POSITIONAL CLONING OF GENES CONTRIBUTING TO VARIABILITY IN NOCICEPTIVE AND ANALGESIC PHENOTYPES

SHAD BENJAMIN SMITH

Department of Psychology

McGill University, Montreal

August, 2006

A thesis submitted to McGill University in partial fulfillment of the requirements of the degree of Doctor of Philosophy in Psychology

Your file Votre référence
ISBN: 978-0-494-32241-3
Our file Notre référence
ISBN: 978-0-494-32241-3

POSITIONAL CLONING OF GENES CONTRIBUTING TO MULTIPLE ANALGESIC AND NOCICEPTIVE PHENOTYPES

Shad Benjamin Smith, B.S.

Department of Psychology

McGill University, 2006

Jeffrey S. Mogil, Ph.D., Advisor

ABSTRACT

Variability between individuals in pain and analgesia phenotypes is often observed in both clinical and experimental settings. The source of this variability has long been attributed to the interplay of environmental and genetic factors, but we have only recently begun identifying these determinants. Experiments comparing isogenic strains of mice have suggested that different pain tests may share a genetic basis; likewise, analgesic magnitude induced by disparate drug classes may be influenced by a common set of genes.

We have presently used a quantitative trait locus mapping strategy to search for genes responsible for variability in analgesic response to five analgesic drugs (the opioids morphine and U50,488, and the non-opioid drugs clonidine, epibatidine, and WIN55,212-2). We first used a B6129PF2 intercross population to map sensitivity to clonidine, morphine, and WIN55,212-2 to a 30 cM region on distal Chromosome 1. *In silico* and congenic strain mapping techniques allowed us to refine this linkage, as well as generalize it to four of the five drugs and seven mouse strains. *Kcnj9* (GIRK3) was identified as a likely candidate gene underlying response to multiple analgesic modalities. We showed that this gene is differentially expressed between C57BL/6 and 129P3 strains

in the periaqueductal gray. We also determined that *Kcnj9* null mutant mice exhibit attenuated analgesic responses.

We previously mapped nociceptive response to the formalin test to two loci on Chr. 9 and 10 using an AB6F2 cross. Using *in silico* mapping, we identified several haplotypes near the *Atp1b3* gene on Chr. 9 (a subunit of the sodium-potassium pump) that correlated highly with early phase formalin response. We then showed that pharmacological antagonism of the sodium-potassium channel eliminates the strain difference observed between A and C57BL/6 mice, supporting a role for this gene in determining response to formalin. Positional cloning of the Chr. 10 locus, employing recombinant and congenic strains, allowed us to refine the location of the locus to a <3 cM interval. A small number of genes in this region were identified as differentially expressed by microarray analysis, providing a short list of candidate genes for follow-up investigation.

ABSTRAIT

Des variabilités en terme de douleur et d'analgésie ont souvent été observées entre individus dans les cadres cliniques et expérimentaux. Ces variabilité phénotypiques ont longtemps été expliquées par le jeu résultant des facteurs environnementaux et génétiques, mais ce n'est que récemment que ces derniers ont attiré l'attention des chercheurs. Des études comparant des lignées isogéniques de souris ont suggéré une base génétique commune pour les différents tests d'évaluation de la douleur; de même, il se pourrait que l'ampleur de l'effet analgésique causée par différentes classes de drogues dépende d'un même ensemble de gènes.

Nous avons présentement utilisé une stratégie de cartographie des loci à effets quantitatifs (ou « QTL ») afin d'identifier les gènes responsables de la variabilité aux effets analgésiques de cinq substances analgésiques (les opiacés morphine et U50,488 et les non-opiacés clonidine, épibatidine et WIN55,212-2). D'abord, une cartographie génétique à partir de souris issues du croisement B6129PF2 nous a permis d'établir que les gènes associés à la sensibilité à la clonidine, à la morphine et au WIN55,212-2 se trouvaient sur la partie distale du chromosome 1, et ce, sur une longueur de 30 centimorgans. Une cartographie selon une approche *in silico* à partir de souris congéniques nous a permis de mieux comprendre ce groupe de liaison de plusieurs gènes et de l'étendre à quatre des cinq drogues et à sept lignée murines. Le gène *Kcnj9* (codant pour GIRK3) a été identifié comme étant le gène candidat sous-tendant le plus probablement la réponse aux multiples modalités analgésiques. Nous avons découvert que ce gène s'exprimait à des niveaux différents chez C57BL/6 et 129P3 dans la matière grise périaqueducale. De plus, des souris mutantes chez lesquelles le gène *Kcnj9* fut rendu non fonctionnel montrait des réponses analgésiques moindres.

Précédemment, à partir de souris issues du croisement AB6F2, nous avons cartographié les gènes associés à la réponse nociceptive au *formalin test* et constaté qu'ils occupaient deux loci, l'un sur le chromosome 9 et l'autre sur le chromosome 10. Une cartographie *in silico* a indiqué la présence sur le chromosome 9 de plusieurs haplotypes fortement impliqués dans la phase du début de réponse au test et situés près du gène *Atp1b3* (codant pour une des sous-unités de la pompe sodium/potassium). Nous avons ensuite montré que le blocage du canal sodium/potassium par un antagoniste pharmacologique chez A et C57BL/6 éliminait la différence de réaction observée normalement entre ces deux lignées de souris lors du *formalin test*, démontrant du même coup le rôle joué par *Atp1b3* dans la réponse à ce test. L'étude de souris recombinantes et congéniques nous a permis, au moyen du clonage positionnel, d'affiner la localisation du locus sur le chromosome 10 jusqu'à une distance d'au moins trois centimorgans. L'analyse de l'expression génique par micropuces à ADN nous a révélé que dans cette région existait un nombre restreint de gènes exprimés à des niveaux différents ce qui nous donne une courte liste de gènes candidats qui pourraient être étudiés dans le cadre de futures recherches.

This work is dedicated to my parents: my father, who passed on to me his enthusiasm for learning purely for its own enjoyment; and my mother, who has always believed I would discover things never before known; and also to Katie, who has always patiently supported my efforts.

ACKNOWLEDGEMENTS

Many people contributed substantially to the success of this research effort:

Steve Bors and animal care staff, for dedication, hard work, and catching my mistakes;

Dr. Elissa Chesler, for R instruction and great advice on the mapping data analysis;

Dr. Michael H. Ossipov, for his AD50 calculation software;

Dr. Anny Fortin, for maintaining and providing recombinant mouse strains;

Dr. Lori Flaherty and Dr. Valerie Bolivar, for the generous gift of subcongenic strains;

Dr. David Clark, Dr. Gouchun Liao, and Roche Bioscience, for haplotype mapping;

Dr. Michael Costigan and Robert Griffin, for microarray technical advice and analysis;

Dr. Kevin Wickman and his students at the University of Minnesota, for sharing their *Kcnj9* findings, providing knockout mice, and contributing their great expertise;

Jennifer Ritchie, for the recombinant inbred and congenic strain panel phenotyping;

Jean-Sebastien Austin and Kara Melmed, for outstanding technical instruction and aid in gene expression studies (and French translation);

Susana G. Sotocinal, Genome Quebec, and numerous undergraduate volunteers, for a tremendous work coordinating the genotyping (and occasional phenotyping) of over 1200 F2 animals and many recombinant/congenic strains, as well as breeding colony management;

My fellow graduate students Mona Lisa Chanda and Dale Langford, for intellectual stimulation, companionship, collaboration, and a lot of thankless favors;

Dr. Sonya G. Lehto, for encouragement, and for getting the whole ball rolling;

and especially, Dr. Jeff Mogil, who has been a true mentor, for voluminously providing advice, challenges, criticism, expertise, funding, inspiration, knowledge, and above all, opportunities.

TABLE OF CONTENTS

LIST OF TABLES

LIST OF FIGURES

CHAPTER 1: A REVIEW OF THE GENETICS OF PAIN AND ANALGESIA

A. Variability in pain and analgesia

A.1. Pain-modulating circuitry

Nociception is a vital sensory mechanism necessary for warning an organism of danger, tissue damage, or illness, and at least in humans, the experience of pain is usually accompanied by an unpleasant emotional component and strong motivational impulses (IASP Subcommittee on Taxonomy, 1979). Until the mid-20th century, medical science did not stray far from the model of pain presented by René Descartes (1664), that the nociceptive signal was carried directly from the cutaneous site of injury to the brain via a single afferent neuron, without any modification of the transmission. The publication of the gate-control theory in 1965 by Melzack and Wall (1965) introduced the idea that pain-transmitting neurons interact with other neurons in the spinal cord, such that the signal can be reduced or even blocked. The past decades have seen many refinements to this concept, and we now know that the multifaceted components of pain are supported by a complex system of neurochemical mediation, which includes both feedback and feedforward regulation as well as signal modulation and dampening mechanisms (Basbaum and Fields, 1984).

Nociception may be initiated by mechanical tissue damage, noxious heat or cold, or inflammatory chemical activation of specialized neurons known as nociceptors (reviewed in Julius and Basbaum, 2001). These nociceptors, small-diameter afferents that may be thinly myelinated (Aδ fibers) or unmyelinated (C fibers), terminate primarily in laminae I and II of the spinal cord dorsal horn. From there, the ascending spinothalamic tract carries the nociceptive signal to the thalamus and then to somatosensory areas of the

cortex, where the sensory-discriminative aspects of sensation are processed (Willis and Westlund, 1997), and to the anterior cingulate and insular cortical areas, which have been implicated in the affective aspects of pain (Rainville et al., 1997). Information is also transmitted through the spinomesencephalic tract to midbrain areas such as the periaqueductal gray (PAG) (Wilberg and Blomqvist, 1987), a vital center for pain inhibition.

It is believed that the PAG is involved in mediating the stress response, allowing an injured animal to make a "fight or flight" response without regard to incapacitating pain (Bandler and Depaulis, 1991). Electrical stimulation of the PAG has been shown to produce substantial attenuation of nociceptive sensation, or analgesia, even sufficient to allow surgery in awake animals (Reynolds, 1969). Microinjection of opioids into the PAG produces profound analgesia, suggesting that the role of the endogenous neurotransmitters is to initiate descending pain inhibitory pathways (Murfin et al., 1976). Activation of neurons in the PAG, whether by electrode or by cortical signaling, results in the release of a number of neurotransmitter molecules, including catecholamines and endogenous opioids, into the midbrain (for a review, see Basbaum and Fields, 1984). Some of these projections release norepinephrine into the dorsolateral pontine tegmentum (DLPT) (Bajic and Proudfit, 1999); however, the bulk of the projections from the PAG terminate in the rostral ventromedial medulla (RVM) (Beitz, 1982). Both of these pathways contribute substantially to pain modulation via further projections to the dorsal horn of the spinal cord, where they inhibit ascending pain signals (Liebeskind et al., 1973). Modulation of nociceptive information may occur at any of the aforementioned levels of the nervous system. Pain, we now recognize, does not represent an unadulterated transduction of the precise qualities of the noxious stimulus; pain is rather a

highly mutable, distinctly subjective experience that (almost) all humans have in common, but which is unique to every individual.

A.2. Variability in pain and analgesia in humans

Humans exhibit an astounding array of responses to aversive stimuli, as noted by the surgeon Henry Beecher (1946), who reported that soldiers wounded in battle would often decline pain-killers for even the most serious of wounds. Libman, a clinician, was among the first to experimentally categorize subjects, designating his patients as "responders" and "non-responders" based on their reaction to moderate pressure placed against their mastoid bone (Libman, 1934). Subsequent studies have shown that individuals vary widely in their pain threshold and tolerance. For example, hyposensitive subjects detect pressure pain at up to double the threshold of hypersensitive individuals (Sherman, 1943; Chapman and Jones, 1944; Brennum et al., 1989); more recent studies show that differences in thermal pain response are equally considerable (Chen et al., 1989b; Sheps et al., 1999; Coghill et al., 2003; Hutchinson et al., 2004). Wide variation in pain experience is not limited to experimental manipulations. Individuals differ in their susceptibility to a number of painful clinical conditions, such as complex regional pain syndrome (CRPS) (Griepp and Thomas, 1991), fibromyalgia (Pellegrino et al., 1989; Stormorken and Brosstad, 1992), migraine (Honkasalo et al., 1995; Mulder et al., 2003), and painful neuropathy following nerve trauma (Devor, 2004), diabetes, or zoster infection (Schmader, 2002).

The variability exhibited between individuals is also evident in response to analgesic compounds. Although this has been anecdotal knowledge to physicians for many years, Lasagna and Beecher (1954) first published findings of a lack of efficacy of

standard doses of morphine in a substantial minority of patients. Individual differences in opiate efficacy have since been documented repeatedly, both in experimental (Chapman et al., 1990) and clinical settings (Portenoy et al., 1990; Galer et al., 1992). Non-steroidal anti-inflammatory drugs, another important group of analgesic compounds including aspirin and ibuprofen, similarly show variation in patient response (Day et al., 1988). Acupuncture, which presumably relies on endogenous analgesic mechanisms, has also been shown to vary in effectiveness between subjects in experimental (Takeshige et al., 1983) as well as clinical (Wong et al., 2003; Brinkhaus et al., 2006) contexts.

A.3. Variability in nociception and antinociception in rodents

Animals have proven useful for basic studies of nociception and its inhibition, and a number of rat and mouse models of painful clinical states have been developed. Pain researchers have compared separate rat and mouse lines for differences between strains on a number of measures of nociception, including response threshold, hypersensitivity, analgesic magnitude, and analgesic tolerance (see Mogil, 1999 for an extensive review of this literature). In general, wide divergence between mouse strains has been observed for all common tests of nociception, ranging from 1.2- to 17.2-fold differences (in the tail-withdrawal and magnesium sulfate abdominal constriction tests, respectively) in strain means (Mogil et al., 1999a; Lariviere et al., 2002). Mice also differ in their susceptibility to neuropathic pain; strains subjected to the same injury (autotomy, or complete denervation of a hindlimb) may respond with minimal (AKR and C58 strains) or extreme (C57BL/6 and C3H/He strains) self-injurious behavior toward the offending paw (Mogil et al., 1999a). Both quantitative and qualitative differences have been noted in analgesic response in mice. We recently compared twelve mouse strains for analgesic magnitude

on five different drug classes against acute thermal pain, and found that the effective dose (AD50) ranged from 2.5- (for the κ-opioid drug U50,488) to 36.8-fold (for the cannabinoid WIN55,212-2) differences between the least- and most-responsive strains (Wilson et al., 2003). Other researchers have shown that analgesia produced by stress or opioid injection arises via different neurochemical mechanisms in different mouse strains (Helmstetter and Fanselow, 1987), or is operational in only a particular subset of strains (Vaccarino et al., 1988). An extreme example was provided by Rady et al. (1998), who proved that heroin analgesia may be mediated by delta-, mu-, or kappa-opioid receptors, depending on the strain tested.

A.4. Sources of variability in pain and analgesia

The major focus of our laboratory is to determine the sources of variability between individuals on measures of nociception and its inhibition. Researchers have found it useful to consider three major components of observed variance (although quantifying the contribution of each component remains a thorny problem): environmental variance, genetic variance, and measurement error. Humans being the heterogeneous, dynamic creatures that we are, a large number of pain-relevant modifiers have been identified within each component of nociceptive variance. Differences in pain and analgesic sensitivity on the basis of race (Edwards et al., 2001; Mechlin et al., 2005) and especially sex (Berkley, 1997) have been observed; however, it is difficult in humans to determine whether such differences are accounted for better by genetic factors (such as gene polymorphisms, androgen effects, etc.) or by environmental influences (like cultural values, gender roles). What may seem to be obviously environmental causes of variability (e.g., stressful life events, motorcycle accidents, exposure to workplace

hazards) frequently interact with heritable susceptibility factors in producing clinical pain states. Psychological factors such as affective state, coping style, pain behavior modeling, hypervigilance, and catastrophizing all contribute to an individual's experience of pain, also in ways affected by both inherent genetic liabilities and the context of the particular painful event (McGrath, 1994). Pain, even at the most basic level of nociceptive sensation, is a remarkably complex trait; partitioning the sources of variance is a daunting challenge in humans, leading many investigators to devise animal models in which either genetic or environmental uniformity may be maximized.

We have recently published a data-mining exercise on variability on the tail-withdrawal test, drawing on an archival data set of over 8000 separate mice tested in our laboratory over an eight year period (Chesler et al., 2002). Both environmental and genetic factors, and their corresponding interaction effects, were observed to influence tail-withdrawal latencies; in fact, the most important factor was *tester*, meaning that the person taking the reading was at least as important as the mouse being tested in determining the mouse's measured sensitivity. The next highest-ranked cluster of factors was related to the genotype of the mouse, however, confirming that heritable strain characteristics are an important determinant of nociceptive phenotypes (Takagi et al., 1966; Frischknecht et al., 1988; Belknap and O'Toole, 1991). Also noted as variables relevant to thermal pain tolerance were season and time of day when tested, housing conditions, sex, ambient humidity, and within-cage order of testing. Independent observers have likewise implicated diet (Shir et al., 1998), ambient temperature (Tjolsen and Hole, 1993), barometric pressure (Sato et al., 1999), and pre- and postnatal maternal behavior (Sudakov et al., 1996; Stephan et al., 2002) as factors contributing to nociceptive behavior in rodents. Although the environment clearly plays a major role in

nociception, the study of genetic differences in mice is a worthwhile endeavor that has already proven to be of value in identifying genes of relevance to pain in humans.

B. Exploiting inbred mouse strain differences to study nociception

B.1. Characterization of inbred strains

The modern laboratory mouse is an exquisitely, but finitely, complex model of mammalian behavior, thanks to the complimentary efforts of 19th century pet breeders and 21st century geneticists. Many of the strains of mice in common use originated from the stocks of "fancy mice" bred by Abbie Lathrop for their interesting color varieties (Beck et al., 2000). Clarence Little, a biologist at nearby Harvard University, recognized the utility of multiple standardized genetic backgrounds in controlling for genetic and environmental variability in his experiments, and began inbreeding Lathrop's mice to create such lines (Silver, 1995). Inbred mice are the product of repeated brother-sister mating, in which each subsequent generation loses roughly half of the genetic heterogeneity of the previous generation. Following 20 generations of inbreeding, all mice of a particular strain are virtual clones of each other, sharing over 99% of their genetic code. Furthermore, inbred mice are homozygous at every locus, eliminating complications related to dominance. Genetically uniform mouse models allow for research performed at one point in space and time to be compared with all other experiments conducted on the same strains; just as importantly, they justify the massive efforts spent to sequence the entire mouse genome (Waterston and al., 2002), and to map markers (Schalkwyk et al., 1999) and haplotype blocks (Wade et al., 2002) that differentiate strains. Researchers will shortly have at their disposal a viable number of commercially available inbred strains in which practically all sources of genetic

variability have been meticulously catalogued. Determining the ways in which such genetic variation is expressed behaviorally remains a daunting, but surmountable, challenge.

B.2. Strain differences in nociception and antinociception

Assuming they are bred and housed in equivalent environments, differences in the phenotypic means of isogenic strains may be attributed entirely to genetic differences. A rich literature of strain differences across many neurobiological parameters has been compiled over several decades, especially between the common strains C57BL/6 and DBA/2 (reviewed in Ingram and Corfman, 1980). More recently, a growing number of studies characterize behavioral differences between strains on measures of nociception and analgesia (Belknap and O'Toole, 1991; Mogil et al., 1999a; Lariviere et al., 2002; Wilson et al., 2003). It is tempting to causally attribute behavioral patterns to underlying physiological divergence between the strains; however, the sheer number of biological differences catalogued between common strains defeats any such attempts. We and others have taken a more systematic approach to documenting strain differences, the *strain survey*, in which a panel of strains (including 10 or more strains selected at random) is tested for sensitivity or resistance to a pain test or analgesic drug. Strain surveys have proven to be useful tools in the dissection of the genetic components of nociceptive behavior; the remainder of this section will describe our use of 12 inbred strains to investigate numerous tests of nociceptive sensitivity, hyperalgesia, and analgesic response (Mogil et al., 1999a; 1999b; Lariviere et al., 2002; Wilson et al., 2003). These data have been submitted to the Mouse Phenome Project (Paigen and

Eppig, 2000), a public database to which researchers from all over the world may contribute phenotypic results for a core group of inbred strains for comparison.

As each member of an inbred strain is genetically identical to all others, the true performance of a strain on a measure of nociception may be precisely assessed by averaging the performance of many individuals. Whereas between-strain variability represents genetic variance, within-strain variability characterizes the influence of environmental factors on the trait. It is possible to estimate the contribution of additive genetic factors to a given phenotype, referred to as "narrow-sense heritability" (or h^2), by comparing the allelic variance (V_A) with the total variance from both genetic and environmental sources (phenotypic variance, or V_P), using a simple formula (Falconer, 1989):

$$h^2 = V_A / V_P .$$

We have experimentally determined estimates of heritability for all major pain tests commonly used in the mouse (Mogil et al., 1999a; Lariviere et al., 2002). These estimates range from h^2=0.30 (for thermal hypersensitivity produced by intraplantar injection of carrageenan) to 0.76 (for the acetic acid writhing test). Our work has shown that genetics and environmental factors share almost equally the mediation of the majority of pain tests in mice. The contribution of genetic factors to pharmacological antinociception is smaller (ranging from h^2=0.12 for the κ-opioid agonist U50,488, to 0.40 for the nicotinic agonist epibatidine and the α_2-adrenergic agonist clonidine), but still substantial (Wilson et al., 2003).

B.3. Genetic correlation

By employing the same strains in multiple surveys, enough statistical power is achieved to investigate *genetic correlations* between phenotypes (Hegmann and Possidente, 1981; Crabbe et al., 1990). Traits that are genetically correlated (i.e., in which the same strains score high or low) are presumed to be so because of their mediation by overlapping sets of genes, due to the ability of individual genes to influence various traits (also known as *pleiotropy*). Observing which phenotypes share genetic mediation offers clues as to the nature of the biological systems underlying the traits. Pain assays may be characterized on a number of parameters (e.g., nociceptive vs. neuropathic, stimulus modality, site of injury, intensity, duration, etc.), any of which may influence the genetic mediation of the phenotype. A multivariate analysis of our strain surveys revealed that genetically correlated assays may be grouped into five "clusters:" nociception produced by thermal or chemical/inflammatory stimuli, thermally or mechanically evoked hypersensitivity, and hypersensitivity driven by afferent activity (Lariviere et al., 2002). Similar sets of strains were sensitive to all tests of thermal sensitivity, but an entirely different set of strains scored high on tests of chemical pain. This principal held true even for neuropathic injury models—the relevant dimension was not the nature of the injury producing hypersensitivity, but rather the stimulus used to evoke pain. Additionally, negative correlations indicate that genes responsible for hypersensitivity (whether to thermal or mechanical stimuli) are the same as those mediating nociception in uninjured animals, but in the opposite direction (i.e., thermal sensitivity genes are protective of thermal hyperalgesia).

We have also used genetic correlation to examine the relationship between nociceptive sensitivity and analgesic response. Genetic correlations between analgesics

of different classes (acting at different receptor types, opioid and non-opioid) range from r_s=0.39-0.77, suggesting that genes downstream from the receptor in the analgesic pathway are responsible for variability in analgesic sensitivity (Wilson et al., 2003). Furthermore, the patterns of analgesic variability evinced in this study correlated significantly with strain means of tail-withdrawal latency (r_s=0.33-0.68) and with formalin-induced licking behavior (r_s=0.79-0.86). Although there is some evidence that analgesic magnitude is specific to the type of pain being inhibited (Mogil et al., 1996; Elmer et al., 1998), our results suggest the striking possibility that variability in analgesic response is an indirect consequence of genes modulating nociceptive sensitivity.

C. Mapping pain and analgesia genes

As noted previously, the genetic determinants of individual differences in a complex trait such as pain are numerous, each contributing a small amount to the overall trait variance. Phenotypes regulated by multiple genes usually have a normal (bell-shaped) distribution in a population, and are referred to as *quantitative traits*; these differ from Mendelian traits, which are controlled by a single gene and are bimodally distributed. Localizing the gene underlying a Mendelian trait is a straightforward (although quite demanding) process of following the trait across multiple generations by tracing its coinheritance with genetic markers (a technique referred to as *linkage mapping*). Finding loci responsible for variability in a quantitative trait (*quantitative trait locus mapping*, or QTL mapping) is much more difficult, as there are many more sources of variation to capture. Inbred mouse strains are the optimum starting point for QTL mapping, as they have quantifiable inherited differences, but can be crossed to produce

mice with only three possible genotypes at any particular locus (two in the case of backcrossed progeny or recombinant inbred strains).

C.1. QTL mapping methods

Properly defined, a quantitative trait locus, or QTL, is simply a region of the genome responsible for variation in the trait of interest (Doerge, 2002). Plant geneticists have followed the coinheritance of morphological characteristics to map QTL since the 1920s (Sax, 1923; see also Rasmusson, 1933; Thoday, 1961), but the application of the technique to mammalian behavior was impractical before the advent of modern genomics. The past two decades have seen tremendous advances in the tools available to geneticists, and it is now feasible to undertake QTL mapping projects as the first step in identifying the precise DNA sequence differences underlying behavioral variation. Optimization of this process is essential for proper evaluation of a QTL's size and location, and requires attention to such features of study design as population construction, genetic marker selection, and statistical modeling (Belknap et al., 1996).

Strain surveys provide valuable information for the selection of starting strains to use in QTL mapping, as strains with polar phenotypes will most likely be those in which allelic variation most directly influences performance. Two parental strains (generation "P1") are chosen such that phenotypic and genetic divergence are maximized; these strains are crossed to produce an F1 ("first filial") generation heterozygous at all loci. All F1 animals are identical, but due to homologous recombination, F1 animals produce offspring (the F2 generation) that are each unique combinations of the P1 strains' alleles (homozygous paternal, homozygous maternal, or heterozygous) when crossed with each other. Another common method is to backcross F1 animals to one of the P1 strains,

thereby producing offspring with random assortments of genes with either one or two alleles from the backcrossed strain. Although backcrosses have been frequently used to map variability loci due to their simplicity (i.e., only one degree of freedom), intercrosses have many advantages; as twice as many meioses are evident in an intercross, only about half the number of progeny need be phenotyped (Lander and Botstein, 1986). Backcrosses are also ill-suited for determining dominance and epistatic effects. However, as mapping precision is directly related to the number of recombination events between markers, two other population types offer potentially greater resolution. Advanced intercross lines (Darvasi and Soller, 1995) and recombinant inbred lines (Plomin et al., 1991) both rely on successive crosses in F2 lines to increase the recombination density in phenotyped animals.

As all F2/backcross individuals are genetically unique, phenotypic variance between them implicates allelic variation at genes involved in its mediation. Although it is impractical (using present technology, at least; Carlson et al., 2004) to assay every gene for association with the phenotype, a smaller number of markers spread across the genome is sufficient to detect linkage. Useful genetic markers are sections of DNA that can be amplified and visualized efficiently, and that differentiate between the parental strains, either by length or by nucleotide sequence. Early QTL mapping projects relied on *restriction fragment length polymorphisms* (RFLPs) (Lander and Botstein, 1986), but the more common repeat polymorphisms called *microsatellites* have supplanted them (Dietrich et al., 1996), and future mapping studies will increasingly take advantage of the ubiquitous *single nucleotide polymorphisms* (SNPs) (Lindblad-Toh et al., 2000). To achieve complete coverage at ~20 cM resolution of all 19 autosomes and the X chromosome in the mouse genome, at least 100 markers are required (Flint et al., 2005).

Because complex, multigenic traits are influenced by numerous factors, linkage to a QTL region is a matter of probability, and numerous statistical techniques have been developed to model phenotype-genotype relationships in the various mapping crosses. The traditional model of *marker regression* is the simplest (Doerge, 2002); an analysis of variance is performed for each marker, contrasting the hypothesis that the allelic status of the marker and the trait cosegregate with the null hypothesis of no linkage. Such single marker tests are inefficient, as the markers themselves are not responsible for QTL effects, nor do they offer much information as to where a quantitative trait gene might be located.

Interval mapping (Lander and Botstein, 1989) is an alternative strategy whereby the genetic map is estimated for entire chromosomes, not just at marker locations, enabling a probabilistic full-genome scan. This method employs an iterative algorithm, such as the EM algorithm (Dempster et al., 1977), to compute maximum likelihood estimates (MLEs) of linkage for missing data points (i.e., all intervals between actual marker locations). At any given location, the MLE is compared to the likelihood estimation under the assumption of no linkage. The strength of linkage at a location is expressed as a LOD (*logarithm of the odds*) score, calculated as the odds of the phenotype distribution given linkage to the genotype, over the odds if the phenotype is unlinked to the genotype:

$$\text{LOD} = \log_{10}(\text{probability of linkage/probability of no linkage}).$$

Several statistical packages have been developed to perform the mapping calculations (e.g., Manly and Olson, 1999; Broman et al., 2003).

C.2. Considerations and limitations for QTL mapping

Even in assiduously characterized experimental populations, quantitative trait genes are needles in immense haystacks, and mapping them in practice requires surmounting a number of technical and statistical hurdles. The very nature of a quantitative trait implies that genes modifying such a trait will likely exert a small effect on the overall variance, typically on the order of 1-10%, and the number of progeny needed to detect differences between genotypes is often over 300. The actual effect size(s) is unknown before the experiment is actually performed; therefore, studies can only be designed to detect loci above a certain threshold (Lander and Schork, 1994). Furthermore, the size of the genome (>1600 cM) necessitates a large number of markers (>100 for ~20 cM resolution) be genotyped in each mouse. The number of potential false positives is great when such a large number of interdependent tests are performed (as in marker regression), with a standard Type I error rate of 0.05%. The method of maximal likelihood used in interval mapping was devised to avoid problems with overcorrecting for multiple tests, but the appropriate LOD threshold for significant linkage has been a controversial topic. Lander and Kruglyak (1995) proposed standardized threshold values of 2.8 (suggestive) and 4.3 (significant) as benchmarks for intercross mapping in the mouse. However, others have proposed permutation testing, based on resampling from the original data, as an empirical means of obtaining thresholds (Churchill and Doerge, 1994), especially for study designs that violate the assumptions of the Lander and Kruglyak model. The criteria for inclusion in the confidence interval (C.I.) are similarly controversial. Lander and Botstein (1986) suggested a 1 LOD drop-off, indicating a reduction in confidence by a factor of 10, although others have advocated for more conservative estimates (1.5 or 2.0 LOD score drop-offs) (Moore and Nagle, 2000).

Although beyond the scope of this review, model selection for QTL analysis remains an area of great research interest. As every data set is unique, care must be taken to ensure the appropriate statistical methods are used to account for phenotype distribution, covariates, missing genotype data, multiple linked QTL (including interaction effects), and any other deviations from linear modeling assumptions. (Discussion of various methods can be found in Jansen, 1993; Kao et al., 1999; Sen and Churchill, 2001; Broman, 2003).

Statistical issues aside, there is considerable argument as to the relative usefulness of QTL mapping in mice as a method to explore the genetic architecture of behavioral traits (e.g., Nadeau and Frankel, 2000). Mapping techniques in common use frequently require hundreds of mice, thousands of individual genotyping reactions, and tens of thousands of dollars. Considering that QTL effects are usually a small proportion of the overall trait variance, and that the resolution of loci is rarely limited to less than 20-30 cM, what exclusive information do these studies provide? In contrast to studies of mutant animals (with either transgenic or spontaneous mutations), QTL mapping detects only those genes that actually cause variation in their naturally appearing forms; genes are never artificially altered. Similarly, genes identified in linkage studies are necessarily the *first cause* of phenotypic variance between two strains; unlike expression techniques such as whole-genome microarrays, the primary DNA sequence differences are implicated, rather than RNA changes that may be several steps removed from the initial difference. Mapping a gene by positional linkage is not hypothesis-driven, meaning it is capable of finding genes for which no functional knowledge exists. Novel trait-relevant pathways may even be discovered, if the implicated gene interacts with the phenotype by a previously unknown mechanism. For example, our investigation of the sex-specific

efficacy of kappa-opioid analgesia led to the gene for the melanocortin-1 receptor (*Mc1r*), a pivotal protein modulating analgesia in females (Mogil et al., 2003). Most importantly, the potential for translation to human pain conditions is high for QTL mapping, as synteny between mice and humans is about 80% (Waterston and al., 2002), and polymorphisms causing minor effects in one species will likely be tolerated (if not common) in another.

D. Identification of quantitative trait genes

D.1. Fine mapping methods

The result of a QTL mapping project is usually a number of 20-30 cM regions where a quantitative trait gene (QTG) is likely to be located. A 30 cM region of the mouse genome may contain, on average, from 400-500 genes, many of which could influence the trait in question based on their known biological functions. The process of narrowing the number of possible QTGs down to one is known as positional cloning, although many steps are usually required to complete the task. From the initial confidence intervals obtained in the initial mapping project, the next step is to fine map the implicated region. Like QTL mapping, this process relies on informative recombinations in progeny of phenotypically-divergent inbred strains. Genotyping more markers around the peak of the QTL in the original F2 population may increase the mapping precision somewhat (5-20 cM), but rarely to the degree necessary for molecular dissection of the QTL (Moisan, 2000).

Mapping variability loci can be accomplished in populations other than backcrosses and intercrosses, and such methods can also be used to accelerate fine mapping efforts. *Recombinant inbred (RI)* strains have been used for decades (Bailey,

1971) to detect and locate major-effect genes, and have been used to find QTLs as well. An RI strain panel is constructed from the progeny of an F2 intercross; repeated brother-sister mating of the F2 animals for multiple generations produces a number of reinbred lines, each of which is a unique (and fixed) mosaic of the parental strains' genotypes. A number of such RI panels have been created, many consisting of over 20 strains each, and these have been extensively genotyped such that the strain of origin is known at virtually every locus in every strain. Because each member of an RI strain is essentially a clone of every other member, variability in a phenotype can be partitioned between genetic (between-strain variance) and non-genetic (within-strain variance) sources, when the means of multiple mice of each strain are considered (Blizard and Bailey, 1979). Between-strain variability can be correlated with the known genetic map in order to locate regions of the genome that predict phenotypic performance across strains (Gora-Maslak et al., 1991). This method of QTL detection is usually underpowered compared with traditional cross methods, due to the limited number of extant RI strains in any given panel; mapping results acquired using RI strains are frequently confirmed using other methods. However, once a QTL has been assigned to a broad confidence interval, RI strains containing recombinations within this interval may be compared in order to pinpoint a tightly linked segment.

A similar strategy may be employed using another genetic model, the *recombinant congenic* strain. Whereas repeated brother-sister mating produces lines of recombinant inbred mice in which half of the alleles derive from each parental strain, a congenic line is produced by backcrossing an F1 animal back to one of the parental strains for a number of generations before inbreeding (Demant and Hart, 1986). This produces a recombinant strain in which from 6.25-12.5% of the genome (depending on the number of generations

of backcrossing) is "donor"-derived, the rest arising from the backcrossed, "recipient" strain. As with recombinant inbred strains, comparing congenic strains with differing alleles in a putative QTL region can associate a marker with variability in a trait.

Recently, techniques to create *marker-assisted* (or *"speed"*) *congenic strains* have been developed that drastically reduce the time and expense of creating a panel of conventional congenic strains. Speed congenic mice are also created by backcrossing F1 intercross progeny with one of the parental strains over 6-8 generations; however, each generation is genotyped at the QTL to select for animals retaining donor strain markers (Bailey, 1981; Markel et al., 1997). This process creates mice that are theoretically equivalent to the recipient strain throughout the genome, except for the interval between the markers used for selection. These animals should exhibit the phenotypic effect of the QTL when compared with the recipient strain, thereby confirming the presence of a QTG in the congenic region. Further congenic substrains may be created by continuing the backcrossing, although in practice this technique is limited by the decreasing frequency of recombination events in ever-narrowing regions (Darvasi, 1997).

Congenic strain construction is a tedious and time-consuming (usually 2 years in rodents) endeavor, but an alternative strategy has recently been proposed by Bolivar et al. (2001). Their method involves exploiting the wealth of knockout strains currently available from commercial suppliers. The construction of a knockout generally involves manipulating the desired gene in 129 strain embryonic stem cells before implantation, then backcrossing the resulting mice onto a C57BL/6 background. This process essentially creates a 129 (donor)/B6 (recipient) congenic region around the deleted gene. Assuming the mutation itself doesn't influence the relevant trait, the "knockout/congenic" can be assessed to determine whether polymorphisms in this region contribute to

observed strain differences. A simple breeding protocol can be employed to verify whether the mutation or neighboring donor DNA is responsible for phenotype differences (Bolivar et al., 2001).

D.2. Positional/molecular cloning techniques

Additional meioses to produce recombination events are impractical after the confidence interval is less than 1-2 cM. Further isolation of the QTL requires direct molecular cloning of tiny sequences, usually maintained as part of a library of large-insert vectors. These libraries are created by inserting small segments of mouse DNA into artificial chromosomes of prokaryotic or simple eukaryotic cells, such as bacteria (BAC clones) or yeast (YAC clones.) Transgenic mice can be produced expressing a few hundred kb of donor strain DNA. This technique has been successfully used to isolate a QTL for asthma (Symula et al., 1999).

Empirical proof of the identity of a quantitative trait polymorphism requires a special type of congenic animal—one in which the precise allelic difference responsible for the QTL has been substituted from one strain onto the other (for example, a C→G nucleotide exchange) without any other modification. Although this is now technically feasible via transgenesis, carrying out the process of cloning a quantitative trait nucleotide by its position alone can take up to a decade, and epistasis can radically alter the expression of a trait when a single nucleotide change is isolated from the context of the full genome (Belknap et al., 1996). Clearly allele transfer is an untenable burden of proof, when other, more practical means are available to implicate single genes beyond a reasonable doubt.

D.3. Candidate gene approach

The assemblage of all identified genes and expressed sequences in publicly accessible databases (e.g., MGI and Ensembl) has made it possible to inventory candidate genes at any point in the process of narrowing QTL intervals. A gene-dense 1 cM region can contain 20 or more genes, but individual genes on this list can be evaluated for evidence supporting a biological mechanism underlying the QTL effect. The standard of proof for accepting a candidate gene as responsible for a QTL is based on three factors: physiologic function, sequence variation, and/or expression differences.

A list of positional candidates from a pain QTL study can be winnowed by searching the literature for evidence implicating each gene in the region in neurotransmission, inflammation, or other relevant biological function. In this regard, gene knockout studies play an invaluable role, as the most direct means of associating genetic variation with a change in phenotype. To date, over 125 genes have shown a pain phenotype in null mutant mice, providing an ever-growing inventory of high-priority candidates (see also Belfer et al., 2004 for a discussion on prioritizing "pain genes" for human association studies). Of the many pain-relevant genes, only those containing actual sequence differences between the original inbred strains are potential candidates. Until very recently, researchers concentrated on exonic polymorphisms affecting the translated protein sequence, predicting that large differences in protein function were behind quantitative trait variability. However, most genetic factors underlying complex traits are subtle, and are more likely to be due to polymorphisms that affect the rate of transcription or translation (e.g., in introns or upstream regulatory regions, or silent point mutations in exons). Consequently, the search for relevant quantitative trait nucleotides cannot be limited to the gene itself, but may also include regulatory regions many

thousands of nucleotides from the start of the gene. RNA expression differences (as quantified by qRT-PCR or microarray) in candidate genes are considered proxies for regulatory modulation in instances where comparing the sequence of the entire neighborhood of the gene in both strains is impractical. Ideally, only one gene within the QTL region will prove to be functionally important to pain processing, contain effectual nucleotide sequence variation, and/or be differentially expressed in the parental strains.

E. *In silico* mapping in the mouse

The technique of *in silico* mapping is a recently proposed alternative to QTL mapping in genetically segregating populations. This method relies on archival datasets of polymorphisms in common inbred strain lines; because all members of a strain are identical, each strain need be genotyped only once. Linkage with a trait is assessed by correlating strain means with known polymorphic regions (called *haplotypes*), rather than by associating genetic markers with phenotypes in individual mice. As more strains are sequenced, *in silico* mapping will become an inexpensive but powerful mapping tool, especially in the localization of QTL.

E.1. Haplotype architecture in inbred strains

The most frequent genetic differences are single nucleotide polymorphisms, or SNPs. The SNPview database (http://snp.gnf.org) has genotyped almost 11,000 SNPs in 48 strains, and Roche (http://mousesnp.roche.com) currently catalogues over 184,000 SNPs in 20 strains, but the true number is much higher. It is estimated that a SNP between mouse strains occurs, on average, every 1000 bases (Lindblad-Toh et al., 2000); however, the density of polymorphism is not consistent throughout the genome, as there

are regions of both high (~40 SNPs per 10 kb) and low (>0.5 SNPs per 10 kb) SNP density (Wade et al., 2002). The vast number of informative SNPs bears great promise for full-genome association studies in humans, which would allow variability genes to be mapped at very high resolution (Risch, 2000). Unfortunately, genotyping millions of SNPs in each subject would require immense resources by today's technology.

In the mouse, it may not be necessary to determine the allelic status of every known SNP in order to perform genome-wide surveys. It has been suggested that the genomes of extant inbred strains are mosaics of European and Asian ancestral stocks, and their relatively recent divergence from a common ancestor is indicated by large regions of conserved sequences among strains (Wade et al., 2002). Genotypes are transmitted together in segments of high linkage disequilibrium called haplotype blocks; haplotype structure allows one to treat the entire block as a unit of inheritance. By some estimates, only 50,000 tag-SNPs (each representing a single haplotype) may be sufficient to characterize the entire genome (Cuppen, 2005), although others argue that a tag-SNP every 10 kb (i.e., 300,000 for complete genome coverage) is needed to preserve power (de Bakker et al., 2005).

E.2. Mapping phenotypes with haplotypes

Grupe et al. (2001) first described a practical strategy to map phenotypes using a SNP database (publicly available at http://mousesnp.roche.com/). As a proof of concept experiment, they attempted to verify 26 published QTL for 10 different behavioral and physical traits. For each pair of strains, they computed distances between genetic loci based on allelic status; they then compared these values with archived phenotypic values, and computed a correlation value between the genetic and phenotypic distances for each

strain-pair comparison. They were able to confirm 15 of the 26 known QTL while excluding 90% of the genome from consideration. Their algorithm employed arbitrary 10 cM haplotype blocks, rather than inherited, empirically-verified haplotypes, thereby compromising the resolution. The appropriate level of significance is also unclear, as the number of strains with both phenotypic and genotypic data was only 4-10 per phenotype (Chesler et al., 2001). However, refinements to this technique promise to vastly improve the detection and localization of QTL as more strains are included in the database, and it was recently reported that this method was able to pinpoint the aromatic hydrocarbon receptor based on its metabolic activity in 13 inbred strains (Liao et al., 2004).

An alternative use for *in silico* mapping has been described by Marshall et al. (2002); they used allelic variation to prioritize coding-region SNPs within QTL attendant to traditional linkage mapping. It is also advantageous to combine haplotype analysis with QTL mapping to disregard areas within a confidence interval that are identical-by-descent between the parental strains, and therefore unlikely to produce phenotypic variability.

F. Current knowledge of genes relevant to nociception and analgesia

We have consistently observed moderate-to-high heritability estimates for a range of nociceptive and analgesic phenotypes in mouse strain surveys (Mogil et al., 1999a; Lariviere et al., 2002; Wilson et al., 2003), indicating that they would be amenable to genetic dissection using the mapping techniques described above. Rather than attempt to separately map each of the dozens of pain tests, we have employed a strategy suggested by genetic correlation analysis. As most pain assays cluster with other tests activating the same stimulus modality (Mogil et al., 1999b), it is likely that QTL mapping of a

representative test from each group will uncover major effect genes common between tests. Thermal, chemical/inflammatory, and neuropathic pain QTL have all been successfully mapped, and in several cases candidate genes have been identified. The genetic mediation of analgesia produced by opioid drugs and stress has also been explored.

F.1. QTL mapping of nociception

Thermal pain was first mapped using the hot plate test in a recombinant inbred population derived from the C57BL/6 and DBA/2 strains (Mogil et al., 1997a). Six regions were implicated in a preliminary scan, and a subsequent replication experiment using an F2 intercross confirmed that distal chromosome 4 harbored a QTL for thermal sensitivity, dubbed *Tnpr1*. Interestingly, the QTL effect was not significant in females, suggesting the gene contributes to thermal pain variability in males only. The δ-opioid receptor gene *Oprd1*, located on Chr. 4 at 65 cM, appeared to be a strong candidate underlying this QTL, and pharmacological studies verified that blockade of this receptor affects sensitivity on the hot plate test in a sex- and strain-dependent manner.

A different thermal pain assay, the radiant heat paw-withdrawal test of Hargreaves et al. (Hargreaves et al., 1988), was used to uncover a second thermal pain gene. Linkage mapping in two different F2 intercrosses (B6xAKR and B6xC) established that a QTL was located on Chr. 7 between 34 and 67 cM (Mogil et al., 2005). This region was further narrowed to a 12 cM interval using the A.B6-*Tyr*$^{+}$/J congenic strain. The most likely candidate gene in this region was *Calca* (54 cM), which encodes the neurotransmitter calcitonin gene-related peptide, alpha (CGRPα), known to be released by nociceptors following noxious activation. Injection of CGRPα into the tested paw

completely eliminates the wide divergence between strains on the Hargreaves test, and other lines of electrophysiological and gene expression evidence support the role of this gene in variability in thermal sensitivity.

The Chr. 7 QTL region was observed in another test of "burning" pain, one which used the chemical capsaicin rather than a thermal stimulus. Capsaicin is the pungent component of chili peppers responsible for the sensation of heat, as it activates the same transduction molecule (the *Trpv1* receptor) that also responds to noxious heat. Furuse et al. (2003) mapped 4 QTL determining capsaicin intake, a measure of oral "burn," in a cross between sensitive C57BL/6 and insensitive KJR mice. None of these QTLs (*Capsq1-Capsq4*, located on Chr. 2, proximal 7, medial 7, and 8 respectively) contained the *Trpv1* gene, serving as a reminder that variability does not have to occur at the activation of a pathway, but can occur at any level downstream as well.

Neuropathic pain has been mapped using the autotomy model, in which transection of the hindlimb nerves produces self-mutilation behaviors (Wall et al., 1979). Seltzer et al. (2001) used a recombinant inbred set derived from the sensitive A and insensitive C57BL/6 strains to map a QTL on Chr. 15 to a 3 cM interval; unfortunately, the large number of potential candidates in this region has precluded positive identification of the QTG. These researchers have subsequently verified this *pain1* locus in a backcross of C3H/HeN and C58/J mice (Devor et al., 2005).

Ongoing work in our lab has focused on two QTL we observed using the biphasic formalin model of chemical/inflammatory pain. Previous strain surveys had identified A and C57BL/6 as strains with low and high incidences, respectively, of licking following intraplantar injection with a dilute solution of formaldehyde (Mogil et al., 1998; Mogil et al., 1999a). Interval mapping with an F2 intercross of these strains revealed a QTL on

Chr. 9 (*Nociq1*, peak~60 cM) that predicted formalin response in the early phase only; a second region on Chr. 10 (*Nociq2*, peak~55 cM) associated with both early and late phases of the formalin test (Wilson et al., 2002). The Chr. 10 region has been linked to collagen-induced arthritis (Dracheva et al., 1999; Yang et al., 1999) and the acetic acid writhing test (H. Hain and J.K. Belknap, unpublished results), suggesting the gene responsible for this QTL is also relevant to other inflammation models. We have employed a number of techniques to identify these two inflammation genes; this work will be fully detailed in this manuscript.

F.2. QTL mapping of analgesia

The genetic mediation of morphine analgesia has been thoroughly dissected using a number of approaches capitalizing on the divergence of C57BL/6 and DBA/2 on inhibition of hot-plate sensitivity. The trait was initially mapped using BXD recombinant inbred (RI) strains; only one significant QTL was observed, on Chr. 10 (Belknap et al., 1995). A number of other putative QTL were found in a follow-up study using the same RI set and in a B6D2F2 intercross; these were investigated using a short-term selected breeding approach and congenic strains in which backcrossing was used to place small intervals of one strain onto the genetic background of the other (Bergeson et al., 2001). Four QTL were reliably confirmed, accounting for up to two-thirds of the genetic variance of the trait. The largest, on Chr. 10, comaps with the μ-opioid receptor gene (*Oprm1*), which encodes the receptor for morphine and which has been implicated in pain variability (Uhl et al., 1999). This region has also been linked to voluntary morphine consumption (Berrettini et al., 1994), but not morphine antinociception on the writhing test (H. Hain and J.K. Belknap, unpublished data). A QTL on mid Chr. 9 appears to be

due to the serotonin 1-B receptor gene *Htr1b*, based on pharmacological evidence (Hain et al., 1999), and a likely candidate for a female-specific QTL on proximal Chr. 1 is the κ-opioid receptor gene *Oprk1*, although more confirmatory evidence is needed. A second Chr. 9 QTL, also observed only in females, has not been identified to date. Details of all previously mapped pain- and analgesia-related QTLs are given in Table 1.

Mapping quantitative trait loci has proven extremely useful in elucidating the nature of female-specific mechanisms of stress-induced and opioid analgesia. Analgesia produced by a short swim in cold water is mediated by NMDA receptors in male mice of most strains, but pharmacological blockade of NMDA activity in females has no effect (Mogil et al., 1993; Mogil and Belknap, 1997). Similarly, NMDA activity is required for κ-opioid analgesia in male deer mice but not females (Kavaliers and Choleris, 1997). Separate mapping projects affirmed that stress-induced analgesia (SIA) and U50,488 (a κ-opioid agonist) analgesia both mapped to distal Chr. 8, but the effect was only observed in females (Mogil et al., 1997b; Mogil et al., 2003). Although no genes in this region were obvious candidates, the melanocortin-1 receptor gene *Mc1r* was investigated due to its expression in the PAG and the antinociceptive properties of its endogenous ligands, α-melanocyte stimulating hormone (α-MSH) and adrenocorticotropic hormone (ACTH). Comparing mutant female mice with non-functional melanocortin-1 receptors to their wild-type counterparts, we observed a "male" (i.e., NMDA-sensitive) pattern of response to U50,488 injection in the mutants only (Mogil et al., 2003). Pharmacological antagonism of this receptor in wild-type females likewise resulted in a switch from the female to male system.

F.3. Simultaneous QTL mapping of multiple nociceptive and analgesic phenotypes

Although we and others have demonstrated some success identifying a number of genes relevant for pain sensation and opioid analgesia, only a small number of nociceptive phenotypes have been explored. Strong genetic correlations between various assays of particular pain modalities, as well as between analgesics of multiple drug classes, suggest that overlapping sets of genes contribute to these traits. We have proposed (Mogil et al., 1999b; Wilson et al., 2003) that an efficient dissection of the genetics of pain should draw upon information gathered from these strain surveys, enabling the prediction of phenotypes that would display common genetic mediation. Specifically, we predict that simultaneous mapping projects of three correlated analgesic drugs will implicate loci in common across all three drugs. Such a finding would likely represent a gene (or genes) acting at a level of the descending modulatory pathway where analgesic mechanisms have converged. To test this hypothesis, we have used a B6129PF2 intercross population to map variability loci responsible for analgesic sensitivity to clonidine, morphine, and WIN55,212-2.

In a separate line of experiments, we have used mice derived from an AxB6 cross to investigate two previously discovered QTLs mediating variability on the formalin test (Wilson et al., 2002). The biphasic formalin test may be considered as two distinct phenotypes, as the early and late phases appear to correspond to different nociceptive mechanisms. The first QTL, located on Chr. 9, was significant for the early phase only, but a QTL on distal Chr. 10 reflected early and late phase variance. We have used a number of genetic, molecular, and pharmacological techniques to determine the identity of genes regulating sensitivity to chemical/inflammatory pain.

CHAPTER 2: QTL MAPPING OF THERMAL NOCICEPTION AND ANALGESIA

A. Experiment Summary

Genetic correlation analysis of five analgesic drugs predicted that overlapping sets of genes may be responsible for sensitivity to analgesic drugs of multiple neurochemical classes (Wilson et al., 2003). We designed simultaneous QTL mapping projects to determine the genetic factors contributing to variability in clonidine, morphine, and cannabinoid analgesia using a common population of 896 B6129PF2 intercross mice. All mice were genotyped at 100 microsatellite markers spread throughout the mouse genome, and the software package R/qtl was employed for interval mapping of all phenotypes. Baseline thermal pain mapped to two major loci on chromosomes 7 and 11, as well as others. A locus exerting moderate effects on analgesia from all three drugs was observed on distal Chr. 1. The peak of linkage for all three drugs was within 5 cM of the 95 cM mark, suggesting a single gene is likely partially responsible for variability across drug types. This region of Chr. 1 has a number of potential candidate genes, of which many have been posited as quantitative trait genes for other neurobehavioral phenotypes. The gene *Kcnj9*, encoding a G protein-coupled inwardly rectifying potassium channel, is located at the peak of linkage and is differentially regulated between 129 and C57BL/6 strains, making it a prime candidate for explaining variability in sensitivity to analgesic drugs.

B. Introduction

Genetic diversity is a major component underlying individual differences in both nociception and analgesia. A growing literature has documented moderate heritability estimates for a number of clinical and experimental pain conditions in humans (Honkasalo et al., 1995; Larsson et al., 1995; MacGregor et al., 1997; Treloar et al., 1998; Hakim et al., 2002). There is also evidence that analgesia produced by opiate drugs is influenced by genetic factors (Liston et al., 1981); allelic variants of several metabolic genes, including *COMT* (Zubieta et al., 2003) and *CYP2D6* (Sindrup et al., 1990; Poulsen et al., 1996), have been associated with deficiencies in opioid activity. The use of isogenic and selectively bred mouse strains has overwhelmingly confirmed that genetic differences contribute significantly to variability in analgesic response from opiates (reviewed in Flores and Mogil, 2001) as well as a number of distinct pain modalities (Mogil et al., 1999a; Lariviere et al., 2002).

Non-opioid drugs are increasingly valued as adjuvant analgesics in conjunction with opioids, and there is considerable interest in developing them for stand-alone use to combat chronic pain. Studies comparing rodent strains have demonstrated a genetic influence on non-opioid analgesics, including the α_2-adrenergic receptor agonist clonidine (Marwaha, 1984; Tiurina et al., 1995) the nicotinic acetylcholine receptor agonist epibatidine (Flores et al., 1999), and cannabinoids (Onaivi et al., 1996), among others. Although the primary receptor for each of these drugs is unique, they are all (except for the nicotinic receptor) G protein-coupled receptors (GPCRs), and they all putatively inhibit pain by activating descending modulatory pathways in the spinal cord. However, the extent to which the genetic mediation of a particular drug class is distinct from others has been largely unexplored.

We recently examined this question by assaying a panel of inbred mouse strains for sensitivity to five analgesic drugs active against the tail-withdrawal and formalin tests (Wilson et al., 2003). These drugs included the κ-opioid agonist U50,488, the cannabinoid WIN55,212-2, clonidine, epibatidine, and (for comparison) the prototypical μ-opioid drug morphine. For each drug, the range of half-maximal antinociceptive doses (AD50s) between strains was quite large, from a 2.5-fold difference between BALB/c and C58 strains in U50,488 sensitivity, to a 36.8-fold difference between A and AKR mice for the cannabinoid agonist. Intriguingly, we observed similar response patterns across drug classes, such that mouse strains sensitive to one analgesic were likely to be sensitive to the others. Genetic correlation analysis (Crabbe et al., 1990; Mogil, 2000) suggested that overlapping sets of genes partially mediate analgesic magnitude regardless of the drug used, possibly by regulating neuronal excitability at CNS sites where analgesic mechanisms have converged. In addition, baseline pain response was shown to be negatively correlated with analgesic sensitivity, implying that the genes responsible for analgesia are also involved in determining nociceptive sensitivity.

Although we can currently only speculate as to the nature of these "master genes" controlling pain and analgesia, quantitative trait locus (QTL) mapping has been used successfully to determine the identity of a number of genes involved in nociceptive modulation. The genetic determinants of baseline thermal sensitivity have been dissected using two commonly used pain tests. Mogil et al. (1997a) detected a locus on chromosome 4 that appears to modulate hot-plate latencies in male but not female mice; this locus likely corresponds to the δ_2-opioid receptor gene. Variation in the *Calca* gene on Chr. 7, which encodes the nociceptive neurotransmitter CGRP, was shown to be

responsible for the greater sensitivity of C57BL/6 over AKR mice (and very likely between all 12 strains tested) on the Hargreaves paw-withdrawal test (Mogil et al., 2005).

Morphine antinociception against hot-plate pain has been thoroughly examined using QTL analysis in multiple populations derived from a C57BL/6 and DBA/2 cross (Bergeson et al., 2001). Five significant loci have been revealed, accounting for most of the genetic variance between the two strains. One of these, on Chr. 10, comaps with *Oprm1*, the μ-opioid receptor gene. Although this result may seem intuitive, this locus was not linked with morphine inhibition of nociceptive behavior in the acetic acid writhing test (H. Hain and J.K. Belknap, unpublished results), indicating that the genetic mediation of analgesia may be dependent on the characteristics of the pain being inhibited. A second locus on mid-Chr. 9 is likely the serotonin-1B receptor gene *Htr1b* (Hain et al., 1999). Two other loci implicated in morphine analgesia are both markedly female-specific; the identities of the responsible genes are as yet unproven, although one on proximal Chr. 1 may be the κ-opioid receptor. Another female-specific locus has been found to mediate analgesia produced by both non-opioid stress mechanisms (Mogil et al., 1997b) and the κ-opioid drug U50,488 (Mogil et al., 2003). This locus, mapped to distal Chr. 8, was shown to be the melanocortin-1 receptor gene, *Mc1r* (Mogil et al., 2003).

Although genetic differences in the receptor to which a particular drug binds may produce variability between individuals (as has been shown for morphine), it is highly unlikely that genes responsible for analgesia across drug classes encode membrane receptors. Rather, the "master genes" will likely be those participating in mechanisms common to multiple analgesic systems, such as G protein-coupled second messenger systems, neuronal excitability, or neurotransmitter metabolism. Alternatively, they may be those genes contributing to variable sensitivity to the pain modality itself. As a first

step in localizing these genes, we performed simultaneous quantitative trait locus mapping projects with three analgesic drugs active against the tail-withdrawal assay of thermal pain: morphine, clonidine, and the cannabinoid WIN55,212-2.

C. Methods

C.1. Subjects

Previous strain surveys revealed that 129P3 mice are relatively sensitive to all of the analgesics under consideration in this study, whereas C57BL/6 mice are among the most resistant to their antinociceptive effects (Wilson et al., 2003). Conversely, these two strains are resistant and sensitive, respectively, to thermal pain as assessed by the tail-withdrawal test (Mogil et al., 1999a). Breeding pairs of B6129PF1/J animals (the reciprocal 129PB6F1 cross is not commercially available) were obtained from The Jackson Laboratory (Bar Harbor, ME) and bred on-site at McGill University. Their F2 hybrid offspring were weaned at 18-21 days and housed in groups of 3-5 same-sex littermates in our humidity- and temperature-controlled vivarium. All mice were given food (Harlan Teklad 8604) and water *ad libitum* and maintained on a 14/10-hr light/dark cycle. They were tested at no less than six weeks of age, in approximately equal numbers of males and females. Testing was performed near the middle of the light phase to minimize circadian effects (Kavaliers and Hirst, 1983). Immediately after testing, subjects were euthanized by cervical dislocation according to ethical guidelines, and their liver, spleen, and tail were harvested for genotyping.

C.2. Phenotyping

Morphine sulfate (National Institute for Drug Abuse, Rockville, MD) was dissolved in 0.9% saline and administered in a dose of 15 mg/kg. Clonidine hydrochloride and WIN55,212-2 (both from Tocris, Ellisville, MO) were also dissolved in saline, in doses of 3 mg/kg and 10 mg/kg, respectively. Doses were chosen on the basis that they robustly distinguish 129P3/J mice from C57BL/6J mice (i.e. 129 mice show marked analgesia while B6 mice are relatively unaffected.) All drugs were administered intraperitoneally to naïve mice in an injection volume of 10 ml/kg.

All mice were phenotyped using the 49° tail-withdrawal assay; testing of all drug groups occurred concurrently over the course of ~1 yr (summer to summer). Each mouse was secured gently inside a cloth/cardboard holder with its tail held outside. The tail was lowered into a hot water bath maintained at 49.0°C and the time for it to withdraw its tail was measured with a stopwatch to the nearest 0.1 s; 15 s was used as a cutoff latency in order to avoid damage to the tail. Readings were taken at baseline (pre-injection) and at 15, 30, and 60 minutes post-injection of the drug. At each time point, two latencies were measured and then averaged to increase accuracy. For purposes of statistical analysis, phenotypic data at each time point were converted into percentage of the maximum possible effect using the formula:

$$\%MPE = (\text{post-injection latency-baseline})/(\text{cutoff-baseline}) \times 100$$

The maximum %MPE for the three time points was used as a measure of analgesic magnitude for QTL analysis; as an alternative way of characterizing the effectiveness of analgesic compounds, we also computed the percent analgesia, or area under the time-

course curve (AUC). Baseline latencies were used as a measure of sensitivity to thermal nociception for use in interval mapping.

C.3. DNA Isolation and Genotyping

Genomic DNA from the mouse spleens was extracted using the DNeasy kit (Qiagen, Mississauga, ON) following the manufacturer's protocol, and PCR was performed using standard procedures. Primers were obtained from Invitrogen (Burlington, Ontario). Samples were genotyped either in our laboratory, by capillary electrophoresis using the CEQ 8000 Genetic Analysis System (Beckman-Coulter, Fullerton, CA), or off-site at the Genome Quebec Innovation Centre using the ABI Model 3100 (Applied Biosystems, Foster City, CA), for 100 microsatellite markers (average intermarker distance: 15.6 cM) across the 19 autosomes and the X chromosome (Fig. 1). Markers were selected using the MGI database (www.informatics.jax.org) to differentiate between 129P3/J and C57BL/6J alleles.

C.4. Statistical Analysis and QTL Mapping

Phenotypic and genotypic data were assembled in Excel (Microsoft, Redmond, WA), and basic statistical analyses were performed in Systat 10 (SPSS, Chicago, IL). Frequency histograms of the phenotypes were generated using Prism 4 (GraphPad, San Diego, CA). Seven mice were excluded as statistical outliers on the basis of their baseline latency >3 s.d. from the mean. The analgesia score used in all subsequent analyses was percent analgesia, as the frequency distribution of this measure in the F2 population exhibited more variability (and therefore more statistical power for mapping) than did maximum %MPE. Analgesia was analyzed within each drug group (clonidine

n=292, morphine n=302, WIN n=295), as well as collectively, regardless of drug (n=889). Baseline latencies of all mice (except outliers) were used to map thermal sensitivity (n=889).

The R/qtl programming environment (version 2.1.1; Broman et al., 2003) was used to perform full-genome scans as well as to evaluate multiple-QTL models for all phenotypes. Utilities within R/qtl were used to calculate recombination frequencies and identify genotyping errors; the estimated genetic map compared favorably with established marker positions (data not shown). Interval mapping was generally performed using the EM algorithm as implemented in R/qtl, except where noted. We assessed the significance level individually for each QTL search by permutation tests with 1000 iterations; this analysis was occasionally done using Haley-Knott regression (Haley and Knott, 1992), when the computational demands were too great to be carried out with the EM algorithm. Except where noted, all results above a full-genome-corrected $p < 0.05$ are reported as significant. "Suggestive" and "highly significant" results correspond to Type I error rates of $p < 0.63$ and 0.001, respectively (Lander and Kruglyak, 1995).

D. Results

The mean of the baseline latencies in all F2 mice was 3.38 ± 0.03 s, intermediate between the means of the parental strains (129P3 = 4.8 s, B6 = 2.2 s; Mogil et al., 1999a). The trait distribution (see Fig. 2a) exhibited wide, non-normal variability around this mean (Shapiro-Wilk normality test W = 0.97, $p<0.001$, kurtosis = 0.3, skewness = 0.7); the baseline scores were therefore normalized using a square root transformation for QTL mapping. The distributions of analgesia measurements appeared to be bimodal in all three drug groups (Fig. 2b-2d); a considerable number of mice exhibited 100%

analgesia across time-points, whereas the remainder was distributed around a peak substantially lower. Such a bimodal distribution suggests that a single main effect gene (or unidentified environmental confound) separates mice into responsive and non-responsive groups, with other smaller-effect loci determining variability around these peaks. At the doses used, morphine produced a greater mean level of analgesia (65.2%) than did clonidine (43.1%) or WIN55,212-2 (42.6%)

Male mice were significantly more sensitive to clonidine ($t_{290} = 3.211, p < 0.001$) than were females, and a trend toward differential responses between males and females was observed in thermal sensitivity ($t_{888} = 1.638, p = 0.10$) and analgesia produced by morphine ($t_{300} = 1.691, p = 0.09$), but not WIN55,212 ($t_{293} = 0.665, p = 0.51$). Baseline latencies correlated weakly with clonidine ($r = 0.24, p < 0.001$) and WIN55,212 ($r = 0.12, p = 0.05$) analgesia, but not with morphine ($r = 0.04, p = 0.48$) analgesia. These genetic correlations partially confirm our previous prediction that overlapping sets of genes are likely to be found contributing to both pain and analgesia variability in this mapping population (Wilson et al., 2003).

As the phenotyping of the three groups was performed simultaneously over an extended period, we looked for trends across months in thermal sensitivity and analgesic magnitude for each group. Baseline latency appeared to decrease, as a main effect of month was noted ($F_{10,907} = 4.78, p < 0.001$). An increase in morphine sensitivity was also observed over time ($F_{6,295} = 10.55, p < 0.001$), but no such trend was apparent for clonidine ($F_{8,306} = 1.28, p = 0.25$) or WIN55,212 ($F_{4,294} = 1.19, p = 0.32$). As the trends were not consistently observed in all groups, nor were they cyclical (i.e., seasonal), we hesitate to speculate as to the nature of any covariates systematically confounding these results.

D.1. Thermal QTL

Interval mapping with a single-QTL model revealed two highly significant loci affecting baseline latencies on the tail-withdrawal test, one on Chr. 7 and one on Chr. 11 (Fig. 3a). Additional suggestive loci were observed on four other chromosomes. A two-dimensional scan was then performed, to detect any epistatic interactions between these QTL. No interactions were observed between the detected loci, but a strong interaction between a region of Chr. 4 and the X chromosome suggested the presence of a sex-specific QTL. Interval mapping with sex as a covariate confirmed a suggestive linkage to Chr. 4 in males only. A multiple QTL model may be constructed with the fitqtl function in R/qtl; this method uses a drop-one-term analysis to compare the full model (all terms included) with the model obtained by dropping a given term. The best-fit model (Table 2) accounts for 14.9% of the phenotypic variance in tail-withdrawal sensitivity (as R/qtl uses the imputation method for modeling, Table 2 does not correspond exactly with Fig. 3a-d, which were created using the EM method.)

D.2. Analgesia QTL

The analgesia scores of the F2 mice were bimodally distributed, with a spike at the upper limit, so the "two-part" model designed for such a pattern of responses was used for interval mapping with the EM algorithm (Broman, 2003). Although this model takes into account the added parameters of non-normal frequency distributions, it can be computationally intensive. Therefore, significance levels were estimated using 1000 permutations of the phenotypes, as analyzed using Haley-Knott regression on a normal model; this method likely overestimates the significance estimates of our datasets.

In order to generate hypotheses regarding the presence and location of a "master analgesia gene," we first analyzed a composite analgesia phenotype including all mice, regardless of which drug was administered. One significant locus was observed on distal Chr. 1, and nine other peaks reached a level of suggestive significance (Fig. 4). We then performed interval mapping of the three drug datasets separately. The Chr. 1 locus was also significant in the clonidine and WIN55,212 groups, but no linkages reached significance in the morphine group (Fig. 5). There was likely a great deal of data censoring in the morphine results, as the 15 mg/kg dose induced high levels of antinociception in the majority of animals. Therefore, we repeated the experiment in a new B6129PF2 population using a 10 mg/kg dose, genotyping only three markers at the distal end of Chr. 1. Significant linkage (peak LOD = 2.8 at 93 cM, 95% threshold LOD = 1.95) to this region was observed in this population, mirroring the peaks seen in the clonidine and WIN55,212 groups (Fig. 6). One other significant locus was observed on Chr. 7 in the WIN55,212 group, as well as numerous suggestive loci. The full QTL models for clonidine and WIN55,212-2 analgesia, as determined by imputation mapping and the drop-a-term method, are given in Table 3.

Additional analyses were conducted using sex and baseline latencies as covariates, in order to partition out the effects of these factors. However, the additional parameters resulted in a corresponding decrease in power, and no credible linkages were observed.

E. Discussion

Major genetic factors underlying variability in a number of nociceptive traits have been localized using quantitative trait locus mapping, and a few of the quantitative trait genes have already been identified. The present experiment extends our knowledge of the genetic determinants of thermal pain, with possible confirmation of previous findings. We have also explored the genetic mediation of multiple analgesic modalities, in particular the hypothesized existence of a set of genes mediating antinociception regardless of the pharmacological binding site.

E.1. Thermal pain QTLs

Performing simultaneous mapping projects from a common F2 intercross population allowed for maximal power in the combined dataset used to map baseline thermal pain. Two loci were detected at high significance, despite having only moderate effects on the overall trait variance. The largest of these peaks, a locus on Chr. 7 (peak at 33 cM, 1-LOD drop-off C.I. 24-38 cM) accounting for 4.7 % of the phenotypic variance, localizes roughly near a known QTL for thermal pain. Using the Hargreaves paw-withdrawal assay, we mapped a QTL at 50 cM (C.I. 34-62 cM) in a B6xAKR intercross (Mogil et al., 2005). Several lines of evidence implicated the gene *Calca*, which encodes the neurotransmitter CGRP, as the responsible gene (Mogil et al., 2005). However, located at 54 cM, *Calca* lies well outside the confidence interval of our present QTL on Chr. 7 and is an unlikely positional candidate. Few obvious pain-related candidate genes reside within our locus, although it does contain several genes with effects on neuronal activity, including subunits of GABA-A and cholinergic receptors and the nerve growth factor necdin. Interestingly, this region of mouse Chr. 7 is syntenic to a region of human

Chr. 15 that is deleted in Prader-Willi syndrome; Prader-Willi patients exhibit deficits in thermal sensation (Holm et al., 1993), and mice lacking the necdin gene *Ndn* (a nerve growth factor, located at 28 cM) have similarly diminished pain sensitivity (Kuwako et al., 2005). Although this QTL may help explain individual differences in normal and abnormal human populations, it does not explain the strain difference in nociceptive sensitivity between 129P3 and C57BL/6 mice, as the more sensitive strain (B6) carries the nociception-resistant allele of the locus.

Conversely, the Chr. 11 QTL at 46 cM (C.I. 30-55 cM) does mirror the direction of the strain difference, and allelic status at this locus accounts for 3.1% of the phenotypic variance in the F2 population. Considering the large number of genes in this region that could be plausible candidates influencing thermal pain sensitivity, it is remarkable that it has not previously been linked to hot-plate (Mogil et al., 1997a), Hargreaves' test (Mogil et al., 2005), or oral capsaicin (Furuse et al., 2003) sensitivity. The primary thermal transducer protein is encoded by *Trpv1* located at 44.1 cM, and a number of ion transport channel proteins linked to pain (including the potassium channel *Kcnj12* at 34.2 cM, the sodium-potassium pump *Atp1b2* at 40 cM, and the amiloride-sensitive sodium channel *Accn1*, the nicotinic acetylcholine receptor *Chrne*, and the serotonin transporter *Slc6a4* at 42 cM) are also found within the confidence interval. Other genes in the region with a known role in pain modulation include a cluster of arachadonic acid metabolism enzymes between 37 and 40 cM, and genes involved in wind-up and inflammation (guanylate cyclase *Gucy2e* at 37 cM and nitric oxide synthase *Nos2* at 45.6 cM) and in opioid antinociception (β-arrestin 2 *Arrb2* at 45 cM).

Four suggestive loci on Chr. 3 (81 cM), Chr. 4 (56 cM), Chr. 6 (28 cM), and Chr. 14 (3 cM) contribute only slightly (>2%) to the phenotypic variance. Of considerable

note, however, is that the chromosome 4 QTL, significant only in males, comaps with a similarly sex-specific QTL for thermal pain sensitivity on the hot-plate test (Mogil et al., 1997a). This QTL, located between 50-80 cM from the centromere, was discovered in the BXD set of recombinant inbred strains, and was subsequently confirmed in a C57BL/6 x DBA/2 intercross. Pharmacological evidenced amassed by Mogil et al. (1997a) concluded that the *Oprd1* gene (65 cM), which codes for the δ-opioid receptor, may partially determine hot-plate sensitivity in a sex- and strain-dependent manner. Based on the parallel localization and sex-specificity of these two loci, it is highly probable that we have replicated the hot-plate QTL using a different pain test in a novel cross, affirming our position that different assays of the same pain modality will share genetic mediation (Mogil et al., 1999b; Mogil, 2000).

E.2. Analgesia QTL

Genetic correlation analysis (Wilson et al., 2003) predicted that QTL mapping of analgesia produced by divergent compounds would implicate common sets of genes. We first looked for linkage in a combined dataset of almost 900 F2 mice, in which analgesic response to one of three drugs had been quantified for each mouse. Only one region, on distal Chr. 1, appeared to be significantly linked, despite the high power of the large dataset. Each subset of F2 animals was then examined to determine if the Chr. 1 QTL generalized to clonidine, morphine, and WIN55,212-2. We found significant linkage to a 26 cM region (84-110 cM) for all three analgesic drugs. Though the peak of linkage differed slightly between drugs (100 cM for clonidine, 90 cM for morphine, and 96 cM for WIN55,212-2), we believe these differences are negligible, due to the imprecision of

QTL mapping. Baseline thermal sensitivity did not significantly map to any region of this chromosome.

These results provide some support for our conjecture that variability in analgesic response is largely mediated by genes common to multiple analgesic modalities, rather than receptors distinct to individual drugs. The gene responsible for the Chr. 1 locus may be involved in GPCR second-messenger processes in neurons activated by drug binding, or it may regulate the excitability of neurons downstream in the analgesic pathway. It is not likely that this gene exerts its influence on analgesia indirectly by affecting pain transmission mechanisms, as the QTL was not linked to tail-withdrawal latency itself.

Distal Chr. 1 is a region rich in behavioral QTLs, many of which could potentially share mediation with the analgesia phenotypes. A search of the Mouse Genome Informatics database (www.informatics.jax.org, March 16, 2006) revealed 34 neurobehavioral- and/or pain-related QTLs mapped to >75 cM; these include seven traits related to alcohol, six to morphine or other drugs, two to painful arthritis, five to emotionality/anxiety, and one to seizure susceptibility. Several of these QTLs have been finely mapped near the peak of linkage of our analgesia QTL. Ferraro et al (2004) mapped susceptibility to seizure (*Szs1*) to a 6.6 Mb region using the B6.D2-*Mtv*-7a/Ty congenic strain; they concluded that of four ion-transport genes in this region (*Atp1a2*, *Atp1a4*, *Kcnj9*, and *Kcnj10*), the potassium channel gene *Kcnj10* (93.5 cM) appeared most likely to underlie the phenotype, due to an amino acid change between B6 and D2 mice. Yalcin et al. (2004) employed a quantitative complementation strategy using *Rgs2* null mutant mice to implicate this gene (78 cM) in regulating anxiety as measure by open-field locomotion. Ethanol-induced locomotion was linked to a distinct but nearby region (82- 85 cM) using a multiple strain cross (Hitzemann et al., 2002); these researchers noted

that *Kcnj9* (94.2 cM) was the only gene near this locus found to be differentially expressed by microarray analysis (Sandberg et al., 2000), making it a good candidate gene. These researchers (Hitzemann et al., 2004) similarly used a multiple cross mapping strategy, combined with novel gene expression and sequence analyses, to map basal locomotor activity to a 10 Mb length (168-178 Mb). Again, *Kcnj9* appeared a likely candidate, as it was the only gene for which gene expression patterns mirrored the behavioral data.

Although none of the previously mentioned QTL studies included a 129 strain, they all used C57BL/6 to contrast with an oppositely responding strain, just as in the present study. It is worth noting, however, that the microarray experiment that established *Kcnj9* as the only differentially expressed gene on distal Chr. 1 was performed using B6 and a 129 substrain, 129SvEv (Sandberg et al., 2000). Future sections of this work will discuss haplotype correspondence between the strain used in this project, 129P3, and strains used in other studies (e.g., other 129 substrains, A, BALB/c, DBA/2, LP, etc.).

Many of the genes evaluated as candidate genes for other phenotypes are also possible quantitative trait genes for our analgesia phenotypes. Several, including *Atp1a2*, *Atp1a4*, *Kcnj9*, and *Kcnj10*, encode cation channels involved in establishing membrane potentials. A number of G protein signaling pathway genes reside in this region, including several of the *Rgs* ("regulator of G protein signaling") family implicated in opioid analgesia (Sanchez-Blazquez et al., 2003), as well as the G protein-coupled potassium channel subunit, *Kcnj9*. Other genes in the QTL region with suspected links to pain include *Psen2* (presenilin 2, 101.0 cM) which is down-regulated in response to inflammation (Saban et al., 2002), and *Mpz* (myelin protein zero, 92.4 cM), a variant of

which causes neurosensory dysfunction and pain in the form of Charcot-Marie-Tooth disease (Gemignani et al., 2004).

Despite these promising results, it does not appear that the gene underlying the Chr. 1 QTL (which we dubbed *Manr1*, for "Multiple analgesic response 1") is a "master analgesia gene" responsible for the genetic correlations between multiple analgesics and baseline thermal pain. The allele associated with sensitivity to analgesia in the F2 mice derives from C57BL/6, the more resistant of the two parental strains. The allelic effect of the responsible gene explains at most 4.7% of the phenotypic variance (in the clonidine group), and as demonstrated by the morphine group, may be highly dose-dependent. The localization of the quantitative trait gene may be problematic, as the 1-LOD drop-off confidence intervals are probably optimistic. Nevertheless, the existence of a gene that partially determines sensitivity to all three common analgesic drugs is a novel and remarkable finding. Identification of this gene holds promise for new drug development targets, as pharmacological manipulation of the relevant protein may be the key to increasing the analgesic sensitivity of opioid-resistant patients.

CHAPTER 3: FINE MAPPING OF *Manr1*

A. Experiment Summary

Quantitative trait locus mapping implicated a broad region of distal chromosome 1 (80-110 cM) harboring a gene influencing antinociception produced by analgesic drugs acting at α_2-adrenergic (clonidine), μ-opioid (morphine), and CB-1 cannabinoid (WIN55,212-2) receptors. Two strategies were used to reduce the confidence interval, in order to facilitate the identification of the gene responsible for variability in analgesic potency. We first employed *in silico* mapping to correlate the normalized analgesic response patterns of 8 inbred strains with an archival database representing the genetic architecture of the strains. This analysis confirmed the role of the Chr. 1 locus in analgesia produced by clonidine, morphine, WIN55,212-2, and the κ-opioid agonist U50,488; additionally, it refined the probable location of the locus to the interval 170-180 Mb. We also began the process of cloning the quantitative trait gene by position by exploiting the congenic region created concomitantly with knockout mouse construction. *Fcgr3* null mice, which have 129-derived genetic material at the QTL region on a C57BL/6 background, exhibited attenuated analgesic response to clonidine and WIN55,212-2 (but not morphine) compared with wild-type mice. These results indicate that we have captured the relevant gene in the congenic interval, and have placed the gene within a 5 Mb region (170-175 Mb).

B. Introduction

Traditional analgesics such as opioids have been used to effectively minimize pain and discomfort for centuries. However, the side effect profile of opioid drugs is often detrimental to successful pain management, as the doses needed to provide relief may be accompanied by intolerable complications such as nausea, constipation, sedation, and respiratory depression, as well as a liability to addiction. Wide interindividual variability has been frequently noted in the potency of morphine and similar drugs, in both clinical (Lasagna and Beecher, 1954; Levine et al., 1981; Maier et al., 2002) and experimental (Wolff et al., 1965; Chapman et al., 1990) contexts. Although much of the variability is produced by environmental (e.g. cultural, sociological, or psychological) factors, evidence is accumulating for a genetic component of analgesic variability (reviewed in Lotsch and Geisslinger, 2006). Polymorphisms of the *OPRM1* (Caraco et al., 2001; Klepstad et al., 2004) and *COMT* (Rakvag et al., 2005) genes have been associated with magnitude of analgesia, and people with non-functional *CYP2D6* alleles are unable to convert codeine into its active metabolite, morphine (Sindrup and Brosen, 1995). Quantitative trait locus mapping has linked genes with a number of analgesic phenotypes: *Mc1r*, which encodes the melanocortin-1 receptor, is involved in determining stress-induced and κ-opioid analgesia (Mogil et al., 2003), and the serotonin receptor gene *Htr1b* has been implicated in morphine sensitivity (Hain et al., 1999). With recent advances in gene mapping and expression profiling producing a revolution in pharmacogenomics (Fagerlund and Braaten, 2001), it is likely that many other genes exerting smaller effects on analgesia will be uncovered. Characterizing the sources of variability in analgesic response is a promising avenue for optimizing pain control, in the form of personalized pharmacotherapy tailored to each individual's genetic propensities.

A number of compounds acting at non-μ-opioid receptor sites have been identified as clinically useful analgesics, either as adjuvants to complement lower doses of opioids, or as alternatives to such drugs. Many of these drugs bind to receptors belonging to the same super-family of G protein-coupled receptors as opioid receptors, including adrenergic, cannabinoid, cholinergic, and GABA-B receptors, and these receptors are located in many of the same CNS sites where opioids are thought to act. The extent to which the genetic factors underlying analgesia produced by disparate classes of drugs remains an unresolved question, however. We performed strain surveys of five such drugs, using mice of 12 different inbred lines, to determine whether analgesic sensitivity to one drug would predict responses to other drugs (Wilson et al., 2003). Moderate to high genetic correlations were observed between morphine (μ-opioid), U50,488 (κ-opioid), clonidine (α_2-adrenergic), epibatidine (nicotinic cholinergic), and WIN55,212-2 (cannabinoid), suggesting that these drugs do in fact share genetic mediation.

Quantitative trait locus (QTL) mapping was subsequently employed to localize the variability genes affecting analgesic magnitude across drug types, as described in the previous section of this work. In three simultaneous mapping projects, clonidine, morphine, and WIN55,212-2 were administered to an F2 population derived from a B6x129P3 intercross, and the resultant inhibition of thermal pain was quantified using the 49° tail-withdrawal test. We used the interval mapping method to correlate phenotypic responses with genotypes at 100 microsatellite markers distributed across all 19 autosomes and the X chromosome. A locus on distal chromosome 1 (80-110 cM), dubbed *Manr1* for "multiple analgesic response 1," was linked to analgesic magnitude in all three drug conditions, supporting our hypothesis that common genes will be found that

affect analgesia regardless of the triggering receptor type. This region contains a number of interesting potential candidate genes, but the size of the confidence interval precludes a systematic evaluation of the hundreds of known or predicted genes contained within it.

We have used two separate strategies to confirm and improve the resolution of our mapping results. The first, known as *in silico* or haplotype mapping, was used to correlate the original strain survey data with a database of thousands of single nucleotide polymorphisms (SNPs), providing a much more refined placement of our variability gene. The second involved the creation of *congenic* mouse lines, in which the QTL region from one strain is placed onto the genetic background of a phenotypically divergent strain. This strategy isolates the QTL from interaction effects, and the congenic line can be further backcrossed to the background strain to narrow the confidence interval to a few Mb.

C. Methods

C.1. *In Silico* Mapping Methods

The procedures used to house and phenotype mice included in the strain surveys have been described previously (Wilson et al., 2003). They are briefly described here.

C.1.1. Subjects

Mice of both sexes of the following 12 inbred strains—129P3, A, AKR, BALB/c, C3H/He, C57BL/6, C57BL/10, C58, CBA, DBA/2, RIIIS and SM (all "J" substrains)—were obtained from The Jackson Laboratory (Bar Harbor, ME). Mice were housed in a temperature-controlled (22±2°C) vivarium at the University of Illinois--Champaign-Urbana on a 12:12 h light/dark cycle. Mice were weaned at 18-21 days of age, housed

with same-sex littermates in groups of 2-5 and given ad lib access to food (Harlan Teklad 8604) and tap water. Mice (n = 6-30/strain/drug/dose) were tested at not less than 6 weeks of age, for a single drug and dose. An approximately equal number of male and female mice were tested in each condition.

C.1.2. Drugs

All drugs except for the cannabinoid were dissolved in physiological saline and administered in the following doses: the selective α_2-adrenergic receptor agonist, clonidine (Sigma, St. Louis, MO), 0.1-5 mg/kg; the nicotinic acetylcholine receptor agonist, (±)-epibatidine dihydrochloride (Sigma), 7.5-150 μg/kg; the μ-opioid receptor agonist, morphine sulfate (National Institute for Drug Abuse, Rockville, MD), 5-200 mg/kg; and the selective κ-opioid receptor agonist, (±)-trans-U50,488 methanesulfonate (Tocris Inc., Ballwin, MO), 10-150 mg/kg. The high affinity cannabinoid CB-1 receptor agonist, R(+)-WIN 55,212-2 mesylate (Tocris), was dissolved in a 50% propylene glycol/saline solution and diluted to the desired concentration with saline; doses ranged from 0.5-480 mg/kg. The vehicle alone has no antinociceptive effects (data not shown). All drugs were administered intraperitoneally (i.p.) in a volume of 10 ml/kg. Full dose response curves were generated by assaying maximum percent antinociception (see below), relative to baseline sensitivity, at a minimum of three doses. Successively higher and lower doses were tested in each strain until the following criteria were fulfilled: a) data from at least 3 doses per strain were obtained; b) the lowest dose yielded maximum percent antinociception of ≤35%; and, c) the highest dose yielded maximum percent antinociception of ≥65%.

C.1.3. Analgesia Phenotyping

The 49°C tail-withdrawal/immersion (TW) test, originally described by Ben-Bassat (1959) and modified by Janssen (1963), was used to measure reflexive responses to thermal nociception. During testing, mice were gently restrained in a cardboard-bottomed cloth holder and the distal half of the tail was immersed in water maintained at 49±0.2°C by a thermal circulator. The latency to a reflexive withdrawal response was measured to the nearest 0.1 s by an experienced observer. For increased accuracy, two latency determinations separated by at least 10 s were made and averaged together at each time point. A 15 s cut-off was imposed to prevent any possible tissue damage and to decrease the possibility of repeated-measures effects. Nociceptive testing in all strains occurred immediately prior to, and 15, 30 and 60 min post-injection for all drugs except for the shorter-acting epibatidine, which occurred immediately prior to and 10, 20 and 30 min post-injection.

Percent antinociception (i.e., percentage of the maximum possible effect) at each time point was calculated for individual mice as: [(post-drug latency – baseline latency)/(cut-off latency – baseline latency)] x 100. The maximal percent antinociception at any time point was used as the dependent measure of drug response. Dose-response curves--comprised of 3-4 doses of each drug within the linear portion of the dose-response relationship for each strain--were used to calculate half-maximal antinociceptive doses (AD50s) (Tallarida and Murray, 1981). The AD50 values across the 12 inbred strains were then transformed to Z-scores for purposes of comparison across drugs, and for *in silico* genetic analysis (Table 4). A composite analgesia Z-score was computed as the arithmetic mean of the five drug scores for each strain.

C.1.4. *In silico* Genetic Mapping

Although 12 strains of mice were characterized in the strain survey (Wilson et al., 2003), the genotyping database includes SNP data for only 6 of those strains (A, AKR, C57BL/6, BALB/c, C3H/He, DBA/2), as well as the 129S1/SvImJ strain, which is closely related to the 129P3/J we phenotyped; therefore, only these 7 strains were considered. The computational genetic analysis of the inbred strain data was performed as previously described (Grupe et al., 2001). In brief, allelic data from the inbred strains was analyzed and a gross haplotype map of the mouse genome was constructed by organizing SNP blocks into 10 Mb segments. The haplotype-based analysis identifies segments in which the haplotypic strain grouping within the block correlates with the distribution of phenotypic data among the inbred strains analyzed. The degree of correlation for each segment is reported as the number of standard deviations from the mean correlation across the entire genome. The haplotype database on which this analysis is based is available at http://mouseSNP.roche.com.

C.2. Knockout/Congenic Mapping Methods

C.2.1. Subjects

Breeder pairs of the B6.129P2-*Fcgr3*^{tm1Sjv}/J (*Fcgr3* KO) mutant strain were obtained from The Jackson Laboratory (Bar Harbor, ME). These mice have an engineered (via homologous recombination) deletion of the *Fcgr3* (92.3 cM) locus; they were produced by introducing the deactivated gene into embryonic stem cells of the 129P2 strain and injecting them into C57BL/6 blastocysts (see Hazenbos, 1996 for details). Homozygous Fcgr3KO and backcrossed B6xFcgr3KO progeny were maintained in our temperature- and humidity-controlled vivarium and given *ad lib* access to tap water

and mouse chow (Harlan Teklad 8604). The approximate extent of the 129 congenic interval was determined by genotyping microsatellite markers throughout Chr. 1 (Fig. 9). Markers at 73 cM (D1Mit102) and 97 cM (*Kmo*) were determined to be 129-derived, whereas flanking markers at 67 cM (D1Mit495) and 107 cM (D1Mit292) were from the background C57BL/6 strain.

We obtained two subcongenic lines derived from the *Fcgr3* KO strain from the Wadsworth Institute (Troy, NY). These lines are the product of backcrossing the KO strain with C57BL/6, and selecting for progeny containing recombination events with the congenic interval. The first subcongenic line, *Fcgr3*-RF1, contains 129-derived DNA between *Rgl1* (152.5 Mb) and *Cdca1* (169.4 Mb), and the second line, *Fcgr3*-RF3, has donor genome between *Mpz* (171.0 Mb) and ~190 Mb (V. Bolivar, personal communication).

C.2.2. Analgesia Phenotyping

Clonidine hydrochloride (Tocris, Ellisville, MO), morphine sulfate (National Institute for Drug Abuse, Rockville, MD), and WIN55,212-2 (Tocris) were dissolved in saline and administered intraperitoneally in three concentrations per drug. All mice (n= 6-17/strain/drug/dose) were between 6-12 weeks of age and drug-naïve at testing.

Both male and female mice were phenotyped using the 49° tail-withdrawal assay (Janssen et al., 1963). The tail of each mouse was lowered into a hot water bath maintained at 49.0°C, and the time for it to withdraw its tail was measured with a stopwatch; 15 seconds was used as a cutoff latency in order to avoid damage to the tail. Readings were taken at baseline (pre-injection) and at 15, 30, and 60 minutes post-

injection of the drug. At each time point, two latencies were measured and then averaged to increase accuracy. We computed the percent analgesia (i.e., area under the time-course curve) by the trapezoidal rule, as a measure of analgesic effect, and used this statistic to infer the AD50 (i.e., the dose providing 50% analgesic relief), where possible (Tallarida and Murray, 1981).

D. Results

D.1. *In silico* Mapping

The Digital Disease (Roche, Palo Alto, CA) algorithm was first used to correlate the analgesia Z-scores with an inbred strain genotype database (Grupe et al., 2001). This database arbitrarily breaks the genome into a low-resolution map of 10 Mb segments, rather than empirically validated haplotypes, to enable rapid QTL mapping. For each trait, the Z-score distribution is compared to the genotypic status of the strains at each 10 Mb block, and a correlation is calculated. The mean correlation across all blocks is computed, and the significance of a given correlation is reported as the number of standard deviations (sd) away from this mean.

The first analysis was performed on the composite analgesia measure, comprised of the average value across all five analgesics for each strain, in order to detect complementary response patterns indicative of a "master analgesia gene." In this analysis (Fig. 7), 10% of the blocks exhibited correlation with the phenotype greater than 0.5 sd from the average correlation, and only 13 blocks were more than 1 sd above it. The largest correlation, at 9.5 sd from the mean, was located on Chr. 1 between 170 and 180 Mb. Other prominent loci were found at proximal Chr. 5 (0-10 Mb), proximal Chr. 7 (20-30 Mb), mid Chr. 11 (80-90 Mb), and distal Chr. 19 (40-50 Mb).

The Chr. 1 locus was common to four of the five analgesics when analyzed separately (Fig. 8a-e). It was the strongest linkage in the clonidine (8.4 sd), morphine (7.6 sd), and U50, 488 (7.4 sd) groups, and was the second strongest correlation in the WIN55,212-2 group (1.5 sd). It did not appear to be linked to epibatidine analgesia. The strong correlation in the 0-10 Mb block of Chr. 5 in the composite analgesia analysis was driven by large correlations to this segment in the epibatidine (13.1 sd) and WIN55,212-2 (14.7 sd) groups. Other prominent linkages were found for the clonidine group (Fig. 8a) on Chr. 1 (130-140 Mb), Chr. 11 (80-90 Mb), and Chr. 19 (40-50 Mb); for epibatidine (Fig. 8b) on Chr. 17 (30-40 Mb); for morphine (Fig. 8c) on Chr. 1 (130-140 Mb) and Chr. 11 (80-90 Mb); and for U50,488 (Fig. 8d) on Chr. 11 (80-90 Mb) and Chr. 19 (40-50 Mb).

D.2. *Fcgr3* Knockout/Congenics

The knockout/congenic strain, in which the "insensitive" 129-derived allele of the *Manr1* QTL has been introgressed onto the C57BL/6 background, was compared with wild-type mice that are fully B6 (i.e., "sensitive") in the QTL interval. The construction of dose-response curves for both strains revealed a significant interaction ($p = 0.05$) between strain and dose in clonidine analgesia (Fig. 10a). Neither strain showed appreciable response at the lowest dose of 3 mg/kg, but higher doses produced attendant increases in analgesia in wild-type mice only ($AD50_{wt} = 4.8$ mg/kg, C.I. = 2.5-9.4; $AD50_{ko}$ = not calculable). WIN55,212-2 (Fig. 10c) also produced analgesia of differing magnitude between strains (genotype main effect $p<0.001$); however, response to this drug did not exhibit dose dependency in either strain (dose main effect $p = 0.67$). Analgesia from the cannabinoid was blunted in both groups, rendering AD50 estimations

meaningless. In contrast, morphine (Fig. 10b) produced equivalent levels of antinociception in both strains at all doses tested (genotype main effect $p = 0.09$). The AD50 for the wild-type strain was 14.4 mg/kg (C.I.=12.1-17.1), and for the congenic, 17.6 mg/kg (C.I.=15.0-20.5); the difference in potency was a non-significant factor of 0.8 (C.I.=0.6-1.0).

We investigated the mode of inheritance of the QTL allele by crossing the *Fcrg3* congenic with wild-type B6, and measuring the sensitivity of the heterozygous progeny to 20 mg/kg clonidine. In a Tukey post-hoc comparison with the two parental strains, the heterozygotes were significantly different from the B6 strain ($p = 0.003$) but not the congenic strain ($p = 0.82$), suggesting that the insensitive 129 allele is dominant (Fig.11a).

We then compared two subcongenic strains derived from the *Fcgr3*KO congenic strain, RF1 and RF3, with wild-type and knockout-congenic mice (Fig. 11b). A main effect between genotypes was detected by ANOVA ($F_{3, 49}=3.083$, $p = 0.016$); Tukey post-hoc tests revealed that only the *Fcgr3*KO mice were significantly different from C57BL/6 ($p = 0.010$).

E. Discussion

Previous quantitative trait locus mapping efforts suggested that a gene influencing analgesic magnitude, regardless of the drug used to produce it, is located on distal Chr. 1. Two limitations of this finding were apparent, however, and needed to be addressed with further investigation. The localization of the QTL was imprecise, as the confidence interval containing the gene was conservatively mapped to a 30 cM region (80-110 cM). Identifying the gene by position alone would require tremendous refinement of this

interval. The other limitation of the QTL was its specificity; the linkage, while strong for the drugs clonidine and the cannabinoid WIN55,212-2, was tenuous for morphine. It was also questionable whether the QTL represented a hypothetical "master analgesia gene" responsible for the differential sensitivities to five analgesics we observed in a survey of 12 inbred strains. We therefore employed two complementary strategies to narrow our QTL confidence interval and extend our conclusions to the full panel of strains and analgesic drugs.

We first correlated the phenotypic data from seven of the twelve strains in our original strain survey (Wilson et al., 2003) with a database of single nucleotide polymorphisms (SNPs). This analysis confirmed that analgesia sensitivity patterns across numerous strains could be predicted by their allelic status at an unidentified gene located between 170 and 180 Mb on Chr. 1. This interval (roughly 90-100 cM) corresponds to the center third of our QTL confidence region, significantly narrowing the region of interest and reducing the number of potential candidate genes by half (see Table 5 for a full list of the 112 genes in this interval). We also confirmed that the *Manr1* locus is relevant to analgesia produced by opioid (morphine and U50,488) and non-opioid (clonidine and WIN55,212-2) analgesics, although it was not linked to sensitivity to the nicotinic cholinergic agonist, epibatidine.

In addition to the *Manr1* QTL, morphine and U50,488 analgesia have also been previously subjected to QTL analysis. An extensive investigation of morphine analgesic variability between DBA/2 and C57BL/6 mice revealed five major loci (Bergeson et al., 2001). The QTL with the largest effect was located on proximal Chr. 10 and is likely *Oprm1*, which encodes the μ-opioid receptor, the high-affinity binding site for morphine. Other loci were detected on proximal and medial Chr. 9 and proximal Chr. 1. Of these

five experimentally verified QTLs, only two loci on Chr. 9 colocalize with regions identified by the *in silico* analysis. A region of distal Chr. 8 was linked to U50,488 analgesia (as well as swim stress-induced analgesia) and was subsequently shown to be the melanocortin-1 receptor gene, *Mc1r* (Mogil et al., 2003). No corresponding linkage to this region was observed in the *in silico* analysis of U50,488 analgesia. One probable reason for the apparent discrepancies between QTL and haplotype mapping is the sex-specific nature of the Chr. 1, proximal Chr. 9, and Chr. 8 loci (Bergeson et al., 2001; Mogil et al., 2003), as the haplotype mapping did not account for sex differences. However, the inability of the *in silico* analysis to detect the Chr. 10 locus is not as readily explained.

In principle, the *in silico* mapping technique holds several advantages over standard QTL mapping methods (Grupe et al., 2001; Wang et al., 2005b), and it has the potential to minimize the expense and time needed to identify variability genes. The practical advantages of haplotype mapping arise from most of the work already having been done; once an inbred strain has been genetically characterized, there is no need to bear the cost of genotyping it again. Likewise, strain surveys are merely the beginning phase of phenotyping in linkage studies, whereas they are the endpoint for *in silico* mapping. Haplotype-based mapping methods derive their power from the entire breeding history of the common inbred strains (Wade et al., 2002), alleviating the need to generate novel recombination events in complicated crosses. The use of a dense SNP database affords resolution on the scale of a single gene. These advantages will become even more significant as more comprehensive haplotype maps featuring added inbred strains are developed, and future strain surveys should be designed to exploit these methods (Wang et al., 2005b). The Digital Disease algorithm presently employed boasts many of these

benefits, but because the genotypic data is grouped into arbitrary 10 Mb segments, its power to exploit the underlying haplotype architecture is compromised.

In addition to the Digital Disease analysis, we also attempted to correlate our phenotypic data with a true haplotype map using the HapMapper (Roche, Palo Alto, CA) algorithm. Numerous genes within our QTL region exhibited linkage (at a liberal $p < 0.02$) with one or more analgesic measures (results are reported in Table 6). However, we do not believe that our study design is appropriate for taking advantage of the potential of dense haplotype mapping. Our current efforts suffer from a lack of power related to the employment of only seven strains in our study. A power analysis conducted by Wang and Peltz (2005) suggested that even for twice the number of strains we used, a similar study would have only 80% power to detect a locus accounting for half the total phenotypic variance at $\alpha = 0.01$. In fact, Darvasi (2001) has estimated that a minimum of 40 strains may be needed to reliably map even the most amenable loci. A cursory analysis of the haplotype structure of the QTL region reveals a disconcerting situation: the most phenotypically divergent strain, C57BL/6, is also the most genotypically distinct, and spurious associations may be common for traits in which B6 is a clear extreme-responding strain. In fact, many of the linkages of haplotype blocks with the analgesia phenotypes result from all strains but C57BL/6 bearing one haplotype, and B6 bearing another. For this reason, we believe the more conservative course is to treat the *in silico* mapping exercise as a confirmation and gross refinement of our previously mapped *Manr1* locus. Any other conclusions that may be drawn from this analysis cannot be distinguished from chance results.

In a separate line of experiments, we used a congenic strain strategy to place the "insensitive" QTL allele from the 129 strain onto a C57BL/6 background. Rather than

undertake the arduous process of backcrossing over multiple generations, we took advantage of the standard transgenic knockout construction protocol, in which a *de facto* 129P2 congenic genotype is maintained around the deleted locus on a C57BL/6 background (Bolivar et al., 2001). Although the 129P2 strain differs somewhat from the 129P3 strain used to discover the *Manr1* QTL, the phenotype was largely preserved, indicating that the 129 strains share the "insensitive" allele. Positional cloning efforts involving 129P2 knockout-related congenic strains should prove as successful, and vastly more expedient, than if we had created a novel 129P3 congenic using marker-assisted selection.

The effect of placing the "insensitive" 129 *Manr1* allele onto the otherwise resistant C57BL/6 background proved to be an almost complete attenuation of analgesic potency in clonidine- and cannabinoid-treated animals. Surprisingly, however, morphine analgesic potency was not significantly reduced in the congenic strain. The reason for this is unclear, but this result does not necessarily negate the convergent evidence of QTL and *in silico* linkage to this phenotype. One possible explanation for the disappearance of the QTL effect is genetic; other unidentified loci may interact epistatically with the Chr. 1 locus, producing differential effects in contrasting genetic backgrounds (Frankel and Schork, 1996). The observance of synergistic and additive interactions between opioid, cannabinoid, and adrenergic mechanisms (Stone and Wilcox, 2004; Tham et al., 2005) suggests that such mechanisms are both common between, and independent of, each other. Morphine is known to act at numerous spinal and supraspinal sites (Yaksh et al., 1988), and epistatic interactions modulating a subset of μ-opioid activity may mask other effects of morphine subject to the QTL. However, until the gene responsible for the QTL

is determined, it is difficult to do more than conjecture as to the nature of such interactions.

The RF1/RF3 subcongenic results are also difficult to interpret, as neither subcongenic was shown to be significantly different from the B6 mice, and therefore to harbor the "insensitive" allele. This unfortunately prevents the use of these strains in the creation of additional subcongenic lines to further isolate the QTL. Failure to replicate the QTL effect in either line may be due to the quantitative trait gene being located between the two non-overlapping subcongenic regions, or it may be due to epistatic factors from isolating the QTL. However, as the two subcongenic strains both appear intermediate between the B6 and *Fcgr3* KO animals, the underlying architecture of the QTL may be more complicated than a single gene. Careful dissection of QTLs for epilepsy (Legare et al., 2000), lupus susceptibility (Morel et al., 2001), exploratory behavior (Yalcin et al., 2004; Zhang et al., 2005), and collagen-induced arthritis (Karlsson et al., 2005) has shown that a single major effect locus frequently separates into numerous small-effect loci. If *Manr1* is an example of such a case, both the RF1 (152-170 Mb) and RF3 (170-190 Mb) intervals could contain one or more genes relevant to analgesia.

As the knockout/congenic strain differs from the wild-type B6 animals, it is necessary to determine whether the deletion of the *Fcgr3* gene is responsible for the phenotype, rather than the 129 segment flanking it. Bolivar et al. (2001) devised a simple breeding program to isolate the effects of the gene knockout from its background; however, we would need numerous additional generations to see the protocol to completion, and the subcongenic results suggest that the QTL effect is not likely to be observable in such an experiment. The *Fcgr3* gene is a particularly unlikely, but still

formally possible, candidate for the *Manr1* locus. This gene encodes an Fc immunoglobulin G receptor, necessary for antigen-directed NK cell and macrophage activity, and null mutants have impaired immune responses (Hazenbos et al., 1996). Although no studies have linked the protein with acute pain or analgesia, it is known to play a role in immune complex-induced arthritis (Nabbe et al., 2005; Skokowa et al., 2005). It is one of the genes possibly linked to the composite analgesia phenotype in the HapMapper analysis (Table 6).

Taken together, our efforts to narrow the *Manr1* confidence region have succeeded in placing the responsible gene (or genes) between 170 Mb and an undelineated crossover distal to the *Kmo* gene at 175.5 Mb. We have confirmed that the *Manr1* gene plays a role in analgesia produced by α_2-adrenergic and cannabinoid mechanisms, and provided evidence that this gene is also likely involved in response to μ- and κ-opioid drugs; however, our results do not support linkage with epibatidine analgesia. Despite the significant refinement of the confidence interval, about 100 genes remain positional candidates. However, of these, only a few appear to be reasonable functional candidates controlling neuronal activity: the potassium channel subunits, *Kcnj9* and *Kcnj10*; two sodium-potassium pump subunits, *Atp1a2* and *Atp1a4*; the G protein regulators, *Rgs4* and *Rgs7*; and the myelin protein, *Mpz*.

An evaluation of the relevant positional, functional, and expression evidence strongly predicts that *Kcnj9* is the most likely candidate gene to determine sensitivity to multiple analgesic modalities. At 94.2 cM, it lies within 6 cM of the peak linkage of all three analgesics. The gene codes for the GIRK3 (Kir3.3) protein, a member of a family of inwardly-rectifying potassium channel subunits, of which GIRK3 is the most abundantly and ubiquitously expressed in the brain. Members of this family (GIRK1-4)

form heterotetramers important for maintaining resting membrane potential in CNS and cardiac cells; these channels are activated following ligand binding of G protein-coupled receptors (GPCRs). Thermal pain sensitivity and at least some effects of morphine are mediated by GIRK3 (Marker et al., 2002; Torrecilla et al., 2002), and GIRK channels have been implicated in analgesic response from a full range of GPCR-binding drugs (Blednov et al., 2003; Mitrovic et al., 2003). The *Kcnj9* gene is expressed in whole-brain tissue at a rate three times higher in 129SvEv than C57BL/6 mice (Sandberg et al., 2000).

In parallel with our positional cloning endeavors, we have conducted experiments to determine whether *Kcnj9* is in fact the gene underlying the *Manr1* locus. We evaluated the candidacy of *Kcnj9* using quantitative gene expression assays and null mutant mice. These studies are described in the next section of this work.

CHAPTER 4: EVALUATION OF *Kcnj9* AS A CANDIDATE GENE UNDERLYING *Manr1*

A. Experiment Summary

A quantitative trait locus common to several opioid and non-opioid analgesia phenotypes was discovered on distal Chr. 1, and subsequently fine mapped to a <10 cM interval. This region contained few obvious candidate genes known to play a role in the neurochemical mediation of pain/antinociception; among these, the most likely gene was *Kcnj9*, which encodes the inwardly-rectifying potassium channel subunit GIRK3. We evaluated the candidacy of this gene by quantifying the effects of variant alleles of this gene on expression levels, as well as by determining the effects of ablation of the gene on behavioral response to analgesic drugs. Mice of the C57BL/6 and 129P3 strains (containing the analgesia-sensitive and –resistant alleles, respectively, of the QTL) were used to determine *Kcnj9* expression in three CNS areas known to be relevant to descending modulatory analgesia: periaqueductal gray (PAG), rostral ventral medulla (RVM), and spinal cord. Differential patterns of expression were observed between the two strains in the PAG, suggesting a possible mechanism for the observed strain difference. We then assayed mice with null mutations of the *Kcnj9* genes for sensitivity to clonidine, morphine, and WIN55,212-2. The mutant mice displayed significantly attenuated analgesia from clonidine and morphine, relative to their wild-type counterparts. These lines of convergent evidence support the involvement of *Kcnj9* in analgesia produced by multiple neurochemical analgesic classes.

B. Introduction

Rapid advances in the tools and understanding of genetics have initiated a revolutionary shift in medicine towards individualized treatment based on the specific genetic liabilities of the patient. The "pharmacogenetic" approach has begun to be applied to the relief of post-operative and chronic pain. The pharmacogenetics of analgesia (reviewed in Flores and Mogil, 2001) holds promise for the significant minority of patients for which current treatments are ineffective, but the number of genes currently known to influence analgesic variability in humans remains small. Up to 10% of Caucasians are non-responsive to codeine because of a mutation in the cytochrome P450 enzyme CYP2D6, rendering them unable to metabolize the drug to morphine (Sindrup and Brosen, 1995). Analgesia from κ-opioid agonists (such as pentazocine) is modulated by the melanocortin-1 receptor (*MC1R*) in a sex-specific manner, as indicated by the greater analgesia produced by these drugs in red-headed women with non-functional MC1Rs (Mogil et al., 2003). Variant alleles of the μ-opioid receptor (*OPRM1*) have been associated with increased analgesia requirement (Caraco et al., 2001; Klepstad et al., 2004; Romberg et al., 2005), although it is unclear whether this is due to insensitivity to opiate drugs or to an increase in the underlying pain.

Researchers have turned to murine genetics to help unravel the many genetic and environmental determinants of analgesic response. Mouse models have proven invaluable in exploring the effects of genetic mutation on nociceptive phenotypes (reviewed in Mogil and Grisel, 1998; Mogil et al., 2000; Malmberg and Zeitz, 2004), and have also been instrumental in resolving the sources of natural individual variability in pain and analgesia. The use of such techniques as quantitative trait locus (QTL) and *in silico* mapping in studies of analgesia has been limited to investigations of the opioids

morphine (Bergeson et al., 2001; Liang et al., 2006a) and U50,488 (Mogil et al., 2003). In an effort to extend these findings to non-opioid drugs, and address the previous finding of genetic correlation between analgesics acting at different receptor sites (Wilson et al., 2003), we performed mapping studies using five drugs: the μ-opioid morphine, the κ-opioid U50,488, the α_2-adrenergic clonidine, the cannabinoid WIN55,212-2, and the nicotinic cholinergic epibatidine. We observed strong evidence for the existence of a gene on distal chromosome 1 (near 95 cM) modulating analgesia produced by clonidine and WIN55,212-2, and likely the μ- and κ-opioid agonists as well.

Efforts to clone this gene by position are underway using a congenic strategy, but a survey of possible candidates genes within the *Manr1* QTL confidence interval suggested a small number of interesting candidates worthy of follow-up investigation. Our criteria for selecting appropriate candidates included position, CNS expression, and functional relevance to multimodal analgesia. It is unlikely that the gene underlying *Manr1* encodes a receptor, as the drugs all have distinct binding sites. However, all of the analgesics bind to members of the superfamily of G protein-coupled receptors (GPCRs), suggesting that the quantitative trait gene (QTG) may play a role in neurochemical signaling mechanisms common to all of them. The analgesics all modulate the PAG-RVM-dorsal horn pathway, and the QTG may exert its influence anywhere in this descending inhibitory system.

Although several genes with relevance to G protein signaling or neuronal excitation are found within the QTL region, we believe that the *Kcnj9* gene (which encodes the GIRK3 protein) is the most likely candidate for the *Manr1* QTL. Located at 94.2 cM, it is found very near the peak of linkage for all of the analgesia phenotypes tested. It belongs to the GIRK family of inwardly-rectifying, G protein-coupled

potassium channel subunits vital to the regulation of membrane potential (Yamada et al., 1998; Wickman et al., 2002), and its homolog is the GIRK subunit most prevalent in human (Schoots et al., 1999) and rodent (Kobayashi et al., 1995; Chen et al., 1997; Karschin and Karschin, 1997) brain. In the mouse, differential *Kcnj9* expression in whole brain tissue between 129 and B6 strains has been established (Sandberg et al., 2000). GIRK channels are known to significantly influence analgesic potency for a wide range of modalities (Ikeda et al., 2002; Blednov et al., 2003; Mitrovic et al., 2003; Marker et al., 2004), and GIRK3 in particular mediates the inhibitory effects of opioids (Marker et al., 2002; Torrecilla et al., 2002).

In order to evaluate the putative contribution of variants of GIRK3 to observed strain differences in analgesic phenotypes, we tested mice homozygous for the deletion of *Kcnj9* for analgesia from clonidine, morphine, and WIN55,212-2. We have also conducted gene expression assays in C57BL/6 and 129P3 strains in areas relevant to nociceptive modulation: spinal cord, rostral ventral medulla, periaqueductal gray, and the anterior cingulate cortex. The purpose of these experiments is to establish whether *Kcnj9* gene knockout has an effect on the inhibition of acute thermal pain by multiple analgesics, and determine where quantitative differences in GIRK3 expression may play a role in interindividual variability.

C. Methods

C.1. Gene expression quantification

C.1.1. Tissue collection

Brain tissue from the periaqueductal gray (PAG) and rostral ventral medulla (RVM), and whole spinal cords were removed from 129P3 and C57BL/6 mice aged from at least six weeks. The harvested tissues were immediately placed in a preservation agent, RNAlater (Ambion, Austin, TX), and stored at 4°C until total RNA isolation. To obtain a sufficient quantity of tissue samples, approximately four mice from each strain were used for each tissue type.

C.1.2. Total RNA isolation and cDNA transcription

Total RNA from the six samples (PAG, RVM, and spinal cord from 129P3 and C57BL/6 mice) was isolated with Trizol (Invitrogen, Burlington, ON) and resuspended in 30 μL of DEPC treated water. The RNA solution was then treated with the DNA-*free* kit (Ambion, Austin, TX) to remove any trace DNA contaminants and purified with the RNeasy Mini kit for RNA cleanup (Qiagen, Germantown, MD). Integrity and concentration of the total RNA samples were evaluated on the Bioanalyzer 2100 (Agilent, Palo Alto, CA). The reverse transcription (RT) reaction was performed according to the protocol of the TaqMan Reverse Transcription Reagents kit (Applied Biosystems, Foster City, CA). In addition to the unknown samples, serial dilutions of known concentrations of mouse brain total RNA (Ambion) acting as standards were reverse transcribed. Briefly, each RT reaction required 1 μL of the total RNA to be added to 9 μL of RT master mix composed of 0.5 μL of 50 μM random hexamers and 0.25 μL of 50U/μL

Multiscribe RT enzyme. Reverse transcription was carried out on a Peltier Thermal Cycler (PTC-100; Bio-Rad, Hercules, CA) at the following cycles: 25°C for 10 min, 48°C for 30 min followed by 95°C for 5 min. The cDNA was stored at 4°C until the PCR reaction was made.

C.1.3. PCR

Two gene-specific TaqMan probe and primer sets for *Kcnj9* and *Gapdh* mouse genes were obtained from ABI. The target gene *Kcnj9* was amplified in different wells of a 96-well reaction plate with the endogenous control gene, *Gapdh*, whose constitutive expression served to normalize quantification of *Kcnj9* expression levels among unknown samples. Each 5 μL cDNA sample of standards and unknowns was added to 20 μL of *Kcnj9* PCR master mix and 20 μL of *Gapdh* PCR master mix. The *Kcnj9* PCR master mix composition was: 12.5 μL of 2X TaqMan Universal PCR Mix with AmpErase UNG, 6.25 μL of DEPC water, and 1.25 μL of 20X *Kcnj9* gene specific probe and primers mix. The *Gapdh* master mix composition was: 12.5 μL of 2X TaqMan Universal PCR Mix with AmpErase UNG, 6.00 μL of DEPC water, and 0.5 μL of 20X *Gapdh* gene specific probe and primers. Standards were run in quadruplicate and unknowns in quintuplicate. Real-time PCR was carried out on an ABI 7000 system at the following cycles: 50°C for 2 min, 95°C for 10 min followed by a round of 40 cycles of 95°C for 15 sec/60°C for 60 sec.

C.1.4. Data analysis

After the PCR reaction was completed, a threshold was fixed across the linear region of all amplification curves. Determining the cycle numbers associated with this

threshold revealed the C_T values for the known standards and unknown samples. C_T values of the unknown samples were then converted into expression values using the corresponding standard curve. The ratio of the average *Kcnj9* amount over the average *Gapdh* amount provided the normalized *Kcnj9* gene expression result.

C.2. GIRK3 knockout animals

C.2.1. Subjects

The use of animals for this study was approved by the University of Minnesota Institutional Animal Care and Use Committee (Protocol 0302A41421). Mice were housed in a temperature-controlled room on a 12 h light/dark cycle, with food and water available *ad libitum*. Efforts were made to minimize the pain and discomfort of the animals throughout the course of this study. The generation of GIRK3 knockout mice was described previously (Torrecilla et al., 2002). The GIRK null mutations were backcrossed through at least 13 rounds against the C57BL/6 mouse strain prior to initiating behavioral testing. Genotypes were determined by PCR of crude DNA samples from tail biopsies (Wickman et al., 1998). Efforts were made to balance the wild-type and knockout groups for each drug condition with respect to gender and age. Drug naïve mice were used for all tests. The experimenter was blind to subject genotype and drug condition during behavioral testing.

C.2.2. Phenotyping

2-(2,6-Dichloroaniline)-2-imidazoline (clonidine), morphine sulfate, and WIN 55,212-2 were purchased from Sigma Chemicals (St. Louis, MO). All drugs were dissolved in 0.9% saline in high concentration stocks, divided into single-use aliquots,

and stored at -20°C. The highest doses of each drug administered were chosen on the basis of pilot studies, where the intent was to identify the drug dose that produced the maximum analgesic effect without causing significant toxicity or motor impairment.

Thermal nociception was assessed using the warm-water-immersion variant of the tail-flick assay on mice 6-7 weeks of age. Mice were acclimated to the testing environment for ≥1 h on the day of testing. During tail-flick testing, mice were secured firmly with the full tail exposed using a soft cloth. Tails were immersed in sequential fashion in water baths set at 49°C, 52.5°C, and 55°C, and were wiped dry between dips. After baseline latencies were determined for each animal, they were given an intraperitoneal (i.p.) injection of drug. Post-drug latencies were determined 15, 30, and 60 min after injection. Cutoff values were set at 20, 12, and 10 s, respectively, for the 49°C, 52.5°C, and 55°C bath exposures to prevent tissue damage. Water bath temperatures were measured daily using a Traceable RTD platinum thermometer (Control Company, Friendswood, TX) and adjusted as necessary to ensure consistency throughout the study. Animals with a baseline latency at 49°C less than 5 s or greater than 9 s were removed from the study. %MPE measures between wild-type and GIRK3 knockout mice at the same dose were analyzed at each temperature and time point by independent measures Student's t-test. %MPE measures between doses within genotype were analyzed by one-way ANOVA and post-hoc analysis was performed using Tukey's HSD test. Statistical analysis showed no difference between male and female mice, therefore, data from both genders were combined to increase the study power. As data from all three temperatures produced similar results and the maximal drug effect was observed at the 30 min post-injection time point, only the subset of data obtained at 49°C and the 30 min time point will be presented here.

D. Results

D.1. Gene expression

For each CNS region assayed, *Kcnj9* gene expression in each strain was compared to the expression of the house-keeping gene *Gapdh*, and reported as a ratio of the two (Fig. 12). Expression of *Kcnj9* was observed in all three tissues; no difference between strains was apparent in the RVM or spinal cord. Expression in the periaqueductal gray was divergent between the two strains, with 129P3 expressing almost three times more transcript than C57BL/6.

D.2. GIRK3 phenotyping

There was no significant difference in baseline latencies between wild-type (7.0±0.1 s) and GIRK3 knockout (6.7±0.1 s). However, there was a trend ($p = 0.06$) for the latencies of GIRK3 knockout mice to be shorter compared to wild-type mice.

Clonidine produced strongly genotype-dependent analgesia (Fig. 13a; wildtype AD_{50}: 0.7 mg/kg, 95% C.I.: 0.4 – 1.3 mg/kg; GIRK3KO AD_{50}: 12.5 mg/kg, 95% C.I.: 3.6 – 43.5 mg/kg). In contrast, morphine produced equivalent levels of analgesia in both strains at all doses tested (Fig. 13b; wildtype AD_{50}: 5.0 mg/kg. 95% C.I.: 4.3 – 5.9 mg/kg; GIRK3KO AD_{50}: 5.6 mg/kg, 95% C.I.: 4.3 – 7.2 mg/kg) (see also Marker et al., 2002; Marker et al., 2004). WIN55,212-2 also produced genotype-dependent analgesia (Fig. 13c), with dose-dependency observed in wildtype mice (AD_{50}: 59.4 mg/kg, 95% C.I.: 22.0 –160.8 mg/kg) but not GIRK3KO mice (AD_{50}: not calculable).

E. Discussion

Simultaneous linkage mapping projects implicated a region of distal Chr. 1 as the site of a gene responsible for analgesia produced by multiple opioid- and non-opioid drugs. We have successfully mapped this quantitative trait locus down to a short (~8 cM) interval through a combination of *in silico* haplotype mapping and congenic strain techniques; however, the ultimate goal of narrowing the confidence interval to a single gene remains distant. Many additional steps of breeding subcongenic animals still remain, and the final step to formally prove the involvement of a gene would require a technically difficult allele-transfer experiment in which the version of the gene from one strain is placed on the background of another strain (Rikke and Johnson, 1998; Nadeau and Frankel, 2000). An alternative to this extensive process is to compile evidence supporting the involvement of a likely "positional candidate gene" in the phenotype in question (Collins, 1997). Criteria which must be validated for a potential candidate gene include: genomic localization within the QTL confidence region; polymorphisms in or near the gene resulting in variant proteins or gene expression level differences; and relevant functionality of the gene, in appropriate organs or tissues, to affect the phenotype. An extensive search of all genes in our confidence region (Table 5) revealed one gene within the region as an especially promising candidate to account for the observed strain differences in analgesic sensitivity: *Kcnj9*.

Located at 94.2 cM (172.2 Mb), *Kcnj9* lies near the peak of linkage in all three analgesic mapping studies: clonidine (100 cM), morphine (90 cM), and WIN55,212-2 (94 cM). It also falls within the region (170-180 Mb) linked by *in silico* mapping with analgesia produced by clonidine, morphine, U50,488, and WIN55,212-2, among seven different inbred strains. The intersection of these mapping efforts implicates the interval

90-96 cM (170-175 Mb), which contains about 100 known genes, including a cluster of ~20 olfactory receptors; *Kcnj9* is one of a small number of genes not excluded by any of our attempts to localize the analgesia QTL.

In order to accept the gene as a strong candidate underlying the *Manr1* QTL, a convincing mechanism by which *Kcnj9* modulates analgesia from multiple drug classes must be postulated; this explanation should preferably account for all of the observed characteristics of the QTL. The relevance of GIRK channels in modulating pain and pharmacological analgesia has been well established (reviewed in Ocana et al., 2004). The GIRK family of G protein-coupled inwardly rectifying potassium channels consists of four subunits (GIRK1-4) encoded by four distinct genes. These four subunits form functional heterotetramers *in vivo*, and the subunit composition seems to be an important factor in the tissue-specific properties of these channels (Kofuji et al., 1995). The purpose of potassium channels in neurons is to regulate membrane conductance by enabling the flow of K^+ ions down their electrochemical gradient (Shieh et al., 2000). GIRK channels are activated by interactions with Gβγ subunits subsequent to the binding of an appropriate ligand to any of a number of G protein-coupled receptors (Kofuji et al., 1995; Sadja et al., 2003). These receptors include opioid, cannabinoid, adrenergic, and other receptor types involved in nociceptive modulation. The ultimate effect of GIRK activity is hyperpolarization of neurons, resulting in a decrease in neural excitability (Signorini et al., 1997).

Null mutant mice for each of the subunits have been generated and tested for altered response to pain and analgesic drugs (Marker et al., 2002; Blednov et al., 2003; Mitrovic et al., 2003; Marker et al., 2004; Marker et al., 2005). Strong evidence especially supports the involvement of the GIRK2 subunit in analgesia from opioid and

non-opioid drugs alike (Ikeda et al., 2000; Blednov et al., 2003; Mitrovic et al., 2003). Mutant mice lacking GIRK2 expression have attenuated postsynaptic inhibitory responses to a number of G protein-coupled receptor agonists with analgesic properties (Luscher et al., 1997), indicating that GIRK channels broadly contribute to analgesia. The role of the GIRK3 subunit in analgesia is less clear, however. Introduction of GIRK3 cRNA into *Xenopus* oocytes does not result in measurable expression (Wischmeyer et al., 1997) or K+ current (Schoots et al., 1999); co-injection of GIRK3 with GIRK1 cRNA into oocytes potentiates G protein-induced currents, but suppresses the current of GIRK2 alone (Kofuji et al., 1995). Although the primary inhibitory channel in the mammalian brain is most likely to consist of GIRK1/2 subunits (Koyrakh et al., 2005), channels composed of 2/3 subunits have been isolated from native mouse brain (Jelacic et al., 2000), and have been shown to modulate the inhibitory effects of opioids in the locus coeruleus (Torrecilla et al., 2002). The function of the GIRK3 subunit in such channels is not yet known, but the availability of GIRK3 may be an important modulatory element, as GIRK2/3 channels are 4.8 times less sensitive to $G_{\beta\gamma}$ compared to GIRK1-containing channels (Jelacic et al., 2000). It has also been proposed (Ma et al., 2002) that a motif on the GIRK3 protein, unique among GIRK subunits, actually diverts channels containing the subunit for lysosomal degradation.

Kcnj9 is an especially attractive candidate for purposes of explaining the contradictory results we have observed between some of our mapping projects. The *Manr1* QTL effect was strong for adrenergic and cannabinoid analgesia, but weaker (and dose-dependent) for morphine. Although *in silico* mapping confirmed the linkage of the QTL to opioid analgesia (from μ as well as κ agonists), no effect was seen in either congenic or GIRK3 knockout strains. This disparity may be explained by the diverse

mechanisms by which morphine inhibits nociception. Postsynaptic opioid receptors are functionally coupled to GIRK channels (Luscher et al., 1997), but a significant component of morphine analgesia arises from action at the presynaptic terminal (Cherubini and North, 1985), where its effects are mediated by G protein-linked calcium channels (Bourinet et al., 1996). Presynaptic inhibition, especially at higher doses of the drug, may mask genotype-specific deficits in postsynaptic antinociception. This hypothesis is bolstered by similar observations in GIRK2 knockout mice; these animals exhibited a drastic reduction in the analgesic potency of clonidine, but that of morphine was only slightly attenuated (Mitrovic et al., 2003). A related explanation may account for the failure of epibatidine analgesia to map to the *Manr1* locus in the haplotype analysis. Epibatidine's target receptor, the nicotinic acetylcholine receptor, is not a G protein-coupled receptor, and epibatidine analgesia would therefore not be strongly influenced by GIRK polymorphisms. It should be noted that the deletion of GIRK2 produces a profound attenuation of nicotine analgesia; however, this effect is probably mediated by deficiencies in monoamine neurotransmission downstream from the nicotinic terminal (Blednov et al., 2003).

Herein we present evidence that *Kcnj9* transcripts are present in differing levels in C57BL/6 and 129P3 strains in an analgesia-relevant CNS region. As previously reported (Marker et al., 2002; Marker et al., 2004), expression of *Kcnj9* mRNA in the spinal cord was minimal, and appeared to be indistinguishable between strains. Expression in the rostral ventral medulla was marginally higher, but likewise equal between 129 and B6. A large strain difference was observed in the periaqueductal gray; expression in 129 mice was almost three times that of B6 mice. This finding replicates the difference between the two strains in six major brain regions assayed by microarray by Sandberg et al.

(2000). The overexpression of GIRK3 (as in 129P3 mice), or lack thereof (as in GIRK3 KO mice), in analgesia-relevant areas of the brain may similarly disrupt the optimal balance of GIRK subunits.

We have used transgenic mutant mice in which the *Kcnj9* locus has been deleted to explore the role of the gene in modulating analgesia. These mice were created by introducing a null mutation into ES cells of the 129Sv/J strain via homologous recombination, producing a chimeric mouse by insertion of transgenic cells at the blastocyst stage, and then backcrossing this mouse with a C57BL/6 background for many generations to eliminate 129-derived genetic material (Torrecilla et al., 2002). Mice homozygous for the deletion exhibited a flattened dose-response relationship, compared with wild-type mice, for both clonidine and WIN55,212-2, indicating that these drugs were largely ineffective at producing any antinociceptive effect (Fig. 13a and 13c). Morphine analgesia was not significantly affected (Fig. 13b). One explanation for this phenotype is that the deletion of the *Kcnj9* gene, and the subsequent loss of any functional GIRK3 protein, resulted in a deactivation of potassium channels necessary for adrenergic and cannabinoid (but not opioid) analgesia. However, the interpretation of knock-out studies is complicated by the "hitch-hiking donor gene" confound: instead of being caused by the non-functional gene, as is usually assumed, the phenotype may be produced by one of the 129-derived genes flanking the deleted locus (Mogil and Grisel, 1998). We have, in fact, exploited such "hitch-hiking genes" already, in the form of the *Fcgr3*KO-congenic mice used to isolate the gene. The pattern of analgesic response of the GIRK3KO mice mirrors that of the *Fcgr3*KO-congenic mice, such that it is impossible to determine whether it is a result of the deletion of either gene, or merely an unexpected side-effect of an unknown 129-derived allele near the knocked-out genes.

Confusion between mutation and strain effects can be resolved using a classical genetic method known as quantitative complementation (Rikke and Johnson, 1998; Yalcin et al., 2004). This method, also termed a "QTL-knockout interaction test" (Darvasi, 2005), uses crosses between null mutants and the high- and low-QTL strains to detect interactions between the mutated gene and the QTL. The test requires that the mutation be non-dominant (i.e., additive or recessive), however, to preserve the possibility of complementation with the QTL. Crossing GIRK3KO mice with B6 wild-types, we found that clonidine analgesic magnitude in heterozygotes was indistinguishable from that of homozygous null mice (data not shown), indicating a dominant mode of inheritance. We can only conclude that the attenuated analgesia phenotype displayed by the GIRK3 mutants is corroborative evidence supporting the role of this gene in antinociception, rather than proof of its involvement.

The precise polymorphism responsible for the difference in *Kcnj9* expression (and possibly the analgesia strain difference) is not easily identifiable. The 129P3 strain is genetically not very well characterized; however, other 129 substrains such as 129S1/SvImJ and 129X1/SvJ, as well as the closely related LP/J strain (Beck et al., 2000), are included in major SNP databases, and can serve as proxies for the 129P3 strain. The sequence of C57BL/6J is in the public domain at www.ensembl.org, and the sequence of 129Sv/J has been made available as well (Wickman et al., 2002). The mouseSNP database (http://mousesnp.roche.com/) catalogues 50 polymorphisms between C57BL/6 and 129/SvImJ in the vicinity of *Kcnj9*, although this may not be an exhaustive list (Table 7). These polymorphisms, any of which may be potential quantitative trait polymorphisms (QTPs), include nucleotide switches (13 within exons, 4 in introns, and 24 outside the gene itself, including the promoter region), and nucleotide deletions

(including a set of three that putatively results in an extra aspartic acid residue in the GIRK3 product of 129 mice). It is likely that at least one of these extra-coding SNPs determines the level of expression of *Kcnj9*, as the gene shows *cis*-regulation as characterized by the Web-QTL method (Hitzemann et al., 2004).

A surprising degree of genetic correlation between numerous opioid and non-opioid analgesic compounds, across a dozen inbred strains, led us to search for a genetic mechanism common to all of the drugs (Wilson et al., 2003). Linkage and *in silico* mapping isolated a short interval at the distal end of Chr. 1 that broadly predicted analgesic response to four of the drugs evaluated, and this locus was successfully transferred from the "analgesia-insensitive" to the "sensitive" strain using a congenic strategy. We then compiled molecular and behavioral evidence implicating *Kcnj9* as the gene responsible for analgesic sensitivity. Although not the "master analgesia gene" we initially predicted, if *Kcnj9* proves to play a role in human sensitivity to analgesics as well, this knowledge may ultimately prove beneficial to the millions of patients currently suffering from insufficient pain relief. The emerging field of pharmacogenetics holds promise for predicting a person's sensitivity to analgesic drugs, and may one day even offer the possibility of increasing drug efficacy through the manipulation of GIRK-related mechanisms.

CHAPTER 5: HAPLOTYPE MAPPING OF *Nociq1*

A. Experiment Summary

Quantitative trait locus mapping revealed the influence of a gene on distal Chr. 9 modulating the response of AB6F2 mice to the early phase of the formalin test, a common measure of chemical nociception. In question, however, remained the identity of this gene, and the extent to which this finding generalized to other mouse strains. By adding new strains to our previous strain survey data, we were able to carry out an *in silico* mapping analysis with enough power to implicate a set of haplotype blocks in the QTL region correlating with the variability observed across multiple strains. These haplotype blocks corresponded to a single gene, *Atp1b3*, a subunit of the ouabain-sensitive sodium-potassium channel. We then showed that pharmacological blockade of this channel eliminated the strain difference between A/J and C57BL/6 in both early and late phases of the formalin test. We also observed that formalin-sensitive C57BL/6 mice exhibit lower expression of *Atp1b3* in the dorsal root ganglia than other, relatively resistant strains, suggesting a mechanism by which the gene may contribute to the behavioral strain difference.

B. Introduction

Inflammation is the body's natural response to tissue damage from burns, injuries, and infection. The release of inflammatory mediators, including cytokines, catecholamines, nerve growth factors, prostaglandins, bradykinin, nitric oxide, and ATP (Dray, 1995), initiates defense mechanisms designed to prevent further injury and stimulate healing. Pain, in the form of hyperalgesia or allodynia, frequently accompanies these processes as an incentive to protect the damaged tissue. Although such pain may be seen as adaptive, inflammatory processes lead to central sensitization (Woolf and Costigan, 1999; Ji, 2004) often manifested as debilitating spontaneous pain (Djouhri et al., 2006), and inflammation underlies numerous pathological states such as arthritis, inflammatory bowel disease, fibromyalgia, and vulvodynia.

Wide psychometric variability in thermal (Chen et al., 1989b; Sheps et al., 1999; Coghill et al., 2003; Hutchinson et al., 2004) and pressure (Sherman, 1943; Chapman and Jones, 1944; Brennum et al., 1989) pain has been convincingly demonstrated, and its determinants enumerated (Chen et al., 1989a; Davis et al., 1998; Fillingim et al., 1998; Myers et al., 2001; Fillingim et al., 2005), but less is known about variability in inflammatory pain in humans. Rodent models of inflammation have therefore been instrumental in establishing a genetic basis for interstrain variability in rats (Rosenthale, 1970; Widy-Tyszkiewicz et al., 1995; Zhang et al., 2003), and we have demonstrated large strain differences in several models of inflammatory pain in mice as well. Strain surveys measuring response to a number of inflammatory agents, such as formalin, acetic acid, magnesium sulfate, bee venom, and the sea moss derivative carrageenan, have shown that strains may vary up to 17-fold in their exhibition of pain behaviors (Mogil et al., 1998; Mogil et al., 1999a; Lariviere et al., 2002). Such variability, while consistent

across chemical agents, does seem to depend on the particular stimulus evoking the pain, whether it be spontaneous or induced by thermal or tactile stimulation (Mogil et al., 1999b). However, the genetic correlation of different inflammation modalities strongly suggests the role of genes causing variation between individuals (Mogil et al., 1999b).

We recently used quantitative trait locus (QTL) mapping to search for genes responsible for variable response to the formalin test between the sensitive C57BL/6J and the resistant A/J strains (Wilson et al., 2002). In this assay (Dubuisson and Dennis, 1977), an injection of 1-5% formalin (itself a dilute solution of formaldehyde) under the plantar surface of the hindpaw produces recognizable pain behaviors (i.e., licking and shaking of the offended limb) in the mouse. Vigorous responses are observed for 5 to 10 min (the early, or *acute*, phase) before subsiding into a short quiescent interval; pain behaviors are renewed a few minutes thereafter (the late, or *tonic*, phase) and last for an hour or more. It is believed that the two phases may represent different nociceptive mechanisms (and therefore, divergent underlying genetic modulation). Overlapping regions on distal Chromosome 10 linked to both the early and late phases suggested that a single locus (*Nociq2*) near 60 cM contributed to variability in both phases. We also observed a locus on Chr. 9 (*Nociq1*, peak 59.8 cM, C.I. 44-68) that accounted for 27.3% of the phenotypic variance of the early phase only.

Mapping a QTL to a ~20 cM interval is only the first step in the identification of the quantitative trait gene (QTG) underlying the locus. Traditionally, an extensive process of cloning the QTG by position, accomplished via the generation of hundreds of recombinant individuals, has been the only recourse to narrow the confidence interval (Moisan, 2000). Recently, however, the completion of the mouse genome sequence and extensive cataloguing of genetic variation between inbred strains have vastly improved

our ability to relate observed phenotypes with essentially all of the basic units of inheritance. Haplotype mapping (Grupe et al., 2001) correlates *in silico* the behavior of a set of inbred strains with an archived database of single nucleotide polymorphism (SNP) variation within the set, such that one can implicate single genes as producing patterns of strain responses. We have subjected our formalin strain survey data to haplotype analysis in order to generate candidate genes with a high probability of producing variability across strains.

C. Methods

C.1. Subjects

Eleven inbred strains, including 129P3, A, AKR, BALB/c, C3H/He, C57BL/6, C58, CBA, DBA/2, RIIIS, and SM (all /J substrains) were assessed in our initial strain survey; they were housed and maintained as previously described (Mogil et al., 1998). SNP data was only available for eight of these strains (after substituting the 129/SvlmJ strain for the closely related 129P3 strain), however, so an additional eight strains were phenotyped for the present study: A/HeJ, B10.D2-H2/oSNJ, BALB/cByJ, MRL/MpJ, NZB/BlnJ, NZW/LaCJ, LG/J, and LP/J. These strains were obtained from The Jackson Laboratory (Bar Harbor, ME), and housed in our environmentally controlled vivarium with ad lib access to food (Harlan Teklad) and tap water. Behavioral candidate gene and expression studies were performed on A/J and C57BL/6J mice reared on-site from breeders obtained from The Jackson Laboratory. Both males and females were tested in all experiments.

C.2. Formalin testing

Response to formalin treatment was assessed as described previously (Tjolsen et al., 1992; Mogil et al., 1998). Briefly, all mice were injected in the plantar surface of the hindpaw with 5% formalin (37% w/w formaldehyde) in a volume of 25 μl, using a 30 gauge needle. Mice were allowed to habituate singly for 1 hr in clear Plexiglas cylinders (12 cm diameter x 15 cm high) on a glass floor before injection. Following the habituation period, each mouse was removed and introduced into a cloth pouch, where it was restrained for injection. Mice were then returned to the Plexiglas cylinder and videotaped from below for 60 min. The recordings were later scored by trained observers blinded to strain or drug condition (as appropriate) using The Observer software package (Noldus, Leesburg, VA). Mice added to the strain survey for purposes of haplotype mapping were scored for early phase response (first ten minutes) only; the total amount of time spent attending to the injected hindpaw (licking or biting) over the duration was measured. For candidate gene studies, the early (0-10 min) and late (10-60 min) phases were both scored. Edema due to inflammation was assessed by weighing the injected and contralateral paws on a microbalance, and computing the percent difference in weight between them.

C.3. Haplotype mapping

Sixteen strains were evaluated for early phase response to formalin treatment, and the mean duration of response was converted to a Z-score for each strain. The phenotype scores were then subjected to computational genetic analysis as previously described (Grupe et al., 2001; Liao et al., 2004). This method uses a haplotype map of the mouse genome, constructed from blocks of SNP alleles of the inbred strains (Wang et al.,

2005a). When this computational analysis was performed, the haplotype map had 5,694 haplotype blocks generated from 215,155 SNPs characterized across 19 inbred strains covering 2,609 genes (see http://mouseSNP.roche.com). Linked haplotype blocks, in which the strain grouping within the block correlates with the distribution of phenotypic data among the inbred strains, are identified *in silico*. A p-value is computed to evaluate the likelihood that genetic variation within each block could underlie the observed distribution of phenotypes among the inbred strains. The haplotype blocks are then ranked based upon the calculated p-value. The p-values for the numerical phenotype evaluated in this experiment were calculated as described using ANOVA (Liao et al., 2004; Wang et al., 2005a; Wang et al., 2005b). As there are no widely recognized standards for significance of full-genome haplotype scans, this analysis is best considered to be exploratory, with follow-up experiments necessary to establish proof of a gene's involvement in the phenotype.

C.4. Candidate gene studies

C.4.1 Nociceptive behavioral testing

Results of the haplotype mapping analysis strongly supported a role for the sodium-potassium ATPase channel in formalin early phase strain variability. We used ouabain (Sigma, St. Louis, MO), an antagonist of this channel, to evaluate behaviorally the effects of blocking the channel on the strain difference. A/J (resistant) and C57BL/6J (sensitive) mice were given a 1 mg/kg dose (in a volume of 0.1 ml/kg i.p.) of the drug, 5 min prior to formalin injection. Formalin response in the early and late phases was quantified as above.

C.4.2 Gene expression studies

Dorsal root ganglia (DRGs) of the L4-L6 level were removed from mice of five strains (A/J, C57BL/6, LG/J, MRL/MpJ, and NZW/LacJ), aged from at least six weeks. Tissues were removed from naïve as well as formalin-challenged mice, in separate experiments. The harvested tissues were immediately placed in a preservation agent, RNAlater (Ambion, Austin, TX), and stored at 4°C until total RNA isolation. To obtain a sufficient quantity of tissue samples, approximately 10-15 mice from each strain were used for each tissue type, and all samples of each type were pooled.

The samples were homogenized with Trizol (Invitrogen, Burlington, ON) and resuspended in 30 μL of DEPC treated water. The RNA solution was then treated with the DNA-*free* kit (Ambion, Austin, TX) to remove any trace DNA contaminants and purified with the RNeasy Mini kit for RNA cleanup (Qiagen, Germantown, MD). Integrity and concentration of the total RNA samples were evaluated on the Bioanalyzer 2100 (Agilent, Palo Alto, CA). The reverse transcription (RT) reaction was performed according to the protocol of the TaqMan Reverse Transcription Reagents kit (Applied Biosystems, Foster City, CA). In addition to the unknown samples, serial dilutions of known concentrations of mouse brain total RNA (Ambion) acting as standards were reverse transcribed. Briefly, each RT reaction required 1 μL of the total RNA to be added to 9 μL of RT master mix composed of 0.5 μL of 50 μM random hexamers and 0.25 μL of 50U/μL Multiscribe RT enzyme. Reverse transcription was carried out on a Peltier Thermal Cycler (PTC-100, Bio-Rad, Hercules, CA) at the following cycles: 25°C for 10 min, 48°C for 30 min followed by 95°C for 5 min. The cDNA was stored at 4°C until the PCR reaction was made.

Gene-specific TaqMan probe and primer sets for the target genes *Atp1b1*, *Atp1b2*, and *Atp1b3*, and the *Gapdh* control were obtained from ABI. The target gene was amplified in different wells of a 96-well reaction plate with the endogenous control gene, *Gapdh*, whose constitutive expression served to normalize quantification of target gene expression levels among unknown samples. Each 5 μL cDNA sample of standards and unknowns was added to 20 μL of target gene PCR master mix and 20 μL of *Gapdh* PCR master mix. The target gene PCR master mix composition was: 12.5 μL of 2X TaqMan Universal PCR Mix with AmpErase UNG, 6.25 μL of DEPC water, and 1.25 μL of 20X target gene specific probe and primers mix. The *Gapdh* master mix composition was: 12.5 μL of 2X TaqMan Universal PCR Mix with AmpErase UNG, 6.00 μL of DEPC water, and 0.5 μL of 20X *Gapdh* gene specific probe and primers. Standards were run in quadruplicate and unknowns in quintuplicate. Real-time PCR was carried out on an ABI 7000 system at the following cycles: 50°C for 2 min, 95°C for 10 min followed by a round of 40 cycles of 95°C for 15 sec/60°C for 60 sec.

After the PCR reaction was completed, a threshold was fixed across the linear region of all amplification curves. C_T values for the unknown samples and known standards were determined as the cycle numbers associated with this threshold. C_T values of the unknown samples were then converted into expression values using the corresponding standard curve. The ratio of the average target gene amount over the average *Gapdh* amount provided the normalized target gene expression result.

D. Results

D.1. Haplotype mapping

Phenotyping additional strains beyond those included in our previous survey (Mogil et al., 1998) did not markedly affect the relative sensitivity rankings of the strains (Table 8). C57BL/6 remained the most sensitive strain, although three of the new strains were less sensitive than BALB/c and A/J, strains formerly identified as most resistant.

The correlation between the phenotype distribution and each haplotype block was assigned a p-value, indicating the likelihood of the correlation being observed by chance. Twenty-six blocks exceeded the arbitrary significance threshold $p<0.01$, corresponding to 19 distinct genes on 14 chromosomes; four genes exceeded a threshold of $p<0.001$. The ten haplotype blocks with the lowest p-value are shown in Table 9. The gene with the highest level of significance in the haplotype mapping analysis was *Gstm3*, located on medial Chr. 3 ($p = 0.00035$). Three genes with significance greater than $p<0.01$ comap with the *Nociq1* locus on distal Chr. 9: *Atp1b3* (51 cM, $p = 0.00039$), *Rbp1* (52 cM, $p=0.0038$), and *Rbp2* (57 cM, $p = 0.007$).

The criteria for an identified gene to be considered a candidate gene underlying *Nociq1* included position (between 44 and 68 cM on Chr. 9), expression in the CNS or relevant peripheral site, and nociception- or inflammation-related function. Only one gene in our haplotype analysis was observed to meet all of these requirements. The sodium-potassium channel subunit *Atp1b3* exhibited a high correlation with the phenotype across all 16 strains tested, and its role in the regulation of neuronal excitability suggests that it is responsible for the observed strain differences. We therefore contrasted the effects of an inhibitor of the sodium-potassium ATPase channel

between a sensitive (C57BL/6) and a resistant strain (A/J) to determine if activity at this site modulates differential formalin response.

D.2. Candidate gene studies

The effect of the sodium-potassium ATPase inhibitor, ouabain, on both the early and late phase, as well as paw edema, was examined using ANOVA (Fig. 14). In the early phase (Fig. 14a), an interaction between strain (A/J versus C57BL/6) and drug (ouabain or saline vehicle) was observed ($F_{1,42}$=4.604, p = 0.038). Post-hoc tests revealed that there was a significant difference in formalin response between the strains when administered saline ($F_{1,21}$=5.016, p = 0.036), but that this difference entirely disappeared after ouabain injection ($F_{1,21}$=0.173, p = 0.682). Similarly, an interaction between strain and drug effects in the late phase ($F_{1,42}$=13.622, p = 0.001, Fig. 14b) was due to the presence of a strain difference in saline-treated ($F_{1,21}$=10.518, p = 0.004) but not ouabain-treated ($F_{1,21}$=3.312, p = 0.083) animals. No significant main effects or interactions were observed in paw edema (Fig. 14c).

D.3. Expression of ATPase subunits

We first compared baseline *Atp1b3* expression in the DRG between A/J and C57BL/6 (Fig. 15a). A/J mice had roughly twice the expression of this gene (5.8 versus 2.7 arbitrary units). Expression of two other β subtypes, β_1 and β_2, however, was not divergent between the two strains (Fig. 15b). *Atp1b3* appeared to be upregulated in both strains following formalin injection (Fig. 15c), but remained higher in A mice. Additionally, other formalin-resistant strains, including LG/J, MRL/MpJ, and NZW/LacJ, also expressed the gene at higher levels than B6.

E. Discussion

The formalin test, a common mouse model of chemical and inflammatory pain, is considered one of the more clinically relevant experimental models of pain, pertinent to the study of chronic inflammatory diseases and conditions such as osteoarthritis and rheumatoid arthritis, inflammatory bowel disease, and vulvar vestibulitis. Mice of different strains exhibit wide variation in nocifensive behaviors (i.e., licking, biting) in response to sub-cutaneous formalin injection, indicating a major genetic component to this model (Mogil et al., 1998; Mogil et al., 1999a). The identification of genetic determinants responsible for individual variability in formalin response would increase understanding of the sequence of events involved in inflammation, and potentially provide novel therapeutic targets. We recently mapped a quantitative trait locus (Wilson et al., 2002) explaining over 27% of the phenotypic variance in the early phase of the formalin test to a region of Chr. 9 (peak LOD 5.2 at 60 cM, C.I. 44-68 cM). This result was limited in several ways: the QTL only appeared to influence early phase responding (i.e., chemosensation), not inflammation; the confidence interval was too large to pinpoint the responsible gene; and the locus was only known to mediate the strain difference between C57BL/6 and A/J.

Haplotype-based mapping is a recently developed technique (Grupe et al., 2001; Liao et al., 2004) that may significantly improve resolution and specificity in conjunction with traditional QTL mapping approaches. By exploiting the natural genetic variation that has arisen in inbred strains over many years, it is possible to implicate single genes contributing to a complex trait (provided the number of strains queried is sufficiently large). Our analysis (Table 9) associated a small number of genes on Chr. 9 correlating highly with the observed pattern of formalin sensitivity across all 16 strains. Two related

genes, *Rbp1* and *Rpb2*, were associated with moderate probability ($p<0.01$) and are located within the confidence interval of the QTL. However, these genes encode retinol-binding proteins with no clear function in pain or inflammation; examination of the MGI and other gene expression databases concluded that these genes are largely active in the eye and small intestine, respectively.

The other gene implicated by the haplotype analysis was *Atp1b3* (highest correlation $p<0.0004$). The protein product of this gene is a β subunit of the Na+, K+-ATPase channel, which in conjunction with an α subunit, regulates ion transfer across neuronal cell membranes (Besirli et al., 1997). The α subunit is responsible for ATP hydrolysis and contains the binding site for the pharmacological antagonist ouabain (Jorgensen et al., 2003). The function of the β subunit is not well-characterized, but it is believed to be necessary for proper assembly of the channel on the membrane. The Na+, K+-ATPase channel has been implicated in two types of painful inflammation. A mutation in the *Atp1a2* gene has been linked to a rare form of familial hemiplegic migraine (DeFusco et al., 2003). An inverse relationship between Na+ ion transfer by this channel and inflammation has been demonstrated in irritable bowel disease, although the dysregulated tissue is the colonic mucosa, rather than neurons (Allgayer et al., 1988). This channel is also believed to modulate opioid antinociception, although both synergistic (Zeng et al., 1999) and antagonistic (Masocha et al., 2003) interactions have been observed between morphine and ouabain.

We used systemic injections of ouabain to look for evidence of strain-dependent activity of the Na+, K+-ATPase channel (Fig. 14). The large strain difference between A/J and C57BL/6 in response to formalin injection was entirely eliminated by the co-administration of the ATPase blocker, ouabain, both in the early phase (Fig. 14a) as

well as the late phase (Fig. 14b). This would suggest that the efficiency of the channel in A mice is lower than that of B6 mice, and that inhibition of the channel equalizes ATPase activity. We cannot deduce from this alone the precise mechanism by which ATPase activity translates to behavioral response to inflammation, but the fact that edema was unchanged by ouabain in either strain (Fig. 14c) supports the assertion that the mechanism does not modulate basic inflammatory processes, but rather the transmission of nociceptive impulses to the CNS.

Interestingly, despite the lower activity of the allele carried by the A strain, expression of the *Atp1b3* gene was higher than B6 (Fig. 15a). This relative increase was consistent across several of the formalin-resistant strains (Fig. 15c), suggesting that lower expression in B6 is responsible for its high sensitivity. Not enough is known about the different β subunits to explain this discrepancy, but it is possible that the β_3 subunit is less functional than other β subtypes competing for dimerization with α subunits. No strain-specific expression differences were observed in either *Atp1b1* or *Atp1b2* (Fig. 15b); B6 mice may therefore have a greater proportion of these subunits than would A mice (although the absolute quantities of mRNA of these two subtypes were considerably smaller than those of *Atp1b3*; data not shown).

The present experiments validate the use of QTL and haplotype mapping to convincingly identify variability genes at very high resolution. Our analysis led us to a single plausible candidate, *Atp1b3*, a gene known to play a role in neuronal excitability and inflammation. Pharmacological manipulation of the Na+, K+-ATPase channel confirmed that this channel was responsible for the differential sensitivity between A/J and C57BL/6. Although we cannot presently postulate a mechanism to explain how variants of the gene manifest as behavioral differences, the level of expression of *Atp1b3*

appears to determine formalin sensitivity. The relevance of these findings to human inflammatory disease may prove to be substantial; the Na+, K+-ATPase channel has already been linked to migraine, and we believe it is likely that association studies of both acute inflammation and inflammatory disease states could implicate genetic variation in *Atp1b3* or any of the other genes involved in ATPase assembly.

CHAPTER 6: POSITIONAL CLONING OF *Nociq2*

A. Experiment Summary

Both the acute/chemical and the tonic/inflammatory phases of the formalin test exhibit wide variety between inbred mouse strains. Using quantitative trait locus mapping, we previously identified a region of distal Chr. 10 harboring a gene contributing to variability in both phases of the formalin test. As no obvious candidate genes were identified within the confidence interval, we have continued our search for this gene using a variety of recombinant mouse strains to clone the gene by its position. We surveyed panels of recombinant inbred and recombinant congenic strains derived from a cross between the A/J and C57BL/6 strains, which confirmed the presence of the QTL on distal Chr. 10. We also constructed congenic and subcongenic lines in order to further isolate the QTL to a <3 cM interval. The expression levels of the genes in this region were queried by microarray analysis, providing a short list of candidate genes with both positional and functional evidence supporting their involvement in formalin test variability.

B. Introduction

Both experimental and clinical pain exhibit robust interindividual variability, and the role of genetic factors in this variability is increasingly appreciated (Mogil, 2004). Although the pace of human genetic association studies of pain is accelerating, much more is known about pain genetics (especially with regards to phenomics) in the mouse. Several quantitative trait loci (QTLs) have been identified for pain-related traits, and functional data provided in support of candidate genes (Mogil et al., 1997a; Hain et al., 1999; Mogil et al., 2003; Mogil et al., 2005). However, much greater progress has been made with thermal pain (and analgesic responsivity against thermal pain) than more clinically relevant pain modalities. The most common current preclinical assay of inflammatory pain is the formalin test (Tjolsen et al., 1992). In this assay, a dilute solution of formaldehyde is injected subcutaneously into the hindpaw, and a temporally biphasic pattern of recuperative behaviors (e.g., licking, biting, lifting) is observed. Of most clinical relevance is the tonic or "late" phase of behavior (F_{late}), which begins approximately 10-15 min after the formalin injection and lasts 30-60 min before subsiding.

Mice show impressive strain-dependence in their licking/biting behavior in the late phase of the formalin test, with the A/J and 129P3/J strains particularly resistant and a number of strains, including C57BL/6J (B6), sensitive (Mogil et al., 1999a). We have shown that these behavioral differences are not due to strain-dependent inflammation (Mogil et al., 1998), and that they correlate highly with immediate-early gene expression in the deep dorsal horn of the spinal cord (Bon et al., 2002). We recently identified two QTLs in an (A/J x B6)F_2 intercross (named *Nociq1* and *Nociq2*). *Nociq1*'s effects were specific to the "early" phase of the formalin test (F_{early}), but *Nociq2* (peak LOD = 4.3; 1-

LOD drop-off confidence interval: >58 cM on chromosome 10) explained 15% of the trait variance in F_{late}. Inheritance of two copies of the B6 allele of the *D10Mit35* marker (69 cM) resulted in an additional 200 s of licking in F_{late} compared to A/J homozygotes. Unfortunately, the only obvious candidate gene in the confidence interval containing this QTL was *Ifng* (interferon-γ, 67 cM), and studies with *Ifng* knockouts and quantitative RT-PCR convincingly excluded its candidacy.

Thus, the purpose of the present study was to work towards the positional cloning of *Nociq2*, a QTL with potentially generalizable influence on inflammatory pain across multiple assays (Hain et al., unpublished data). To this end, we obtained or constructed recombinant inbred strains, recombinant congenic strains, and speed congenic lines to confirm the existence and refine the location of *Nociq2*.

C. Methods

C.1. Subjects

Subjects of all experiments were naïve, adult (6-12 weeks old) mice of both sexes. Genotypes tested included A/J, C57BL/6J (B6), and several recombinant inbred (RI; from the AXB/BXA set), recombinant congenic (RC; AcB/BcA set), and congenic strains to be described below. Inbred and RI strains were purchased from The Jackson Laboratory (JAX; Bar Harbor, ME). RC strains were transferred to our vivarium from a breeding colony at the Montreal General Hospital. All congenic strains were bred in-house. Upon weaning (at 18-21 d) or immediately after arrival, mice were housed in standard shoebox cages of 2-4 with same-sex littermates in a temperature-controlled (20±1°C) environment (14 h:10 h light/dark cycle; lights on at 07:00 h), and with *ad lib* access to food (Harlan

Teklad 8604) and tap water. Mice were habituated to the laboratory for at least one week before any behavioral testing commenced.

C.2. Formalin Test

Mice were habituated for 30 min in individual transparent Plexiglas cylinders (15 cm diameter; 22.5 cm high) placed atop a glass surface suspended over high-resolution video cameras. All subjects were then given a subcutaneous injection of 5% formalin into the plantar right hindpaw (20 μl volume), and videotaped digitally for 60 min following the formalin injection. Videotape observations were later sampled for 5 sec at 1-min intervals, and the presence or absence of right hindpaw licking/biting in that 5-sec period was scored. The early/acute phase of the formalin test (F_{early}) was defined as 0-5 min post-injection, and the tonic/late phase (F_{late}) as 5-60 min post-injection. Data are presented as the percentage of samples in each phase in which licking/biting was detected. We and others have shown previously that this method of scoring is highly accurate compared to conventional assessment of total time spent licking/biting (Abbott et al., 1999; Chesler et al., 2003).

Hindpaw edema was quantified in the following manner (Wilson et al., 2002). Immediately at the cessation of testing, mice were sacrificed by cervical dislocation and both hindpaws were severed at the ankle joint and weighed. Edema was expressed as the difference in the weight of the injected versus uninjected paw, as a percentage of body weight.

C.3. RI Strains

The AXB/BXA set of RI strains includes 28 separate strains that have been reinbred to homozygosity from an F_2 hybrid cross between A/J and B6 strains (Nesbitt and Skamene, 1984). Each strain possesses approximately half of its genome derived from the two parental strains, but in different patterns. A consultation of the 811-marker microsatellite database of parental contributions in each strain (Prows and Horner, 2002) revealed nine strains with crossovers in the distal region of Chr. 10. Of these nine RI strains, eight were available from JAX for delivery: AXB-4, AXB-8, AXB-18, AXB-19, BXA-4, BXA-8, BXA-17 and BXA-26. These strains were tested on the formalin test along with A/J and B6 mice (n=5-7/strain) (see Fig. 16).

C.4. RC Strains

The AcB/BcA set of RC strains includes 37 separate strains that have been reinbred to homozygosity from a (F_1 x A/J) x A/J and (F_1 x B6) x B6 double backcross (Fortin et al., 2001). Strains of the AcB set possess approximately 13.25% of their genome from the B6 strain (on an A/J background); strains of the BcA set possess approximately 13.25% of their genome from the A/J strain (on a B6 background). A consultation of the 625-marker microsatellite database of parental contributions in each strain (Fortin et al., 2001) revealed three strains with crossovers in the distal region of Chr. 10. Of these three RC strains, two were available: AcB64 and BcA72. These strains were tested on the formalin test along with A/J and B6 mice and four AcB/BcA "control" RC strains (n=12-29/strain) (see Fig. 17).

C.5. Congenic Line Construction

AcB64 and BcA72 have donor genome from B6 and A/J, respectively, at regions other than distal mouse Chr. 10, including commonly recombinant genome on proximal Chr. 2 (0-15 cM) and mid-Chr. 15 (39-48 cM). Therefore, we used the AcB64 and BcA72 strains to construct speed congenics (A.AcB64^{Nociq2} and B6.BcA72^{Nociq2} lines, respectively). These were generated with marker-assisted selection of breeding males (Wong, 2002), in each backcross generation selecting for marker heterozygosity in the already recombinant Chr. 10 region (i.e., 65-70 cM for AcB64, *D10Mit14-D10Mit103*; 49-70 cM for BcA72, *D10Mit230-D10Mit297*). AcB64 and BcA72 mice were backcrossed to A/J and B6, respectively, for five generations, intercrossed, and separate wild-type and congenic lines then formed. We attempted to form four wild-type and four congenic lines in each case; in the BcA72 project three wild-type and one congenic strain were lost to poor fecundity. The purity of the congenic strains was confirmed by genotyping, and extant strains were tested on the formalin test (n=12-25/strain) (see Fig. 18).

C.6. Microarray Study

Dorsal root ganglia (DRGs) of the L4-L6 level were removed from mice of A/J and C57BL/6 strains, aged from at least six weeks. All mice were injected, as described previously, with either formalin or vehicle. The mice were sacrificed by cervical dislocation after 45 minutes, and tissue extraction immediately followed. The harvested ganglia were immediately placed in a preservation agent, RNAlater (Ambion, Austin, TX), and stored at 4°C until total RNA isolation. Three mice per strain per condition

were used, with no pooling of samples; RNA for each chip was taken from a single individual.

The samples were homogenized with Trizol (Invitrogen, Burlington, ON) and resuspended in 13 μL of nuclease-free water. Integrity and concentration of the total RNA samples were evaluated on the Bioanalyzer 2100 (Agilent, Palo Alto, CA). Isolated RNA (40 ng/μl samples, in a volume of 6 μg) was then sent to the Genome Quebec Innovation Centre, for conversion to labeled cRNA using the small sample protocol established by Affymetrix. Briefly, oligo(dT) primers and reverse transcriptase were used to synthesize double-stranded cDNA using a two step PCR amplification process. The cDNA was then converted by *in vitro* transcription to biotin-labeled cRNA, which was fragmented into roughly 100 bp segments and then hybridized to probes on the chip. Staining with streptavidin phycoerythrin and signal detection were performed on a GeneChip Scanner 3000 (Affymetrix, Santa Clara, CA). The chip used to assay gene expression levels was the Affymetrix MOE430v2 chip, which contains probe sets for about 39,000 transcripts.

We used a 2x2 class comparison experimental design in order to detect expression differences between strains and as a result of formalin treatment. This design also enabled us to look for interactions between strain and treatment conditions. The raw signal intensity data from each condition was normalized using the Robust Multiple-array Average (RMA) method (to account for systematic differences in signal between chips), and averaged across the three replicates. Differences between conditions were assessed by ANOVA, and p-values were computed to test for strain, treatment, and interaction effects. Additionally, a transformed fold change was computed using the formula:

$$\text{fold change} = \log_2([\text{condition 1}]/[\text{condition2}])$$

where condition was defined as signal intensity for either B6/A, or formalin/control, depending on the analysis. A fold change is reported (Table 10) for all genes in which a significant effect was observed ($\alpha = 0.05$), regardless of the magnitude of the change. As this was considered an exploratory analysis, no corrections were made for multiple testing in order to minimize Type II errors.

D. Results

D.1. RI Strains

One-way ANOVAs revealed no significant effect of genotype on F_{early} responding ($F_{10,55} = 1.6, p = 0.14$) or edema ($F_{10,55} = 1.8, p = 0.08$). By contrast, the main effect of genotype on F_{late} licking behavior was highly significant ($F_{10,55} = 11.3, p < 0.001$). Dunnett's (one-way) post-hoc test revealed the following RI strains as *not* significantly higher scoring than A/J: AXB-4, BXA-4. Dunnett's (one-way) case-comparison test revealed the following RI strains as *not* significantly lower scoring than B6: AXB-8, AXB-18, AXB-29, BXA-8, BXA-17, BXA-26. Results, summarized in Fig. 16, were consistent with the presence of a QTL for F_{late} sensitivity distal to *D10Mit35* at 121.9 Mb on Chr. 10.

D.2. RC Strains

One-way ANOVAs revealed no significant effect of genotype on F_{early} responding ($F_{8,171} = 1.9, p = 0.06$). By contrast, the main effect of genotype on F_{late} responding was highly significant ($F_{8,171} = 6.6, p < 0.001$), as was the main effect of genotype on edema ($F_{8,171} = 5.8, p < 0.001$). Note, however, that strain-dependent edema did not show any correlation with F_{late} responding ($r = -0.01$). Dunnett's (one-way) post-hoc performed on

data from A/J and AcB RC strains revealed AcB64 (but not AcB63) as showing significantly higher F_{late} licking behavior than A/J ($p<0.001$). Dunnett's (one-way) post-hoc performed on data from B6 and BcA RC strains revealed BcA72 only as showing significantly lower F_{late} licking behavior than B6 ($p<0.01$). Results, summarized in Fig. 17, were consistent with the presence of a QTL for F_{late} sensitivity between *D10Mit237* (at 119.6 Mb) and *D10Mit103* (at 125.4 Mb).

D.3. Congenic Lines

We collapsed the various A.AcB64^{Nociq2} and B6.BcA72^{Nociq2} wild-type and congenic lines together for analysis. For A.AcB64^{Nociq2}, a highly significant effect of genotype was observed for F_{early} ($F_{1,121} = 17.4$, $p < 0.001$; due to the low F_{early} licking of two wild-type lines, data not shown) and F_{late} ($F_{1,121} = 14.9$, $p < 0.001$), but not for edema ($F_{1,121} = 0.4$, $p = 0.51$). Congenic A.AcB64^{Nociq2} lines displayed higher licking in F_{late} than their wild-type counterparts in every case (see Fig. 18a). For B6.BcA72^{Nociq2}, the effect of genotype on F_{early} and edema was non-significant ($F_{1,77} = 0.04$, $p = 0.84$ and $F_{1,77} = 0.03$, $p = 0.86$, respectively). However, a significant effect of genotype on F_{late} licking was observed ($F_{1,77} = 6.1$, $p < 0.05$), with Dunnett's one-way post-hoc test showing the wild-type line having higher licking than any of the congenic lines (see Fig. 18b).

D.4. Microarray Study

As we were specifically looking for gene expression differences underlying the *Nociq2* QTL, only probe sets derived from Chr. 10 genes will be discussed presently. The microarray analysis (Table 10) identified 54 genes and expressed sequences as differentially regulated ($p<0.05$) between A and B6, only 12 of which were expressed

higher in B6 mice. An interaction between strain and treatment was observed for an additional four genes, two for which expression went up following formalin injection in A and down in B6, and two for which the opposite occurred. No genes on Chr. 10 were detected as being significantly regulated by formalin treatment alone. Of all of the genes identified on Chr. 10, only five are located in the QTL region (roughly corresponding to cytoband D3): *Hmga2* (log-transformed B6 expression 1.1-fold higher than A, $p<0.001$), *Rdh5* (1.4-fold higher in A, $p = 0.002$), *Rnf41* (2.9-fold higher in B6, $p<0.001$) , *Baz2a* (1.7-fold higher in A, $p = 0.003$), and an unidentified RIKEN cDNA clone (1.7-fold higher in A, $p = 0.011$).

E. Discussion

The genetic determinants of nociceptive variability are not yet understood, and although several quantitative trait loci have been implicated in individual differences in pain sensitivity (Mogil et al., 1997a; Furuse et al., 2003; Devor et al., 2005; Mogil et al., 2005), only a couple of the underlying genes have been identified. These genes include the delta-opioid receptor gene *Oprd1* (Mogil et al., 1997a), which appears to be linked to latencies on the hot-plate test, and *Calca*, which predicts paw withdrawal from a radiant heat source (Mogil et al., 2005). Both of the pain tests mentioned assay sensitivity to an acute thermal stimulus, which poorly reflects the types of pain for which patients commonly seek analgesic relief. More clinically relevant pain tests include models of inflammation (e.g., formalin, acetic acid writhing), muscle pain (intramuscular injection of acidic saline) and nerve trauma (e.g., chronic constriction injury, partial-nerve injury).

We have shown that the patterns of strain sensitivity to different pain tests are often highly correlated, such that "clusters" of genetically correlated tests may be

identified (Mogil et al., 1999b; Lariviere et al., 2002). The defining attribute of most of these clusters is the stimulus modality used to evoke the nociceptive response (i.e., thermal, chemical, or mechanical). For example, Spearman rank correlations between tests of chemical/inflammatory pain ranged from 0.41 (for formalin late phase with abdominal constriction induced by magnesium sulfate) to 0.79 (for formalin early phase with abdominal constriction induced by acetic acid) (Mogil et al., 1999b). Such high correlations suggest that a single set of genes is largely responsible for variability in all tests of chemosensation and inflammatory pain. Separate QTL mapping projects have supported this premise; linkage to distal Chr. 10 has been observed in both early and late phase formalin responses (Wilson et al., 2002), the acetic acid writhing test (Hain and Belknap, unpublished data), and arthritis (Dracheva et al., 1999; Yang et al., 1999). Based on these findings, we hypothesized that a single gene within the QTL region (>58 cM) is broadly important to the modulation of inflammatory pain.

Few genes in this interval are recognized as having a role in pain or inflammation, however, so we first endeavored to minimize the confidence region of the QTL. A major limitation of QTL mapping is the poor resolution it allows, due to the small number of crossovers in the F2 generation. In contrast, recombinant populations by definition offer substantially more recombination sites, greatly increasing the precision of QTL localization. We tested several recombinant inbred lines from the AXB/BXA set, which collectively dissected the QTL region into 1.5-3 Mb segments defined by five microsatellite markers. The QTL effect was observed most strongly in the region between 119.6 and 124.7 Mb. An additional analysis, using recombinant AcB/BcA congenic lines, supported the existence of a QTL between 119.6 and 125.4 Mb. Finally,

pure congenic lines confirmed the bidirectional transfer of the QTL locus from A/J and B6 backgrounds between 119.6 and 124.7 Mb, corresponding to 67.5-70 cM.

Despite the tremendous refinement of the QTL interval, over 100 known genes may still be conservatively considered positional candidates (see Table 11 for a full list). A small number may have a tenuous link to pain or inflammation, such as the neuropeptide tachykinin 2 (*Tac2*), the neuronal membrane structural protein tetraspanin 31 (*Tspan31*), prostaglandin E synthase 3 (*Ptges3*), and cyclin-dependent kinase 2 (*Cdk2*). However, none of the genes in the interval suggest themselves as obvious candidates mediating a broad spectrum of inflammatory conditions.

As a complementary approach to our positional localization of the quantitative trait gene, we looked for expression differences in Chr. 10 genes that might be responsible for behavioral variability between A and B6. By identifying significantly strain-regulated genes within the QTL interval, we should be able to distinguish candidates with both linkage and functional evidence supporting a role in formalin response (Aitman et al., 1999; Eaves et al., 2002; Matthews et al., 2005). This strategy has previously been used to explore a number of neurobehavioral phenotypes, including ethanol use (Tabakoff et al., 2003), open field activity (Rodriguez de Ledesma et al., 2005), and the pain-related phenotypes irritable bowel disease (de Buhr et al., 2006) and arthritis (Johannesson et al., 2005). Our analysis demonstrated that distal Chr. 10 harbors many genes with large expression differences between A and B6 strains (strain main effect $p<0.05$); interestingly, however, only a few genes were differentially regulated as a result of formalin treatment (strain x treatment interaction effect $p<0.05$), and none on Chr. 10 were found to be regulated in the same direction in both strains (treatment main effect $p<0.05$). It is probable that behavioral differences produced by the *Nociq2* locus

are related to baseline gene expression patterns in the two strains, rather than a difference in how the strains react to formalin.

If the QTL effect is in fact due to detectable transcript level differences, only regulated genes in the confidence region (67.5-70 cM) can be considered candidates underlying the QTL. A small number of potential candidates were identified by the microarray analysis, but little is known about their function, especially as relating to inflammation or nociceptive mechanisms. The chromosomal architectural transcription factor *Hmga2* (70 cM) is known to be involved in tumorigenesis (Tallini and Dal Cin, 1999). Mutations of the retinol dehydrogenase gene *Rdh5* (72 cM) can have severe implications in the eye (Jang et al., 2001), but no activity is known in the DRG. *Baz2a* and *Rnf41* (located in cytoband D3) both regulate the activity of other genes, but little is known regarding their specific functions. *Baz2a* belongs to a family of bromodomain-containing genes that interact with chromatin remodeling complexes (Jones et al., 2000). *Rnf41* targets proteins, such as epidermal growth factors (Qiu and Goldberg, 2002), neuregulin receptors (Diamonti et al., 2002), and parkin (Zhong et al., 2005), for lysosomal degradation.

The microarray results should be considered exploratory, as they are intended to generate hypothetical candidates for further testing. The specific expression level differences we observed need to be replicated by qRT-PCR, an ongoing effort in our laboratory. A critical next step is to discover functional links between genes with confirmed strain-specific regulation and inflammatory mechanisms, by either interrupting the transcription/translation of the gene, or by pharmacological manipulations at the level of the proteins. Once a gene has been found that appears to regulate the behavioral response to formalin, it should be possible to find the SNP variation within this gene (or

in nearby regulatory regions) between the A/J and C57BL/6 strains responsible for the QTL effects. Alternately, another limitation of this study was its focus on gene expression in the primary nociceptors; extending the search for differentially regulated genes to other CNS structures involved in pain processing may be useful if the QTG is not involved in peripheral nociception, but rather in higher-level pain processing. It is probably imprudent at this point to speculate as to how these findings may translate to clinical advances in pain management, but continuing this work promises to uncover novel gene targets contributing to individual differences in inflammation. Such discoveries may have important implications in the treatment of arthritis, irritable bowel disease, and many other inflammatory disease states.

CHAPTER 7: GENERAL DISCUSSION

The studies described in this work significantly advance our understanding of the genetic determinants of nociception and analgesia in a number of ways. Our most apparent conclusions are the novel candidate genes we have proposed to underlie individual differences in thermal pain, analgesic sensitivity, and formalin response. Additionally, our findings lend support to hypotheses we generated through the use of genetic correlation analysis, confirming the validity of this approach. Finally, the wide range of mapping methodologies we employed has allowed us to evaluate the utility of convergent strategies in QTL discovery.

A. Discovery and evaluation of candidate genes for multiple pain phenotypes

We explored the genetic basis of thermal nociception and its inhibition by opioid and non-opioid drugs in three simultaneous quantitative trait locus mapping projects in a single B6129PF2 population. Combining baseline thermal sensitivity scores from all three experiments allowed us remarkable power to detect small-effect QTLs at high significance levels. Loci on six chromosomes contributed to a multiple QTL model accounting for almost 15% of the phenotypic variability on the 49°C tail-withdrawal test. The two most prominent QTLs, on mid-Chr. 7 (peak 33 cM, C.I. 24-38 cM) and mid-Chr. 11 (peak 46 cM, C.I. 30-55 cM), have not been previously linked to any pain phenotype. These regions contain a number of well-known pain modulatory genes, including those for necdin, the heat transducer, TRPV1, nitric oxide synthase, β2-arrestin, and ion channels of GABAergic and cholinergic types, among others. The identity of the specific genes responsible for the QTLs, however, remains to be investigated.

The full power of our combined dataset also allowed us to map a QTL for sensitivity to multiple analgesic drugs to distal Chr. 1 (80-110 cM), which was subsequently confirmed in separate analyses for the α_2-adrenergic clonidine, the cannabinoid WIN55,212-2, and the μ-opioid morphine. We confirmed and refined the location of this QTL (dubbed *Manr1*) to 90-100 cM (roughly 170-180 Mb) using haplotype-based and congenic strategies. *Kcnj9*, located at 94.2 cM, was identified as the candidate in this interval best suited to modulate analgesia from multiple drug classes. This gene encodes a subunit of the GIRK (G protein-coupled, inwardly rectifying potassium) channel, which is functionally coupled to post-synaptic neurotransmitter receptors of many types; ligand binding at these receptors results in an inhibitory hyperpolarization of the neuron. We demonstrated that mice with the *Kcnj9* gene deleted exhibit substantially attenuated analgesia from clonidine and WIN55,212-2, and that *Kcnj9* expression in the periaqueductal gray is strain-dependent.

Haplotype mapping also pinpointed *Atp1b3* as the gene responsible for the *Nociq1* QTL we previously mapped to Chr. 9 for early phase formalin response. This gene, involved in sodium and potassium exchange across neuronal cell membranes, is differentially regulated in the dorsal root ganglia of mice with different sensitivities to chemosensation. We were able to completely eliminate the strain difference in formalin response using a sodium/potassium channel inhibitor, ouabain.

We used a traditional positional cloning strategy to locate another gene underlying formalin response on Chr. 10. We were able to minimize the confidence interval of the *Nociq2* QTL, using recombinant inbred, recombinant congenic, and speed congenic lines, to about 5 Mb. Although this region contains no obvious candidate genes capable of modulating inflammatory pain response, we generated a short list of differentially

regulated genes in this region using microarray technology. These genes, including *Baz2a and Rnf41*, among others, are currently being investigated for their potential involvement in formalin response.

B. Validation of genetic correlation among pain phenotypes

The impetus for QTL mapping of multiple analgesic phenotypes was a series of strain surveys in which the analgesic potencies of five descending-modulatory drugs were found to be correlated (Wilson et al., 2003), such that a strain's sensitivity to morphine, for example, would predict its relative sensitivity to another drug. The correlation of two different complex traits implies that many of the same determining factors regulate both traits in a similar direction, and such a correlation observed between inbred strains suggests that the relevant factors are genetic (Crabbe et al., 1990). The results of our analgesia strain surveys led us to search for a gene (or genes) broadly involved in descending antinociception, regardless of the initiating receptor type. Our prediction proved correct, as four of the five drugs mapped in our *in silico* analysis were linked to the same interval on distal Chr. 1 we previously mapped using QTL methodology. Convergent evidence suggested that the protein producing the Chr.1 effect was GIRK3, which interacts with the individual receptors for all four drugs (clonidine, morphine, U50,488, and WIN55,212-2) via G protein signaling. The only drug not linked to Chr. 1 was epibatidine, a nicotinic receptor agonist which does not activate G protein mechanisms. It is apparent that other genes must also contribute to analgesia produced by multiple analgesic mechanisms, as the *Manr1* QTL does not itself explain the direction or magnitude of the strain differences we observed. However, we believe that a better understanding of GIRK channel mechanisms has great potential for increasing the

effectiveness of clinical analgesics, especially for people genetically resistant to their therapeutic properties. Although the GIRK channel has been implicated in analgesia produced by multiple drug classes (Blednov et al., 2003; Mitrovic et al., 2003), the primary role of the GIRK3 subunit in variability between normal mouse strains would likely have gone unnoticed without the demonstration of linkage of the phenotype.

Another prediction of our genetic correlation experiments is that pain tests of the same stimulus modality (e.g., thermal, mechanical) partially share genetic mediation (Mogil et al., 1999b). Several loci influencing the withdrawal threshold to an acute heat stimulus have been found using QTL mapping (Mogil et al., 1997a; Mogil et al., 2005), but no overlapping genomic regions have been identified between different pain tests. We mapped two additional prominent thermal pain loci to chromosomes 7 and 11, but interestingly, a smaller effect locus on Chr. 4 appeared very similar to one previously linked to hot-plate sensitivity (Mogil et al., 1997a). Both QTLs were between 45-80 cM, and both appeared to regulate thermal pain sensitivity in male mice only. Pharmacological evidence supported the candidacy of the δ-opioid receptor gene, *Oprd1*, underlying hot-plate sensitivity, and it is highly likely that this gene is similarly responsible for variability in tail-withdrawal latencies in male mice.

C. Evaluation of complementary approaches in complex trait analysis

Although researchers have prolifically identified QTL regions for hundreds of different structural, physiological, and behavioral traits, very few of the nucleotide polymorphisms underlying individual variability in these traits have been conclusively identified. It has therefore been a historically frequent criticism of the technique, that despite the great expenditures of time and resources involved in QTL mapping, it has

been too difficult to translate QTL findings into clinically useful knowledge (Nadeau and Frankel, 2000). Recently, however, a number of mapping strategies have been developed that promise to vastly increase the efficiency of quantitative trait genetics.

The traditional method of isolating a quantitative trait gene has been to clone it by its position, relying on ever-finer recombinant maps in complicated crosses. We successfully employed this technique to reduce the confidence interval of the *Nociq2* QTL to <3 cM. Unfortunately, this appears to be the reasonable extent of the resolution this technique currently allows, with the limited number of recombinant inbred and congenic strains commercially available. In the very near future, however, a powerful tool for the dissection of complex traits will become widely available. A panel of about 1,000 recombinant inbred strains, known as the Collaborative Cross, will be derived from eight parental strains, such that maximal genetic diversity is achieved (Complex Trait Consortium, 2004). This resource will drastically increase the power and resolution of positional cloning efforts.

An alternative to constructing panels of recombinant mice is to take advantage of the genetic diversity already present between inbred strains. Hundreds of thousands of single nucleotide polymorphisms differentiate these strains, and vast numbers of these SNPs have been catalogued in electronic databases (Wang et al., 2005b). We correlated strain means from our analgesia and formalin strain surveys with patterns of SNP variation using *in silico* gene mapping algorithms, with varying levels of success. We only obtained data for seven genotyped strains in the analgesia project, and therefore had to be conservative in our estimation of the QTL location. However, we were able to confirm our prediction that a gene on distal Chr.1 was influencing analgesic magnitude from multiple drugs with this analysis. In the formalin experiment, however, we were

able to correlate the SNP database with the means of sixteen strains, and the added power allowed us to implicate a single gene in early phase formalin response. Clearly, the *in silico* mapping strategy is an efficient and powerful method of pain gene discovery, as we and others (Liang et al., 2006a; Liang et al., 2006b) have demonstrated, provided the number of strains assayed is sufficient. The number of strains needed for adequate statistical power remains controversial (Darvasi, 2001), but as more strains are genotyped, the utility of this technique is sure to increase.

The use of knockout strains to confirm the presence of a QTL can be useful, but there are a number of caveats that must be applied in such an experiment. Even beyond the well-established confounds of epistatic interactions and compensation (Mogil and Grisel, 1998), knockout experiments are especially difficult to interpret in the context of candidate gene identification. Knockout strains serve as useful ready-made B6.129 congenics, in the form of "hitch-hiking" donor genome surrounding the deleted locus near the QTL location (Bolivar et al., 2001). Comparing the knockout/congenic with the corresponding wild-type can confirm the transfer of the QTL allele from the donor to the background strain (assuming the deleted locus itself does not manifest a phenotype). This strategy can eliminate the many months needed to create a new congenic line and breed it to homozygosity. We employed such a strategy using *Fcgr3* knockout mice to isolate the *Manr1* QTL. However, the most common use of knockouts is to confirm the active role of the deleted gene in a phenotype, by noting differences in mice that do not express normal copies of the gene. In most knockout experiments, there is a small chance that a donor gene is responsible for the effect, rather than the deletion. However, if it is already known that a QTL is in the area of the knocked-out gene, it can be practically impossible to eliminate the possibility of a hitch-hiking neighbor causing the effect. This situation

arose in our work with the GIRK3 knockout mice; a robust analgesia phenotype was observed in these mice, but we could not conclusively prove that it was the product of a lack of *Kcnj9* expression. The use of knockouts to confirm a QTL candidate gene is not a reliable standard of proof; future candidate gene studies (in fact, all studies that use knockouts to explore the function of a gene) should be designed to minimize the chance of misinterpretation.

Finally, we examined the global gene expression patterns of formalin-treated mice of two strains by microarray analysis, in order to identify genes within the *Nociq2* interval whose regulation might generate the behavioral differences we observed. Although this strategy is becoming popular, only a few studies of pain-related phenotypes have made use of it (e.g., Johannesson et al., 2005; de Buhr et al., 2006), and we know of no example where a gene has been positively identified as responsible for a QTL by this method. However, for QTL studies in which no candidate genes in the confidence interval are obvious, obtaining expression profiles of all of the genes in the region may prove useful. Our own experiments demonstrated that only a handful of genes within our QTL are differentially regulated between strains, but more work needs to be done to confirm these expression changes and assess their functional consequences. We cannot presently evaluate the value of this strategy with the limited results we have so far obtained, although its potential may shortly be realized as more laboratories make use of it.

D. Translating findings from mice to humans

Our gene mapping experiments have already offered significant insights into the mediation of nociception and descending analgesic mechanisms, but the value of these results is best measured by their practical impact on the clinical relief of pain. In order to

translate our findings to human populations, it must be established that the variability genes we have identified in mice also contribute to individual differences in human pain perception. The most direct means to ascertain the effect of variation within a gene is by association of polymorphisms with the trait, using a case-control study design, for example. Our results suggest that a difference in sensitivity to clonidine would be observed in humans with functionally different alleles of the *KCNJ9* gene; likewise, variation in the *ATP1B3* gene might play a role in differential response to inflammation or inflammatory diseases. Of course, the observance of linkage to a particular gene in the mouse does not necessarily imply that the phenotype will also be linked to that gene in humans, for a number of reasons. The exact polymorphisms between two inbred strains will not be the same among human populations, and the structure and function of the gene itself may be quite dissimilar between species. However, by implicating the GIRK channel in analgesia variability in mice, we have identified an important pathway that probably modulates to some degree analgesic sensitivity in humans as well. Examining all of the genes in this pathway (GIRK1-4, G protein subunits, etc.) for association with analgesia phenotypes should distinguish genes important for human pain variability.

The ultimate goal of such research would be to identify the genetic determinants of pain phenotypes, as risk factors for chronic pain diseases as well as novel targets for therapeutic treatments. A small literature of the pharmacogenomics of analgesia has begun to describe variation in response to opiates and cyclooxygenase inhibitors (Ikeda et al., 2005; Lee, 2006; Lotsch, 2006. However, much more understanding of the genetic mediation of analgesic drugs is needed before a truly individualized approach to medicine is achieved. Similarly, the genetic factors underlying human inflammatory pain conditions are too poorly characterized to adequately predict the onset and development

of chronic disease. As we identify more of the genetic variants and mechanisms which lead to chronic pain diseases, we will better be able to treat the source of the pain, rather than merely alleviate the symptoms. One day, the diagnosis of disease and the prognosis for various treatment possibilities may all be made on a single chip, uniquely tailored to the personal characteristics of the patient.

REFERENCES

Abbott FV, Ocvirk R, Najafee R, Franklin KBJ. Improving the efficiency of the formalin test. Pain 1999;83:561-569.

Aitman TJ, Glazier AM, Wallace CA, Cooper LD, Norsworthy PJ, Wahid FN, Al-Majali KM, Trembling PM, Mann CJ, Shoulders CC, Graf D, St. Lezin E, Kurtz TW, Kren V, Pravenec M, Ibrahimi A, Abumrad NA, Stanton LW, Scott J. Identification of *Cd36* (Fat) as an insulin-resistance gene causing defective fatty acid and glucose metabolism in hypertensive rats. Nat Genet 1999;21:76-83.

Allgayer H, Kruis W, Paumgartner G, Wiebecke B, Brown L, Erdmann E. Inverse relationship between colonic (Na^+, K^+)-ATPase activity and degree of mucosal inflammation in inflammatory bowel disease. Digest Dis Sci 1988;33:417-422.

Bailey DW. Recombinant-inbred strains: An aid to finding identity, linkage and function of histocompatibility and other genes. Transplantation 1971;11:325-327.

Bailey DW. Recombinant inbred strains and bilineal congenic strains. In: HL Foster, JD Small, JG Fox, editors. *The Mouse in Biomedical Research*, Vol. 1. New York: Academic Press, 1981; 223-239.

Bajic D, Proudfit HK. Projections of neurons in the periaqueductal gray to pontine and medullary catecholamine cell groups involved in the modulation of nociception. J Comp Neurol 1999;405:359-379.

Bandler R, Depaulis A. Midbrain periaqueductal gray control of defensive behavior in the cat and the rat. In: R Bandler, A Depaulis, editors. *The Midbrain Periaqueductal Gray Matter*. New York: Plenum Press, 1991; 175-187.

Basbaum AI, Fields HL. Endogenous pain control systems: brainstem spinal pathways and endorphin circuitry. Annu Rev Neurosci 1984;7:309-338.

Beck JA, Lloyd S, Hafezparast M, Lennon-Pierce M, Eppig JT, Festing MFW, Fisher EMC. Genealogies of mouse inbred strains. Nat Genet 2000;24:23-25.

Beecher HK. Pain in men wounded in battle. Ann Surg 1946;123:96-105.

Beitz AJ. The sites of origin of brainstem neurotensin and serotonin projections to the rodent nucleus raphe magnus. J Neurosci 1982;2:829-842.

Belfer I, Wu T, Kingman A, Krishnaraju RK, Goldman D, Max MB. Candidate gene studies of human pain mechanisms: a method for optimizing choice of polymorphisms and sample size. Anesthesiology 2004;100:1562-1572.

Belknap JK, Dubay C, Crabbe JC, Buck KJ. Mapping quantitative trait loci for behavioral traits in the mouse. In: K Blum, EP Noble, editors. *Handbook of Psychiatric Genetics*. New York: CRC Press, 1996;435-453.

Belknap JK, Mogil JS, Helms ML, Richards SP, O'Toole LA, Bergeson SE, Buck KJ. Localization to chromosome 10 of a locus influencing morphine analgesia in crosses derived from C57BL/6 and DBA/2 mouse strains. Life Sci 1995;57:PL117-124.

Belknap JK, O'Toole LA. Studies of genetic differences in response to opioid drugs. In: RA Harris, JC Crabbe, editors. *The Genetic Basis of Alcohol and Drug Actions*. New York: Plenum Press, 1991; 225-252.

Ben-Bassat J, Peretz E, Sulman FG. Analgesimetry and ranking of analgesic drugs by the receptacle method. Arch int Pharmacodyn Ther 1959;122:434-447.

Bergeson SE, Helms ML, O'Toole LA, Jarvis MW, Hain HS, Mogil JS, Belknap JK. Quantitative trait loci influencing morphine antinociception in four mapping populations. Mamm Genome 2001;12:546-553.

Berkley KJ. Sex differences in pain. Behav Brain Sci 1997;20:371-380.

Berrettini WH, Ferraro TN, Alexander RC, Buchberg AM, Vogel WH. Quantitative trait loci mapping of three loci controlling morphine preference using inbred mouse strains. Nat Genet 1994;7:54-58.

Besirli CG, Gong TL, Lomax MI. Novel β_3 isoform of the Na,K-ATPase B subunit from mouse retina. Biochim Biophys Acta 1997;1350:21-26.

Blednov YA, Stoffel M, Alva H, Harris RA. A pervasive mechanism for analgesia: activation of GIRK2 channels. Proc Natl Acad Sci USA 2003;100:277-282.

Blizard DA, Bailey DW. Genetic correlation between open-field activity and defecation: analysis with the CXB recombinant-inbred strains. Behav Genet 1979;9:349-357.

Bolivar VJ, Cook MN, Flaherty L. Mapping of quantitative trait loci with knockout/congenic strains. Genome Res 2001;11:1549-1552.

Bon K, Wilson SG, Mogil JS, Roberts WJ. Genetic evidence for the correlation of deep dorsal horn Fos protein immunoreactivity with tonic formalin pain behavior. J Pain 2002;3:181-189.

Bourinet E, Soong TW, Stea A, Snutch TP. Determinants of the G protein-dependent opioid modulation of neuronal calcium channels. Proc Natl Acad Sci USA 1996;93:1486-1491.

Brennum J, Kjeldsen M, Jensen K, Jensen TS. Measurements of human pressure-pain thresholds on fingers and toes. Pain 1989;38:211-217.

Brinkhaus B, Witt CM, Jena S, Linde K, Streng A, Wagenpfeil S, Irnich D, Walther HU, Melchart D, Willich SN. Acupuncture in patients with chronic low back pain. Arch Intern Med 2006;166:450-457.

Broman KW. Mapping quantitative trait loci in the case of a spike in the phenotype distribution. Genetics 2003;163:1169-1175.

Broman KW, Wu H, Sen S, Churchill GA. R/qtl: QTL mapping in experimental crosses. Bioinformatics 2003;19:889-890.

Caraco Y, Maroz Y, Davidson E. Variability in alfentanil analgesia may be attributed to polymorphism in the μ opioid receptor. Clin Pharmacol Ther 2001;69:63/OII-A-64.

Carlson CS, Eberle MA, Kruglyak L, Nickerson DA. Mapping complex disease loci in whole-genome association studies. Nature 2004;429:446-452.

Chapman CR, Hill HF, Saeger L, Gavrin J. Profiles of opioid analgesia in humans after intravenous bolus administration: alfentanil, fentanyl and morphine compared on experimental pain. Pain 1990;43:47-55.

Chapman WP, Jones CM. Variations in cutaneous and visceral pain sensitivity in normal subjects. J Clin Invest 1944;23:81-91.

Chen ACN, Dworkin SF, Haug J. Human pain responsivity in a tonic pain model: psychological determinants. Pain 1989a;37:143-160.

Chen ACN, Dworkin SF, Haug J, Gehrig J. Topographic brain measures of human pain and pain responsivity. Pain 1989b;37:129-141.

Chen SC, Ehrhard P, Goldowitz D, Smeyne RJ. Developmental expression of the GIRK family of inward rectifying potassium channels: implications for abnormalities in the weaver mutant mouse. Brain Res 1997;778:251-264.

Cherubini E, North RA. Mu and kappa opioids inhibit transmiter release by different mechanisms. Proc Natl Acad Sci USA 1985;82:1860-1863.

Chesler EJ, Ritchie J, Kokayeff A, Lariviere WR, Wilson SG, Mogil JS. Genotype-dependence of gabapentin and pregabalin sensitivity: the pharmacogenetic mediation of analgesia is specific to the type of pain being inhibited. Pain 2003;106:325-335.

Chesler EJ, Rodriguez-Zas SL, Mogil JS. In silico mapping of mouse quantitative trait loci. Science 2001;294:2423.

Chesler EJ, Wilson SG, Lariviere WR, Rodriguez-Zas SL, Mogil JS. Identification and ranking of genetic and laboratory environment factors influencing a behavioral trait, thermal nociception, via computational analysis of a large data archive. Neurosci Biobehav Rev 2002;26:907-923.

Churchill GA, Doerge RW. Empirical threshold values for quantitative trait mapping. Genetics 1994;138:963-971.

Coghill RC, McHaffie JG, Yen Y-F. Neural correlates of interindividual differences in the subjective experience of pain. Proc Natl Acad Sci USA 2003;100:8538-8542.

Collins FS. Positional cloning moves from perditional to traditional. Nat Genet 1997;9:347-350.

Complex Trait Consortium T. The Collaborative Cross, a community resource for the genetic analysis of complex traits. Nat Genet 2004;36:1133-1137.

Crabbe JC, Phillips TJ, Kosobud A, Belknap JK. Estimation of genetic correlation: interpretation of experiments using selectively bred and inbred animals. Alcohol: Clin Exp Res 1990;14:141-151.

Cuppen E. Haplotype-based genetics in mice and rats. Trends Genet 2005;21:318-322.

Darvasi A. Interval-specific congenic strains (ISCS): an experimental design for mapping a QTL into a 1-centimorgan interval. Mamm Genome 1997;8:163-167.

Darvasi A. In silico mapping of mouse quantitative trait loci. Science 2001;294:2423.

Darvasi A. Dissecting complex traits: the geneticists' *'Around the world in 80 days'*. Trends Genet 2005;21:373-376.

Darvasi A, Soller M. Advanced intercross lines, an experimental population for fine genetic mapping. Genetics 1995;141:1199-1207.

Davis KD, Kwan CL, Crawley AP, Mikulis DJ. Functional MRI study of thalamic and cortical activations evoked by cutaneous heat, cold, and tactile stimuli. J Neurophysiol 1998;80:1533-1546.

Day RO, Graham GG, Williams KM, Brooks PM. Variability in response to NSAIDs: fact or fiction? Drugs 1988;36:643-651.

de Bakker PIW, Yelensky R, Pe'er I, Gabriel SB, Daly MJ, Altshuler D. Efficiency and power in genetic association studies. Nature Genet 2005;37:1217-1223.

de Buhr MF, Mahler M, Geffers R, Hansen W, Westendorf AM, Lauber J, Buer J, Schlegelberger B, Hedrich HJ, Bleich A. CD14. Gbp1, and Pla2g2a: three major candidate genes for experimental IBD identified by combining QTL and microarray analyses. Physiol Genomics 2006;25:426-434.

DeFusco M, Marconi R, Silvestri L, Atorino L, Rampoldi L, Morgante L, Ballabio A, Aridon P, Casari G. Haploinsufficiency of *ATP1A2* encoding the Na^+/K^+ pump $\alpha 2$ subunit associated with familial hemiplegic migraine type 2. Nat Genet 2003;33:192-196.

Demant P, Hart AA. Recombinant congenic strains--a new tool for analyzing genetic traits determined by more than one gene. Immunogenetics 1986;24:416-422.

Dempster AP, Laird NM, Rubin DB. Maximum likelihood from incomplete data via the EM algorithm. J Roy Stat Soc 1977;39:1-38.

Descartes R. *L'homme*. Cambridge: Cambridge University Press, 1664.

Devor M. Evidence for heritability of pain in patients with traumatic neuropathy. Pain 2004;108:200-201.

Devor M, Gilad A, Arbilly M, Yakir B, Raber P, Pisante A, Darvasi A. *pain1*: A neuropathic pain QTL on mouse chromosome 15 in a C3HxC58 backcross. Pain 2005;116:289-293.

Diamonti AJ, Guy PM, Ivanof C, Wong K, Sweeney C, Carraway KLr. An RBCC protein implicated in maintenance of steady-state neuregulin receptor levels. Proc Natl Acad Sci USA 2002;99:2866-2871.

Dietrich WF, Miller J, Steen R, Merchant MA, Damron-Boles D, Husain Z, Dredge R, Daly MJ, Ingalls KA, O'Connor TJ, Evans CA, DeAngelis MM, Levinson DM, Kruglyak L, Goodman N, Copeland NG, Jenkins NA, Hawkins TL, Stein L, Page DC, Lander ES. A comprehensive genetic map of the mouse genome. Nature 1996;380:149-152.

Djouhri L, Koutsikou S, Fang X, McMullan S, Lawson SN. Spontaneous pain, both neuropathic and inflammatory, is related to frequency of spontaneous firing in intact C-fiber nociceptors. J Neurosci 2006;26:1281-1292.

Doerge RW. Mapping and analysis of quantitative trait loci in experimental populations. Nature Rev Genet 2002;3:43-52.

Dracheva SV, Remmers EF, Gulko PS, Kawahito Y, Longman RE, Reese VR, Cannon GW, Griffiths MM, Wilder RL. Identification of a new quantitative trait locus on chromosome 7 controlling disease severity of collagen-induced arthritis in rats. Immunogenetics 1999;49:787-791.

Dray A. Inflammatory mediators of pain. Br J Anaesth 1995;75:125-131.

Dubuisson D, Dennis SG. The formalin test: a quantitative study of the analgesic effects of morphine, meperidine, and brain stem stimulation in rats and cats. Pain 1977;4:161-174.

Eaves IA, Wicker LS, Ghandour G, Lyons PA, Peterson LB, Todd JA, Glynne RJ. Combining mouse congenic strains and microarray gene expression analyses to study a complex trait: the NOD model of Type 1 diabetes. Genome Res 2002;12:232-243.

Edwards CL, Fillingim RB, Keefe F. Race, ethnicity and pain. Pain 2001;94:133-137.

Elmer GI, Pieper JO, Negus SS, Woods JH. Genetic variance in nociception and its relationship to the potency of morphine-induced analgesia in thermal and chemical tests. Pain 1998;75:129-140.

Fagerlund TH, Braaten O. No pain relief from codeine.? An introduction to pharmacogenomics. Acta Anaesth Scand 2001;25:140-149.

Falconer DS. Introduction to Quantitative Genetics, Vol. 3. New York: Wiley & Sons, 1989.

Ferraro TN, Golden GT, Smith GG, Martin JF, Lohoff FW, Gieringer TA, Zamboni D, Schwebel CL, Press DM, Kratzer SO, Zhao H, Berrettini WH, Buono RJ. Fine mapping of a seizure susceptibility locus on mouse Chromosome 1: nomination of *Kcnj10* as a causative gene. Mamm Genome 2004;15:239-251.

Fillingim RB, Kaplan L, Staud R, Ness TJ, Glover TL, Campbell CM, Mogil JS, Wallace MR. The A118G single nucleotide polymorphism of the μ-opioid receptor gene (OPRM1) is associated with pressure pain sensitivity in humans. J Pain 2005;6:159-167.

Fillingim RB, Maixner W, Kincaid S, Silva S. Sex differences in temporal summation but not sensory-discriminative processing of thermal pain. Pain 1998;75:121-127.

Flint J, Valdar W, Shifman S, Mott R. Strategies for mapping and cloning quantitative trait genes in rodents. Nature Rev Genet 2005;6:271-286.

Flores CM, Mogil JS. The pharmacogenetics of analgesia: toward a genetically-based approach to pain management. Pharmacogenomics 2001;2:1771-1794.

Flores CM, Wilson SG, Mogil JS. Pharmacogenetic variability in neuronal nicotinic receptor-mediated antinociception. Pharmacogenetics 1999;9:619-625.

Fortin A, Diez E, Rochefort D, Laroche L, Malo D, Rouleau GA, Gros P, Skamene E. Recombinant congenic strains derived from A/J and C57BL/6J: a tool for genetic dissection of complex traits. Genomics 2001;74:21-35.

Frankel WN, Schork NJ. Who's afraid of epistasis? Nat Genet 1996;14:371-373.

Frischknecht H-R, Siegfried B, Waser PG. Opioids and behavior: genetic aspects. Experientia 1988;44:473-481.

Furuse T, Miura Y, Yagasaki K, Shiroishi T, Koide T. Identification of QTLs for differential capsaicin sensitivity between mouse strains KJR and C57BL/6. Pain 2003;105:169-175.

Galer BS, Coyle N, Pasternak GW, Portenoy RK. Individual variability in the response to different opioids: report of five cases. Pain 1992;49:87-91.

Gemignani F, Melli G, Alfieri S, Inglese C, Marbini A. Sensory manifestations in Charcot-Marie-Tooth disease. J Peripher Nerv Syst 2004;9:7-14.

Gora-Maslak G, McClearn GE, Crabbe JC, Phillips TJ, Belknap JK, Plomin R. Use of recombinant inbred strains to identify quantitative trait loci in psychopharmacology. Psychopharmacology 1991;104:413-424.

Griepp ME, Thomas AF. Familial occurrences of reflex sympathetic dystrophy. Clin J Pain 1991;7:48.

Grupe A, Germer S, Usuka J, Aud D, Belknap JK, Klein RF, Ahluwalia MK, Higuchi R, Peltz G. In silico mapping of complex disease-related traits in mice. Science 2001;292:1915-1918.

Hain HS, Belknap JK, Mogil JS. Pharmacogenetic evidence for the involvement of 5-hydroxytryptamine (serotonin)-1B receptors in the mediation of morphine antinociceptive sensitivity. J Pharmacol Exp Ther 1999;291:444-449.

Hakim AJ, Cherkas L, El Zayat S, MacGregor AJ, Spector TD. The genetic contribution to carpal tunnel syndrome in women: a twin study. Arthritis Rheum 2002;47:275-279.

Haley CS, Knott SA. A simple regression method for mapping quantitative trait loci in line crosses using flanking markers. Heredity 1992;69:315-324.

Hargreaves K, Dubner R, Brown F, Flores C, Joris J. A new and sensitive method for measuring thermal nociception in cutaneous hyperalgesia. Pain 1988;32:77-88.

Hazenbos WLW, Gessner JE, Hofhuis FMA, Kuipers H, Meyer D, Heijnen IAFM, Schmidt RE, Sandor M, Capel PJA, Daeron M, van de Winkel JGJ, Verbeek JS. Impaired IgG-dependent anaphylaxis and Arthrus reaction in FcγRIII (CD16) deficient mice. Immunity 1996;5:181-188.

Hegmann JP, Possidente B. Estimating genetic correlations from inbred strains. Behav Genet 1981;11:103-114.

Helmstetter FJ, Fanselow MS. Strain differences in reversal of conditional analgesia by opioid antagonists. Behav Neurosci 1987;101:735-737.

Hitzemann B, Malmanger B, Cooper S, Coulombe S, Reed C, Demarest K, Koyner J, Cipp L, Flint J, Talbot CJ, Radmacher B, Buck KJ, McCaughran JA, Jr. Multiple cross mapping (MCM) markedly improves the localization of a QTL for ethanol-induced activation. Genes Brain Behav 2002;1:214-222.

Hitzemann R, Malmanger B, Reed C, Lawler M, Hitzemann B, Coulombe S, Buck K, Rademacher B, Walter N, Polyakov Y, Sikela J, Gensler B, Burgers S, Williams RW, Manly K, Flint J, Talbot C. A strategy for the integration of QTL, gene expression, and sequence analyses. Mamm Genome 2004;14:733-747.

Holm VA, Cassidy SB, Butler MG, Hanchett JM, Greenswag LR, Whitman BY, Greenberg F. Prader-Willi syndrome: consensus diagnostic criteria. Pediatrics 1993;91:398-402.

Honkasalo M-L, Kaprio J, Winter T, Heikkila K, Sillanpaa M, Koskenvuo M. Migraine and concomitant symptoms among 8167 adult twin pairs. Headache 1995;35:70-78.

Hutchinson MR, LaVincente SF, Somogyi AA. In vitro opioid induced proliferation of peripheral blood immune cells correlates with in vivo cold pressor pain tolerance in humans: a biological marker of pain tolerance. Pain 2004;110:751-755.

IASP Subcommittee on Taxonomy T. Pain terms: a list with definitions and notes on usage. Pain 1979;6:249.

Ikeda K, Ide S, Han W, Hayashida M, Uhl GR, Sora I. How individual sensitivity to opiates can be predicted by gene analyses. Trends Pharmacol Sci 2005;26:311-317.

Ikeda K, Kobayashi T, Kumanishi T, Niki H, Yano R. Involvement of G-protein-activated inwardly rectifying K^+ (GIRK) channels in opioid-induced analgesia. Neurosci Res 2000;38:113-116.

Ikeda K, Kobayashi T, Kumanishi T, Yano R, Sora I, Niki H. Molecular mechanisms of analgesia induced by opioids and ethanol: is the GIRK channel one of the keys? Neurosci Res 2002;44:121-131.

Ingram DK, Corfman TP. An overview of neurobiological comparisons in mouse strains. Neurosci Biobehav Rev 1980;4:421-435.

Jang GF, Van Hooser JP, Kuksa V, McBee JK, He YG, Janssen JJ, Driessen CA, Palczewski K. Characterization of a dehydrogenase activity responsible for oxidation of 11-cis-retinol in the retinal pigment epithelium of mice with a disrupted RDH5 gene. A model for the human hereditary disease fundus albipunctatus. J Biol Chem 2001;276:32456-32465.

Jansen RC. Interval mapping of multiple quantitative trait loci. Genetics 1993;205-211:205-211.

Janssen PAJ, Niemegeers CJE, Dony JGH. The inhibitory effect of fentanyl and other morphine-like analgesics on the warm water induced tail withdrawal reflex. Arzneim-Forschung (Drug Res) 1963;13:502-507.

Jelacic TM, Kennedy ME, Wickman K, Clapham DE. Functional and biochemical evidence for G-protein-gated inwardly rectifying K^+ (GIRK) channels composed of GIRK2 and GIRK3. J Biol Chem 2000;275:36211-36216.

Ji RR. Peripheral and central mechanisms of inflammatory pain, with emphasis on MAP kinases. Curr Drug Targets Inflamm Allergy 2004;3:299-303.

Johannesson M, Olsson LM, Lindqvist A-KB, Moller S, Koczan S, Wester-Rosenlof L, Thiesen H-J, Ibrahim S, Holmdahl R. Gene expression profiling of arthritis using a QTL chip reveals a complex gene regulation of the Cia5 region in mice. Genes Immunol 2005;6:575-583.

Jones MH, Hamana N, Nezu J, Shimane M. A novel family of bromodomain genes. Genomics 2000;63:40-45.

Jorgensen PL, Hakansson KO, Karlish SJD. Structure and mechanism of Na, K-ATPase: functional sites and their interactions. Annu Rev Phsysiol 2003;65:817-849.

Julius D, Basbaum AI. Molecular mechanisms of nociception. Nature 2001;413:203-210.

Kao CH, Zeng Z-B, Teasdale RD. Multiple interval mapping for quantitative trait loci. Genetics 1999;152:1203-1216.

Karlsson J, Johannesson M, Lindvall T, Wernhoff P, Holmdahl R, Andersson A. Genetic interactions in *Eae2* control collagen-induced arthritis and the CD4+/CD8 T cell ratio. J Immunol 2005;174:533-541.

Karschin C, Karschin A. Ontogeny of gene expression of Kir channel subunits in the rat. Mol Cell Neurosci 1997;10:131-148.

Kavaliers M, Choleris E. Sex differences in *N*-methyl-D-aspartate involvement in κ opioid and non-opioid predator-induced analgesia in mice. Brain Res 1997;768:30-36.

Kavaliers M, Hirst M. Daily rhythms of analgesia in mice: effects of age and photoperiod. Brain Res 1983;279:387-393.

Klepstad P, Rakvag TT, Kaasa S, Holthe M, Dale O, Borchgrevink PC, Baar C, Vikan T, Krokan HE, Skorpen F. The 118 A>G polymorphism in the human μ-opioid receptor gene may increase morphine requirements in patients with pain caused by malignant disease. Acta Anaesth Scand 2004;48:1232-1239.

Kobayashi T, Ikeda K, Ichikawa T, Abe S, Togashi S, Kumanashi T. Molecular cloning of a mouse G-protein-activated K^+ channel (mGIRK1) and distinct distributions of three GIRK (GIRK1, 2, and 3) mRNAs in mouse brain. Biochem Biophys Res Commun 1995;208:1166-1173.

Kofuji P, Davidson N, Lester H. Evidence that neuronal G-protein-gated inwardly rectifying K+ channels are activated by Gβγ subunits and function as heteromultimers. Proc Natl Acad Sci USA 1995;92:6542-6546.

Koyrakh L, Lujan R, Colon J, Karschin C, Kurachi Y, Karschin A, Wickman K. Molecular and cellular diversity of neuronal G-protein-gated potassium channels. J Neurosci 2005;25:11468-11478.

Kuwako K, Hosokawa A, Nishimura I, Uetsuki T, Yamada M, Nada S, Okada M, Yoshikawa K. Disruption of the paternal necdin gene diminishes TrkA signaling for sensory neuron survival. J Neurosci 2005;25:7090-7099.

Lander ES, Botstein D. Mapping complex genetic traits in humans: new methods using a complete RFLP linkage map

Lander ES, Botstein D. Mapping Mendelian factors underlying quantitative traits using RFLP linkage maps. Genetics 1989;121:185-199.

Lander ES, Kruglyak L. Genetic dissection of complex traits: guidelines for interpreting and reporting linkage results. Nat Genet 1995;11:241-247.

Lander ES, Schork NJ. Genetic dissection of complex traits. Science 1994;265:2037-2048.

Lariviere WR, Wilson SG, Laughlin TM, Kokayeff A, West EE, Adhikari SM, Wan Y, Mogil JS. Heritability of nociception. III. Genetic relationships among commonly used assays of nociception and hypersensitivity. Pain 2002;97:75-86.

Larsson B, Bille B, Pedersen NL. Genetic influence in headaches: a Swedish twin study. Headache 1995;35:513-519.

Lasagna L, Beecher HK. The optimal dose of morphine. J Am Med Assoc 1954;156:230-234.

Lee Y-S, Kim H, Wu, T-X, Wang X-M, Dionne RA. Genetically mediated interindividual variation in analgesic responses to cyclooxygenase inhibitory drugs. Clin Pharmacol Ther 2006; 79:407-418.

Legare ME, Bartlett FS, II, Frankel WF. A major effect QTL determined by multiple genes in epileptic EL mice. Genome Res 2000;10:42-48.

Levine JD, Gordon NC, Smith R, Fields HL. Analgesic responses to morphine and placebo in individuals with postoperative pain. Pain 1981;10:379-389.

Liang D-Y, Guo TZ, Liao G, Kingery WS, Peltz G, Clark JD. Chronic pain and genetic background interact and influence opioid analgesia, tolerance, and physical dependence. Pain 2006a;121:232-240.

Liang D-Y, Liao G, Wang J, Usuka J, Guo Y, Peltz G, Clark JD. A genetic analysis of opioid-induced hyperalgesia in mice. Anesthesiology 2006b;104:1054-1062.

Liao G, Wang J, Guo J, Allard J, Cheng J, Ng A, Shafer S, Puech A, McPherson JD, Foernzler D, Peltz G, Usuka J. In silico genetics: identification of a functional element regulating *H2-Eα* gene expression. Science 2004;306:690-695.

Libman E. Observations on individual sensitiveness to pain. J Am Med Assoc 1934;102:335-341.

Liebeskind JC, Guilbaud G, Besson JM, Oliveras JL. Analgesia from the electrical stimulation of the periaquaductal gray matter in the cat: behavioral observations and inhibitory effects on spinal cord interneurons. Brain Res 1973;50:441-446.

Lindblad-Toh K, Winchester E, Daly MJ, Wang DG, Hirschhorn JN, Laviolette J-P, Ardlie K, Reich DE, Robinson E, Sklar P, Shah N, Thomas D, Fan J-B, Gingeras T, Warrington J, Patil N, Hudson TJ, Lander ES. Large-scale discovery and genotyping of single-nucleotide polymorphisms in the mouse. Nat Genet 2000;24:381-386.

Liston EH, Simpson JH, Jarvik LF, Guthrie D. Morphine and experimental pain in identical twins. Prog Clin Biol Res 1981;69:105-116.

Lotsch J, Geisslinger G. Current evidence for a genetic modulation of the response to analgesics. Pain 2006;121:1-5.

Luscher C, Jan LY, Stoffel M, Malenka RC, Nicoll RA. G protein-coupled inwardly rectifying K^+ channels (GIRKs) mediate postsynaptic but not presynaptic transmitter actions in hippocampal neurons. Neuron 1997;19:687-695.

Ma D, Zeranque N, Raab-Graham K, Fried SR, Jan YN, Jan LY. Diverse trafficking patterns due to multiple traffic motifs in G protein-activated inwardly rectifying potassium channels from brain and heart. Neuron 2002;33:715-729.

MacGregor AJ, Griffiths GO, Baker J, Spector TD. Determinants of pressure pain threshold in adult twins: evidence that shared environmental influences predominate. Pain 1997;73:253-257.

Maier C, Hildebrandt J, Klinger R, Henrich-Eberl C, Lindena G, Group MS. Morphine responsiveness, efficacy and tolerability in patients with chronic non-tumor associated pain -- results of a double-blind placebo-controlled trial (MONTAS). Pain 2002;97:223-233.

Malmberg AB, Zeitz KP. Studies of pain mechanisms in genetically manipulated mice. In: JS Mogil, editor Book Title|, Vol. Volume|. City|: Publisher|, Year|. p.^pp. Pages|.

Manly KF, Olson JM. Overview of QTL mapping software and introduction to Map Manager QT. Mamm Genome 1999;10:327-334.

Markel P, Shu P, Ebeling C, Carlson GA, Nagle DL, Smutko JS, Moore KJ. Theoretical and empirical issues for marker-assisted breeding of congenic mouse strains. Nat Genet 1997;17:280-284.

Marker CL, Cintora SC, Roman MI, Stoffel M, Wickman K. Hyperalgesia and blunted morphine analgesia in G protein-gated potassium channel subunit knockout mice. Neuroreport 2002;13:2509-2513.

Marker CL, Lujan R, Loh HH, Wickman K. Spinal G-protein-gated potassium channels contribute in a dose-dependent manner to the analgesic effect of μ- and δ- but not κ-opioids. J Neurosci 2005;25:3551-3559.

Marker CL, Stoffel M, Wickman K. Spinal G-protein-gated K+ channels formed by GIRK1 and GIRK2 subunits modulate thermal nociception and contribute to morphine analgesia. J Neurosci 2004;24:2806-2812.

Marshall KE, Godden EL, Yang F, Burgers S, Buck KJ, Sikela JM. *In silico* discovery of gene-coding variants in murine quantitative trait loci using strain-specific genome sequence databases. Genome Biol 2002;3:78.71-78.79.

Marwaha J. Supersensitivity of analgesic responses to α_2-adrenergic agonists in genetically hypertensive rats. Brain Res 1984;304:363-366.

Masocha W, Horvath G, Agil A, Ocana M, Del Pozo E, Szikszay M, Baeyens JM. Role of Na(+), K(+)-ATPase in morphine-induced antinociception. J Pharmacol Exp Ther 2003;306:1122-1128.

Matthews DB, Bhave SV, Belknap JK, Brittingham C, Chesler EJ, Hitzemann RJ, Hoffmann PL, Lu L, McWeeney S, Miles MF, Tabakoff B, Williams RW. Complex genetics of interactions of alcohol and CNS function and behavior. Alcohol: Clin Exp Res 2005;29:1706-1719.

McGrath PA. Psychological aspects of pain perception. Archs Oral Biol 1994;39, Suppl.:55S-62S.

Mechlin MB, Maixner W, Light KC, Fisher JM, Girdler SS. African Americans show alterations in endogenous pain regulatory mechanisms and reduced pain tolerance to experimental pain procedures. Psychosom Med 2005;67:948-956.

Melzack R, Wall PD. Pain mechanisms: A new theory. Science 1965;150:971-979.

Mitrovic I, Margeta-Mitrovic M, Bader S, Stoffel M, Jan LY, Basbaum AI. Contribution of GIRK2-mediated postsynaptic signaling to opiate and α_2-adrenergic analgesia and analgesic sex differences. Proc Natl Acad Sci USA 2003;100:271-276.

Mogil JS. The genetic mediation of individual differences in sensitivity to pain and its inhibition. Proc Natl Acad Sci USA 1999;96:7744-7751.

Mogil JS. Genetic correlations among common nociceptive assays in the mouse: how many types of pain? In: M Devor, MC Rowbotham, Z Wiesenfeld-Hallin, editors. *Proceedings of the 9th World Congress on Pain.* Seattle: IASP Press, 2000; 455-470.

Mogil JS editor. *The Genetics of Pain.* Seattle: IASP Press; 2004.

Mogil JS, Belknap JK. Sex and genotype determine the selective activation of neurochemically-distinct mechanisms of swim stress-induced analgesia. Pharmacol Biochem Behav 1997;56:61-66.

Mogil JS, Grisel JE. Transgenic studies of pain. Pain 1998;77:107-128.

Mogil JS, Kest B, Sadowski B, Belknap JK. Differential genetic mediation of sensitivity to morphine in genetic models of opiate antinociception: influence of nociceptive assay. J Pharmacol Exp Ther 1996;276:532-544.

Mogil JS, Lichtensteiger CA, Wilson SG. The effect of genotype on sensitivity to inflammatory nociception: characterization of resistant (A/J) and sensitive (C57BL/6) inbred mouse strains. Pain 1998;76:115-125.

Mogil JS, Meirmeister F, Seifert F, Strasburg K, Zimmermann K, Reinold H, Austin J-S, Bernardini N, Chesler EJ, Hoffman HA, Hordo C, Messlinger K, Nemmani KVS, Rankin AL, Ritchie J, Siegling A, Smith SB, Sotocinal SB, Vater A, Lehto SG, Klussmann S, Quirion R, Michaelis M, Devor M, Reeh PW. Variable sensitivity to noxious heat is mediated by differential expression of the CGRP gene. Proc Natl Acad Sci USA 2005;102:12938-12943.

Mogil JS, Richards SP, O'Toole LA, Helms ML, Mitchell SR, Belknap JK. Genetic sensitivity to hot-plate nociception in DBA/2J and C57BL/6J inbred mouse strains: possible sex-specific mediation by δ_2-opioid receptors. Pain 1997a;70:267-277.

Mogil JS, Richards SP, O'Toole LA, Helms ML, Mitchell SR, Kest B, Belknap JK. Identification of a sex-specific quantitative trait locus mediating nonopioid stress-induced analgesia in female mice. J Neurosci 1997b;17:7995-8002.

Mogil JS, Sternberg WF, Kest B, Marek P, Liebeskind JC. Sex differences in the antagonism of swim stress-induced analgesia: effects of gonadectomy and estrogen replacement. Pain 1993;53:17-25.

Mogil JS, Wilson SG, Bon K, Lee SE, Chung K, Raber P, Pieper JO, Hain HS, Belknap JK, Hubert L, Elmer GI, Chung JM, Devor M. Heritability of nociception. I. Responses of eleven inbred mouse strains on twelve measures of nociception. Pain 1999a;80:67-82.

Mogil JS, Wilson SG, Bon K, Lee SE, Chung K, Raber P, Pieper JO, Hain HS, Belknap JK, Hubert L, Elmer GI, Chung JM, Devor M. Heritability of nociception. II. "Types" of nociception revealed by genetic correlation analysis. Pain 1999b;80:83-93.

Mogil JS, Wilson SG, Chesler EJ, Rankin AL, Nemmani KVS, Lariviere WR, Groce MK, Wallace MR, Kaplan L, Staud R, Ness TJ, Glover TL, Stankova M, Mayorov A,

Hruby VJ, Grisel JE, Fillingim RB. The melanocortin-1 receptor gene mediates female-specific mechanisms of analgesia in mice and humans. Proc Natl Acad Sci USA 2003;100:4867-4872.

Mogil JS, Yu L, Basbaum AI. Pain genes? natural variation and transgenic mutants. Annu Rev Neurosci 2000;23:777-811.

Moisan M-P. From QTL detection to gene identification. In: BC Jones, P Mormede, editors. *Neurobehavioral Genetics: Methods and Applications*. Boca Raton: CRC Press, 2000.

Moore KJ, Nagle DL. Complex trait analysis in the mouse: the strengths, the limitations and the promise yet to come. Annu Rev Genet 2000;34:653-686.

Morel L, Blenman KR, Croker BP, Wakeland EK. The major murine systematic lupus erythematosus susceptibility locus, Sle1, is a cluster of functionally related genes. Proc Natl Acad Sci USA 2001;98:1787-1792.

Mulder EJ, Van Baal C, Gaist D, al. e. Genetic and environmental influences on migraine: a twin study across six countries. Twin Res 2003;6:422-431.

Murfin R, Bennett J, Mayer DJ. The effect of dorsolateral spinal cord (DLF) lesions on analgesia from morphine microinjections into the periaquaductal gray matter (PAG) of the rat. Soc Neurosci Abstr 1976;2:946.

Myers CD, Robinson ME, Riley JL, III, Sheffield D. Sex, gender, and blood pressure: contributions to experimental pain report. Psychosom Med 2001;63:545-550.

Nabbe KC, Boross P, Holthuysen AE, Sloetjes AW, Kolls JK, Verbeek S, van Lent PL, van Den Berg WB. Joint inflammation and chondrocyte death become independent of Fcgamma receptor type III by local overexpression of interferon-gamma during complex-mediated arthritis. Arthritis Rheum 2005;52:967-974.

Nadeau JH, Frankel WN. The roads from phenotypic variation to gene discovery: mutagenesis versus QTLs. Nat Genet 2000;25:381-384.

Nesbitt MN, Skamene E. Recombinant inbred mouse strains derived from A/J and C57BL/6J: a tool for the study of genetic mechanisms in host resistance to infection and malignancy. J Leukoc Biol 1984;36:357-364.

Ocana M, Cendan CM, Cobos EJ, Entrena JM, Baeyens JM. Potassium channels and pain: present realities and future opportunities. Eur J Pharmacol 2004;500:203-219.

Onaivi ES, Chakrabarti A, Gwebu ET, Chaudhuri G. Neurobehavioral effects of D9-THC and cannabinoid (CB1) receptor gene expression in mice. Behav Brain Res 1996;72:115-125.

Paigen K, Eppig JT. A mouse phenome project. Mamm Genome 2000;11:715-717.

Pellegrino MJ, Waylonis GW, Sommer A. Familial occurrence of primary fibromyalgia. Arch Phys Med Rehabil 1989;70:61-63.

Plomin R, McClearn GE, Gora-Maslak G, Neiderhiser JM. Use of recombinant inbred strains to detect quantitative trait loci associated with behavior. Behav Genet 1991;21:99-116.

Portenoy KM, Foley KM, Inturrisi CE. The nature of opioid responsiveness and its implications for neuropathic pain: new hypotheses derived from studies of opioid infusions. Pain 1990;43:273-286.

Poulsen L, Brosen K, Arendt-Nielsen L, Gram LF, Elbaek K, Sindrup SH. Codeine and morphine in extensive and poor metabolizers of sparteine: pharmacokinetics, analgesic effect and side effects. Eur J Clin Pharmacol 1996;51:289-295.

Prows DR, Horner ML. Parental genetic contributions in the AXB and BXA recombinant inbred mouse strains. Mamm Genome 2002;13:127-133.

Qiu XB, Goldberg AL. Nrdp1/FLRF is a ubiquitin ligase promoting ubiquitination and degredation of the epidermal growth factor receptor family member, ErbB3. Proc Natl Acad Sci USA 2002;99:14843-14848.

Rady JJ, Elmer GI, Fujimoto JM. Opioid receptor selectivity of heroin given intracerebroventricularly differs in six strains of inbred mice. J Pharmacol Exp Ther 1998;288:438-445.

Rainville P, Duncan GH, Price DD, Carrier B, Bushnell MC. Pain affect encoded in human anterior cingulate but not somatosensory cortex. Science 1997;277:968-971.

Rakvag TT, Klepstad P, Baar C, Kvam T-M, Dale O, Kaasa S, Krokan HE, Skorpen F. The Val158Met polymorphism of the human catechol-*O*-methyltransferase (COMT) gene may influence morphine requirements in cancer pain patients. Pain 2005;116:73-78.

Rasmusson JM. A contribution to the theory of quantitative character inheritance. Hereditas 1933;18:245-261.

Reynolds DV. Surgery in the rat during electrical analgesia induced by focal brain stimulation. Science 1969;164:444-445.

Rikke BA, Johnson TE. Towards the cloning of genes underlying murine QTLs. Mamm Genome 1998;9:963-968.

Risch NJ. Searching for genetic determinants in the new millennium. Nature 2000;405:847-856.

Rodriguez de Ledesma AM, Desai AN, Bolivar VJ, Symula DJ, Flaherty L. Two new behavioral QTLs, *Emo4* and *Reb1*, map to mouse chromosome 1: congenic strains and candidate gene identification studies. Mamm Genome 2005;17:111-118.

Romberg RR, Olofsen E, Bijl H, Taschner PE, Teppema LJ, Sarton EY, van Kleef JW, Dahan A. Polymorphism of mu-opioid receptor gene (OPRM1:c.118A>G) does not protect against opioid-induced respiratory depression despite reduced analgesic response. Anesthesiology 2005;102:522-530.

Rosenthale ME. A comparative study of the Lewis and Sprague Dawley rat in adjuvant arthritis. Arch int Pharmacodyn 1970;188:14-22.

Saban MR, Nguyen NB, Hammond TG, Saban R. Gene expression profiling of mouse bladder inflammatory responses to LPS, substance P, and antigen-stimulation. Am J Pathol 2002;160:2095-2110.

Sadja R, Alagem N, Reuveny E. Gating of GIRK channels: details of an intricate, membrane-delimited signaling complex. Neuron 2003;39:9-12.

Sanchez-Blazquez P, Rodriguez-Diaz M, Lopez-Fando A, Rodriguez-Munoz M, Garzon J. The GBeta5 subunit that associates with the R7 subfamily of RGS proteins regulates mu-opioid effects. Neuropharmacology 2003;45:82-95.

Sandberg R, Yasuda R, Pankratz DG, Carter TA, Del Rio JA, Wodicka L, Mayford M, Lockhart DJ, Barlow C. Regional and strain-specific gene expression mapping in the adult mouse brain. Proc Natl Acad Sci USA 2000;97:11038-11043.

Sato J, Morimae H, Seino Y, Kobayashi T, Suzuki N, Mizumura K. Lowering barometric pressure aggravates mechanical allodynia and hyperalgesia in a rat model of neuropathic pain. Neurosci Lett 1999;266:21-24.

Sax K. The association of size differences with seed-coat pattern and pigmentation in *Phaseolus vulgaris*. Genetics 1923;8:552-560.

Schalkwyk LC, Jung M, Daser A, Weiher M, Walter J, Himmelbauer H, Lehrach H. Panel of microsatellite markers for whole-genome scans and radiation hybrid mapping and a mouse family tree. Genome Res 1999;9:878-887.

Schmader KE. Epidemiology and impact on quality of life of postherpetic neuralgia and painful diabetic neuropathy. Clin J Pain 2002;18:350-354.

Schoots O, Wilson JM, Ethier N, Bigras E, Hebert TE, van Tol HHM. Co-expression of human Kir3 subunits can yield channels with different functional properties. Cell Signal 1999;11:871-883.

Seltzer Z, Wu T, Max MB, Diehl SR. Mapping a gene for neuropathic pain-related behavior following peripheral neurectomy in the mouse. Pain 2001;93:101-106.

Sen S, Churchill GA. A statistical framework for quantitative trait mapping. Genetics 2001;159:371-387.

Sheps DS, McMahon RP, Light KC, Maixner W, Pepine CJ, Cohen JD, Goldberg AD, bonsall R, Carney R, Stone PH, Sheffield D, Kaufmann PG. Low hot pain threshold predicts shorter time to exercise-induced angina: results from the psychophysiological investigations of myocardial ischemia (PIMI) study. J Am Coll Cardiol 1999;33:1855-1862.

Sherman ED. Sensitivity to pain. Can Med Assoc J 1943;45:437-441.

Shieh CC, Coghlan M, Sullivan JP, Gopalakrishnan M. Potassium channels: molecular defects, diseases, and therapeutic opportunities. Pharmacol Rev 2000;52:557-594.

Shir Y, Ratner A, Raja SN, Campbell JN, Seltzer Z. Neuropathic pain following partial nerve injury in rats is suppressed by dietary soy. Neurosci Lett 1998;240:73-76.

Signorini S, Liao YJ, Duncan SA, Jan LY, Stoffel M. Normal cerebellar development but susceptibility to seizures in mice lacking G protein-coupled, inwardly rectifying K^+ channel GIRK2. Proc Natl Acad Sci USA 1997;94:923-927.

Silver LE. Mouse Genetics: Concepts and Applications. New York: Oxford University Press, 1995.

Sindrup SH, Brosen K. The pharmacogenetics of codeine hypoalgesia. Pharmacogenetics 1995;5:335-346.

Sindrup SH, Brosen K, Bjerring P, Arendt-Nielsen L, Larsen U, Angelo HR, Gram LF. Codeine increases pain thresholds to copper vapor laser stimuli in extensive but not poor metabolizers of sparteine. Clin Pharmacol Ther 1990;48:686-693.

Skokowa J, Ali SR, Felda O, Kumar V, Konrad S, Shushakova N, Schmidt RE, Piekorz RP, Nurnberg B, Spicher K, Birnbaumer L, Zwirner J, Claassens JW, Verbeek JS, van Rooijen N, Kohl J, Gessner JE. Macrophages induce the inflammatory response in the pulmonary Arthrus reaction through G alpha i2 activation that controls C5aR and Fc receptor cooperation. J Immunol 2005;174:3041-3050.

Stephan M, Helfritz F, Pabst R, von Horsten S. Postnatally induced differences in adult pain sensitivity depend on genetics, gender and specific experiences: reversal of maternal deprivation effects by additional postnatal tactile stimulation or chronic imipramine treatment. Behav Brain Res 2002;13:149-158.

Stone LS, Wilcox GL. Alpha-2-adrenergic and opioid receptor additivity in rat locus coeruleus neurons. Neurosci Lett 2004;361:265-268.

Stormorken H, Brosstad F. Fibromyalgia: family clustering and sensory urgency with early onset indicate genetic predisposition and thus a "true" disease. Scandinavian Journal of Rheumatology 1992;21:207.

Sudakov SK, Borisova EV, Lyupina YV. Influence of inheritance and fostering on sensitivity to effects of morphine on nociception and locomotor activity in two inbred rat strains. Neuropharmacology 1996;35:1131-1134.

Symula DJ, Frazer KA, Ueda Y, Denefle P, Stevens ME, Wang Z-E, Locksley R, Rubin EM. Functional screening of an asthma QTL in YAC transgenic mice. Nat Genet 1999;23:241-244.

Tabakoff B, Bhave SV, Hoffman PL. Selective breeding, quantitative trait locus analysis, and gene arrays identify candidate genes for complex drug-related behaviors. J Neurosci 2003;23:4491-4498.

Takagi H, Inukai T, Nakama M. A modification of Haffner's method for testing analgesics. Japan J Pharmacol 1966;16:287-294.

Takeshige C, Murai M, Tanaka M, Hachisu M. Parallel individual variations in the effectiveness of acupuncture, morphine analgesia, and dorsal PAG-SPA and their abolition by D-phenylalanine. Adv Pain Res Ther 1983;5:563-569.

Tallarida RJ, Murray RB. *Manual of Pharmacologic Calculation.* New York: Springer-Verlag, 1981.

Tallini G, Dal Cin P. HMGI(Y) and HMGI-C dysregulation: a common occurrence in human tumors. Adv Anat Pathol 1999;6:237-246.

Tham SM, Angus JA, Tudor EM, Wright CE. Synergistic and additive interactions of the cannabinoid agonist CP55,940 with mu opioid receptor and alpha2-adrenoceptor agonists in acute pain models in mice. Br J Pharmacol 2005;144:875-884.

Thoday JM. Location of polygenes. Nature 1961;191:368-370.

Tiurina IV, Rusakov DI, Sudakov SK. The genetic characteristics of the brain alpha$_2$-adrenergic and S_2-serotonergic systems in the realization of the tail-jerk pain reflex

and its morphine suppression in rats. Eksperimentalnaia i Klinicheskaia Farmakologiia 1995;58:22-24.

Tjolsen A, Berge O-G, Hunskaar S, Rosland JH, Hole K. The formalin test: an evaluation of the method. Pain 1992;51:5-17.

Tjolsen A, Hole K. The tail-flick latency is influenced by skin temperature. APS J 1993;2:107-111.

Torrecilla M, Marker CL, Cintora SC, Stoffel M, Williams JT, Wickman K. G-protein-gated potassium channels containing Kir3.2 and Kir3.3 subunits mediate the acute inhibitory effects of opioids on locus ceruleus neurons. J Neurosci 2002;22:4328-4334.

Treloar SA, Martin NG, Heath AC. Longitudinal genetic analysis of menstrual flow, pain, and limitation in a sample of Australian twins. Behav Genet 1998;28:107-116.

Uhl GR, Sora I, Wang Z. The μ opiate receptor as a candidate gene for pain: polymorphisms, variations in expression, nociception, and opiate responses. Proc Natl Acad Sci USA 1999;96:7752-7755.

Vaccarino AL, Tasker RAR, Melzack R. Systemic administration of naloxone produces analgesia in BALB/c mice in the formalin pain test. Neurosci Lett 1988;84:103-107.

Wade CM, Kulbokas EJ, III, Kirby AW, Zody MC, Mullikin JC, Lander ES, Lindblad-Toh K, Daly MJ. The mosaic structure of variation in the laboratory mouse genome. Nature 2002;420:574-578.

Wall PD, Devor M, Inbal R, Scadding JW, Schonfeld D, Seltzer Z, Tomkiewicz MM. Autotomy following peripheral nerve lesions: experimental anaesthesia dolorosa. Pain 1979;7:103-113.

Wang J, Liao G, Cheng J, Nguyen A, Guo J, Chou C, Hu S, al. e. Haplotype structure of the mouse genome. In: G Peltz, editor. *Computational Genetics and Genomics: New Tools for Understanding Disease*. Totowa, NJ: Humana Press, 2005; 71-84.

Wang J, Liao G, Usuka J, Peltz G. Computational genetics: from mouse to human. Trends Genet 2005b;21:526-532.

Wang J, Peltz G. Haplotype-based computational genetic analysis in mice. In: G Peltz, editor. *Computational Genetics and Genomics: Tools for Understanding Disease*. Totowa, NJ: Humana Press, 2005; 51-70.

Waterston RH, al. e. Initial sequencing and comparative analysis of the mouse genome. Nature 2002;420:520-562.

Wickman K, Nemec J, Gendler SJ, Clapham DE. Abnormal heart rate regulation in *GIRK4* knockout mice. Neuron 1998;20:103-114.

Wickman K, Pu WT, Clapham DE. Structural characterization of the mouse *Girk* genes. Gene 2002;284:241-250.

Widy-Tyszkiewicz E, Mierzejewski P, Kohutnicka M, Czlonkowski A. Cold water stress induced analgesia in unilateral inflammation of the hindpaw in hypertensive and normotensive rats. Pol J Pharmacol 1995;47:313-320.

Wilberg M, Blomqvist A. Somatosensory projection to the mesencephalon: an anatomical study in the monkey. J Comp Neurol 1987;264:92-117.

Willis WD, Westlund KN. Neuroanatomy of the pain system and of the pathways that modulate pain. J Clin Neurophysiol 1997;14:2-31.

Wilson SG, Chesler EJ, Hain HS, Rankin AL, Schwarz JZ, Call SB, Murray MR, West EE, Teuscher C, Rodriquez-Zas S, Belknap JK, Mogil JS. Identification of

quantitative trait loci for chemical/inflammatory nociception in mice. Pain 2002;96:385-391.

Wilson SG, Smith SB, Chesler EJ, Melton KA, Haas JJ, Mitton BA, Strasburg K, Hubert L, Rodriguez-Zas SL, Mogil JS. The heritability of antinociception: common pharmacogenetic mediation of five neurochemically distinct analgesics. J Pharmacol Exp Ther 2003;304:547-559.

Wischmeyer E, Doring F, Wischmeyer E, Spauschus A, Thomzig A, Veh R, Karschin A. Subunit interactions in the assembly of neuronal Kir3.0 inwardly rectifying K^+ channels. Mol Cell Neurosci 1997;9:194-206.

Wolff BB, Kantor TG, Jarvik ME, Laska E. Response of experimental pain to analgesic drugs. I. Morphine, aspirin, and placebo. Clin Pharmacol Ther 1965;7:224-238.

Wong AMK, Leong CP, Su TY, Yu SW, Tsai WC, Chen CPC. Clinical trial of acupuncture for patients with spinal cord injuries. Am J Phys Med Rehabil 2003;82:21-27.

Wong GT. Speed congenics: applications for transgenic and knock-out mouse strains. Neuropeptides 2002;36:230-236.

Woolf CJ, Costigan M. Transcriptional and posttranslational plasticity and the generation of inflammatory pain. Proc Natl Acad Sci USA 1999;96:7723-7730.

Yaksh TL, Al-Rodhan NR, Jensen TS. Sites of action of opiates in production of analgesia. Prog Brain Res 1988;77:371-394.

Yalcin B, Willis-Owen SAG, Fullerton J, Meesaq A, Deacon RM, Rawlins JNP, Copley RR, Morris AP, Flint J, Mott R. Genetic dissection of a behavioral quantitative trait locus shows that *Rgs2* modulates anxiety in mice. Nat Genet 2004;36:1197-1202.

Yamada M, Inanobe A, Kurachi Y. G protein regulation of potassium ion channels. Pharmacol Rev 1998;50:723-757.

Yang H-T, Jirholt J, Svensson L, Sundvall M, Jansson L, Pettersson U, Holmdahl R. Identification of genes controlling collagen-induced arthritis in mice: striking homology with susceptibility loci previously identified in the rat. J Immunol 1999;163:2916-2921.

Zeng W, Dohi S, Shimonaka H, Asano T. Spinal antinociceptive action of Na^+, K^+ pump inhibitor ouabain and its interaction with morphine and lidocaine in rats. Anesthesiology 1999;90:500-508.

Zhang R-X, Lao L, Qiao J-T, Ruda MA. Strain differences in pain sensitivity and expression of preprodynorphin mRNA in rats following peripheral inflammation. Neurosci Lett 2003;353:213-216.

Zhang S, Lou Y, Amstein TM, Anyango M, Mohibullah N, Osoti A, Stancliffe D, King R, Iraqi F, Gershenfeld HK. Fine mapping of a major locus on Chromosome 10 for exploratory and fear-like behavior in mice. Mamm Genome 2005;16:306-318.

Zhong L, Tan Y, Zhou A, Yu Q, Zhou J. RING finger ubiquitin-protein isopeptide ligase Nrdp1/FLRF regulates parkin stability and activity. J Biol Chem 2005;280:9425-9430.

Zubieta J-K, Heitzeg MM, Smith YR, Bueller JA, Xu K, Xu Y, Koeppe RA, Stohler CS, Goldman D. COMT *val*^{158}*met* genotype affects μ-opioid neurotransmitter responses to a pain stressor. Science 2003;299:1240-1243.

Appendix A: Tables

Table 1: Quantitative trait loci contributing to variability in pain- and analgesia phenotypes

QTL name	Chrom.	Location (cM)[a]	Phenotype	Population[b]	Candidate gene	Reference
Nociception						
Capsq1	2	17 – 47.5	Capsaicin intake	KJRB6F2		(Furuse *et al.*, 2003)
Tpnr1	4	50 – 80	Hot-plate	BXD/Ty RI, B6D2F2	*Oprd1*	(Mogil et al., 1997a)
Capsq2	6	3.5 – 24.5	Capsaicin intake	KJRB6F2		(Furuse *et al.*, 2003)
Capsq3	6	44 – 57.5	Capsaicin intake	KJRB6F2		(Furuse *et al.*, 2003)
Tpnr2	7	34 – 62	Hargreaves' test	B6AKRF2, B6CF2, A.B6-*Tyr*$^{+}$/J congenic	*Calca*	(Mogil *et al.*, 2005)
Capsq4	8	21 – 43	Capsaicin intake	KJRB6F2		(Furuse *et al.*, 2003)
Nociq1	9	44 – 68	Formalin (early)	B6AF2, haplotype		(Wilson *et al.*, 2002)
Nociq2	10	69 – 70	Formalin (late)	B6AF2, AcB/BcA RC, ISSC		(Wilson *et al.*, 2002)
Nociq3	12	50 – 54	Formalin (late)	B6.MOLF congenic, ISSC		Unpublished data
Pain1	15	41 – 46	Autotomy	AXB/BXA RI		(Seltzer *et al.*, 2001)
Tpnr3	17	6.5 – 19	Hot-plate, tail-withdrawal, Hargreaves' test	B6.MOLF congenic		Unpublished data
Analgesia						
Morph1	1	0 – 20	Morphine	BXD/Ty RI, B6D2F2		(Bergeson *et al.*, 2001)
Siafq1	8	51 – 81	Stress-induced analgesia, U50,488	BXD/Ty RI, B6D2F2	*Mc1r*	(Mogil *et al.*, 2003)
Morph2	9	10 – 30	Morphine	BXD/Ty RI, B6D2F2		(Bergeson *et al.*, 2001)
Morph3	9	32 – 52	Morphine	BXD/Ty RI, B6D2F2	*Htr1b*	(Bergeson *et al.*, 2001)
Morph4	10	0 – 18	Morphine	BXD/Ty RI, B6D2F2	*Oprm*	(Bergeson *et al.*, 2001)

All of the QTLs shown above are significant based on permutation analysis, with LOD scores > 3 in every case.
[a]Confidence interval (95%) based on a 1-LOD drop off. In some cases, confidence intervals are based on known congenic donor regions.
[b]Mapping population abbreviations are by standard nomenclature or as stated in the text. Other abbreviations: haplotype: *in silico* haplotype mapping using inbred strain means; ISSC: interval-specific subcongenic; RC: recombinant congenic strains.

Table 2. Multiple QTL model for tail-withdrawal sensitivity

Chr	Pos	LOD	%Var	F value	p value
3	81	3.0	1.3	6.7	0.001 **
4	56	2.9	1.3	3.3	0.011 *
6	28	3.7	1.6	8.4	0.0003 ***
7	28	10.4	4.7	24.2	6.2e-11 ***
11	40	6.8	3.0	15.7	2.1e-07 ***
14	3	3.3	1.5	7.6	0.0005 ***
sex		3.3	1.5	5.0	0.002 **
4*sex		2.4	1.1	5.4	0.005 **
Full Model		**31.3**	**14.9**		**0*** **

Signif. codes: `***' p<0.001 `**'p< 0.01 `*'p< 0.05

Table 3. Multiple QTL models for clonidine and WIN55,212-2 analgesia

Chr	Pos	LOD	%Var	F value	p value
Clonidine					
1	100	3.2	4.7	7.4	0.00072 ***
19	15	1.9	2.8	4.4	0.013 **
Full Model		**5.4**	**8.3**		**5.49e-05*** **
WIN55,212					
1	100	3.7	4.4	8.2	0.00033 ***
4	60	1.5	1.8	3.3	0.039 *
7	40	4.0	4.8	8.9	0.00017 ***
9	15	3.5	4.2	7.9	0.00044 ***
10	20	1.8	2.1	3.9	0.021*
11	75	3.6	4.3	8.0	0.00041***
19	52	3.2	3.8	7.1	0.00099***
Full Model		**18.5**	**25.1**		**9.15e-12*** **

Signif. codes: `***' p<0.001 `**' p<0.01 `*' p<0.05

Table 4. Z-scores of analgesia sensitivity in 12 inbred strains

	CLON	EPI	MOR	U50	WIN	Average
129	-0.96	-0.81	-0.92	-0.95	-0.61	-0.85
A	-0.88	-1.05	-0.47	-0.74	-0.62	-0.75
AKR	-0.88	1.69	-0.34	-0.37	2.78	0.57
C57BL/10	*1.22*	*0.25*	*0.75*	*0.19*	*1.10*	*0.70*
C57BL/6	1.53	-0.29	0.63	1.46	-0.06	0.65
BALB/c	-0.76	-1.05	-0.16	-1.07	-0.56	-0.72
C3H/He	*-0.68*	*1.13*	*-0.85*	*0.60*	*-0.53*	*-0.07*
C58	*1.13*	*0.07*	*2.48*	*1.63*	*0.09*	*1.08*
CBA	-0.52	1.69	-0.52	1.15	-0.39	0.28
DBA/2	-0.85	-0.77	-0.86	-0.98	-0.60	-0.81
RIIIS	*0.95*	*-0.61*	*-0.53*	*-0.90*	*-0.40*	*-0.30*
SM	0.71	-0.24	0.80	-0.02	-0.20	0.21

Strains not included in the haplotype analysis (see text) are in *italics*.

Table 5: Known genes in the *Manr1* QTL region

112 genes between 90.0 and 100.0 cM

cM	Genome Coordinates	Symbol, Name
92.6	162739089-162775862 (-)	***Fmo1***, flavin containing monooxygenase 1
92.6	162863114-162893805 (-)	***Fmo3***, flavin containing monooxygenase 3
90.0	169911824-170044739 (-)	***Ddr2***, discoidin domain receptor family, member 2
90.0		***py***, polydactyly
92.1		***ge***, greige
92.1		***sea***, sepia
	170076181-170109124 (-)	***Uap1***, UDP-N-acetylglucosamine pyrophosphorylase 1
	170133434-170149571 (-)	***Uhmk1***, U2AF homology motif (UHM) kinase 1
	170211498-170220947 (+)	***Sh2dib***, SH2 domain protien 1B
	170252650-170555485 (-)	***Nos1ap***, nitric oxide synthase 1 (neuronal) adaptor protein
	170579571-170617530 (+)	***Olfml2b***, olfactomedin-like 2B
	170641955-170802509 (-)	***Atf6***, activating transcription factor 6
	170808930-170820205 (-)	***Dusp12***, dual specificity phosphatase 12
	170852642-170863035 (-)	***Fcrla***, Fc receptor-like A
92.3	170895468-170911110 (-)	***Fcgr2b***, Fc receptor, IgG, low affinity IIb
92.29	170954178-170964934 (+)	***Fcgr3a***, Fc fragment of IgG, low affinity IIIa, receptor
92.3	170986419-170994876 (-)	***Fcgr3***, Fc receptor, IgG, low affinity III
	171056007-171079446 (-)	***Sdhc***, succinate dehydrogenase complex, subunit C, integral membrane protein
92.4	171079554-171089963 (+)	***Mpz***, myelin protein zero
	171102106-171125875 (-)	***Pcp411***, Purkinje cell protein 4-like 1
92.6	171142876-171147684 (+)	***Nr1i3***, nuclear receptor subfamily 1, group I, member 3
92.6	171153929-171155210 (+)	***Apoa2***, apolipoprotein A-II
93.3	171158412-171163129 (-)	***Fcer1g***, Fc receptor, IgE, high affinity I, gamma polypeptide
	171163700-171175952 (-)	***Ndufs2***, NADH dehodrogenase (ubiquinone) Fe-S protein 2
92.3	171179261-171189477 (+)	***Adamts4***, a disintegrin-like and metallopeptidase (reprolysin type) with thrombospondin type 1 motif, 4
92.6	171199228-171205735 (+)	***B4galt3***, UDP-Gal:betaGlcNAc beta 1,4-galactosyltransferase, polypeptide 3
	171205832-171210000 (-)	***Ppox***, protoporphyrinogen oxidase
92.6	171210798-171216801 (-)	***Usp21***, ubiquitin specific peptidase 21
93.0	171217404-171223822 (-)	***Ufc1***, ubiquitin-fold modifier conjugating enzyme 1
90.0	171260093-171270456 (+)	***Dedd***, death effector domain-containing
92.6	171269418-171274446 (-)	***Nit1***, nitrilase 1
92.6	171274539-171287010 (+)	***Pfdn2***, prefoldin 2
	171299238-171317438 (+)	***Pvrl4***, poliovirus receptor-related 4
	171317852-171339082 (+)	***Arhgap30***, Rho GTPase activating protein 30
93.3	171340521-171347583 (+)	***Usf1***, upstream transcription factor 1
93.3	171366401-171393433 (+)	***F11r***, F11 receptor
	171432318-171433590 (+)	***Refbp2***, RNA and export factor binding protein 2
	171446963-171464133 (-)	***Itlna***, intelectin a
	171446963-171464124 (-)	***Itlnb***, intelectin b
93.0	171488165-171514158 (+)	***Cd244***, CD244 natural killer cell receptor 2B4
93.1		***Lsd***, lymphocyte stimulating determinant
93.3	171517472-171536198 (-)	***Ly9***, lymphocyte antigen 9
	171561243-171581877 (-)	***Slamf7***, SLAM family member 7
93.3	171610849-171634096 (+)	***Cd48***, CD48 antigen
93.3	171695971-171730016 (+)	***Slamf1***, signaling lymphocytic activation molecule family member 1
93.3	171769444-171817526 (+)	***Cd84***, CD84 antigen
93.4	171931510-171957364 (-)	***Ltap***, loop tail associated protein

93.4	171981215-171986491 (-)	***Nhlh1***, nescient helix loop helix 1
93.5	171994941-172011669 (-)	***Ncstn***, nicastrin
93.5	172011723-172051248 (+)	***Copa***, coatomer protein complex subunit alpha
93.6	172055682-172065417 (+)	***Pex19***, peroxisome biogenesis factor 19
93.7	172077062-172125309 (+)	***Wdr42a***, WD repeat domain 42A
93.8	172081688-172129499 (-)	***Pea15***, phosphoprotein enriched in astrocytes 15
94.0	172138821-172148753 (-)	***Casq1***, calsequestrin 1
94.0	172152718-172186954 (-)	***Atp1a4***, ATPase, Na+/K+ transporting, alpha 4 polypeptide
94.2	172203036-172234636 (-)	***Atp1a2***, ATPase, Na+/K+ transporting, alpha 2 polypeptide
94.2	172241327-172248757 (+)	***Igsf8***, immunoglobulin superfamily, member 8
94.2	172249953-172258202 (-)	***Kcnj9***, potassium inwardly-rectifying channel, subfamily J,
93.5	172270321-172303005 (+)	***Kcnj10***, potassium inwardly-rectifying channel, subfamily J, member 10
94.0	172305476-172309453 (+)	***Pigm***, phosphatidylinositol glycan, class M
	172404288-172407495 (+)	***Slamf9***, SLAM family member 9
94.0	172411140-172427798 (+)	***Igsf9***, immunoglobulin superfamily, member 9
94.2	172428967-172436300 (+)	***Tagln2***, transgelin 2
94.2	172438295-172474790 (+)	***Ccdc19***, coiled-coil domain containing 19
	172510678-172519408 (-)	***Slamf8***, SLAM family member 8
	172559691-172561802 (-)	***Dusp23***, dual specificity phosphatase 23
94.2	172626986-172628882 (+)	***Crp***, C-reactive protein, petaxin related
94.2	172827594-172828675 (-)	***Apcs***, serum amyloid P-component
94.2	173156636-173162566 (-)	***Fcer1a***, Fc receptor, IgE, high affinity I, alpha polypeptide
94.0	173267298-173269025 (-)	***Darc***, Duffy blood group, chemokine receptor
94.2		***Igsf4l***, immunoglobulin superfamily, member 4-like member 9
	173269606-173303047 (-)	***Igsf4b***, immunoglobulin superfamily, member 4B
95.0		***Nba2***, New Zealand Black autoimmunity 2
95.2	173816645-173845332 (-)	***Ifi204***, interferon activated gene 204
	173828773-173845312 (-)	***Mnda***, myeloid cell nuclear differentiation antigen
95.2		***Ifi201***, interferon activated gene 201
95.31	173852817-173874904 (-)	***Ifi203***, interferon activated gene 203
95.3	173944409-173964166 (-)	***Ifi205***, interferon activated gene 205
95.32		***Ifi202a***, interferon activated gene 202A
95.4	174105279-174180475 (+)	***Spna1***, spectrin alpha 1
96.0	174435221-174813052 (+)	***Fmn2***, formin 2
	174766770-174854521 (-)	***Grem2***, gremlin 2 homolog, cysteine knot superfamily (Xenopus laevis)
99.3	174991922-175425100 (-)	***Rgs7***, regulator of G protein signaling 7
	175534094-175558298 (-)	***Fh1***, fumarate hydratase 1
97.0	175619198-175621063 (-)	***Chml***, choroideremia-like
	175564890-175594826 (+)	***Kmo***, kynurenine 3-monooxygenase (kynurenine 3-hydroxylase)
	175595131-175625300 (-)	***Opn3***, opsin (encephalopsin)
97.0	175813508-175842003 (+)	***Exo1***, exonuclease 1
	175896538-176207985 (-)	***Pld5***, phospholipase D family, member 5
	176711103-176746835 (-)	***Cep170***, centrosomal protein 170
	176747374-176953730 (+)	***Sdccag8***, serologically defined colon cancer antigen 8
	176953382-177182067 (-)	***Akt3***, thymoma viral proto-oncogen 3
	177380065-177388420 (+)	***Zfp238***, zinc finger protein 238
	177700836-177734174 (-)	***Adss***, adenylosuccinate synthetase, non muscle
	178139987-178361220 (-)	***Hnrpu***, heterogeneous nuclear ribonucleoprotein U
	178360780-178438722 (+)	***Efcab2***, EF-hand calcium binding domain 2
97.58		***Kif26b***, kinesin family member 26B
97.59	178910023-179472250 (-)	***Smyd3***, SET and MYND domain containing 3
97.6	179482302-179500464 (-)	***Tfb2m***, transcription factor B2, mitochondrial

98.0		***Scfr1***, stem cell frequency regulator 1
100.0	180285326-180377370 (+)	***Itpkb***, inositol 1,4,5-trisphosphate 3-kinase B
98.6	180523220-180555500 (+)	***Parp1***, poly (ADP-ribose) polymerase family, member 1
98.7	180679955-180707986 (+)	***Acbd3***, acyl-Coenzyme A binding domain containing 3
98.5	180943379-180971337 (-)	***Ephx1***, epoxide hydrolase 1, microsomal
97.3	181773478-181800807 (-)	***Lbr***, lamin B receptor
98.7	181862432-181978534 (-)	***Enah***, enabled homolog (Drosophila)
98.7	182271238-182300553 (-)	***Fbxo28***, F-box protein 28
95.0	182387966-182421394 (+)	***Trp53bp2***, transformation related protein 53 binding protein 2
98.0	182933121-182936988 (+)	***Tlr5***, toll-like receptor 5
99.5	184225321-184230786 (-)	***Hlx1***, H2.0-like homeo box 1 (Drosophila)
100.0		***H25***, histocompatibility 25

MGI queried April 21, 2006.

Table 6: Haplotype blocks correlated with analgesia phenotypes by HapMapper

location (Mb)	gene	*p* value	phenotype
171.14	*Fcgr3*	0.0036	composite
171.31	*Ndufs2*	0.00049	epibatidine
		0.00052	composite
171.78	*Igsf8*	0.015	clonidine
172.4	*Kcnj9*	0.000022	WIN55,212-2
		0.015	clonidine
172.44	*Kcnj10*	0.00016	clonidine
		0.0067	morphine
173.09	*Apcs*	0.0021	clonidine
173.35	*Fcer1a*	0.00008	clonidine
		0.0058	U50,488
173.86	*Al607873*	0.000038	clonidine
174.03	*Mnda*	0.00028	WIN55,212-2
		0.015	clonidine
174.07	*Ifi203*	0.00019	WIN55,212-2
		0.00039	clonidine
		0.0028	morphine
		0.01	composite
174.08	*Ifi202a*	0.000056	WIN55,212-2
		0.0021	clonidine
178.27	*Ebaf*	0.000033	WIN55,212-2
182.56	*Capn2*	0.000011	WIN55,212-2
		0.0005	clonidine
182.66	*Capn8*	0.00000011	WIN55,212-2
		0.00098	clonidine
		0.0076	morphine
		0.014	composite

Table 7: Single nucleotide polymorphisms near the *Kcnj9* locus

Number	Position	Gene	Location	129	B6
1	172.393288	Kcnj9	exon	C	G
2	172.393295	Kcnj9	exon	A	G
3	172.393821	Kcnj9	exon	G	A
4	172.393833	Kcnj9	exon	C	T
5	172.393855	Kcnj9	exon	G	-
6	172.393856	Kcnj9	exon	A	-
7	172.393857	Kcnj9	exon	T	-
8	172.394321	Kcnj9	exon	A	G
9	172.394322	Kcnj9	exon	A	G
10	172.394327	Kcnj9	exon	A	G
11	172.394438	Kcnj9	exon	G	C
12	172.394439	Kcnj9	exon	G	C
13	172.397251	Kcnj9	exon	A	C
14	172.397489	Kcnj9	exon	G	C
15	172.397597	Kcnj9	exon	C	T
16	172.398050	Kcnj9	intron	C	G
17	172.398054	Kcnj9	intron	A	G
18	172.399095	Kcnj9	intron	G	A
19	172.399427	Kcnj9	intron	G	A
20	172.400477	Kcnj9	exon	A	G
21	172.401108	Kcnj9,Kcnj10	between	T	C
22	172.401256	Kcnj9,Kcnj10	between	G	A
23	172.401258	Kcnj9,Kcnj10	between	T	G
24	172.401339	Kcnj9,Kcnj10	between	T	C
25	172.401363	Kcnj9,Kcnj10	between	C	T
26	172.401416	Kcnj9,Kcnj10	between	T	C
27	172.401434	Kcnj9,Kcnj10	between	T	C
28	172.401516	Kcnj9,Kcnj10	between	C	A
29	172.401686	Kcnj9,Kcnj10	between	T	G
30	172.401688	Kcnj9,Kcnj10	between	T	G
31	172.401691	Kcnj9,Kcnj10	between	G	-
32	172.401749	Kcnj9,Kcnj10	between	G	A
33	172.401773	Kcnj9,Kcnj10	between	A	G
34	172.401783	Kcnj9,Kcnj10	between	A	C
35	172.401814	Kcnj9,Kcnj10	between	-	T
36	172.401815	Kcnj9,Kcnj10	between	-	A
37	172.401816	Kcnj9,Kcnj10	between	-	A
38	172.401817	Kcnj9,Kcnj10	between	-	A
39	172.401833	Kcnj9,Kcnj10	between	A	G
40	172.402236	Kcnj9,Kcnj10	between	G	A
41	172.402345	Kcnj9,Kcnj10	between	A	G
42	172.402399	Kcnj9,Kcnj10	between	G	A
43	172.402407	Kcnj9,Kcnj10	between	A	-
44	172.402494	Kcnj9,Kcnj10	between	G	A
45	172.402495	Kcnj9,Kcnj10	between	T	C
46	172.411182	Kcnj9,Kcnj10	between	G	T
47	172.411616	Kcnj9,Kcnj10	between	T	C
48	172.411789	Kcnj9,Kcnj10	between	G	T
49	172.412339	Kcnj9,Kcnj10	between	C	A
50	172.412487	Kcnj9,Kcnj10	between	T	G

Table 8: Z-score-transformed formalin early phase responses of 16 strains

Mouse Strain	MRL	NZW	B/B	B/C	A/J	LGJ	A/H	B10	LPJ	C3H	DBA	129	AKR	SMJ	NZB	C57
Mean Response	**-1.22**	**-1.15**	**-.57**	**-.42**	**-.39**	**-.37**	**-.36**	**-.14**	**-.07**	**-.03**	**.08**	**.17**	**.18**	**.24**	**.32**	**.38**

Table 9. Haplotype mapping of formalin response

P value	Genetic effect	Chr.	Position (Mb)	# SNP	Symbol	Description
0.00035	0.57	3	108.346 - 108.392	34	*Gstm3*	Glutathione S-methyl transferase, mu 3
0.00039	0.64	9	96.1771 - 96.1775	9	*Atp1b3*	ATPase, Na+/K+ transporting, beta 3
0.00073	0.6	3	108.344 - 108.346	17	*Gstm3*	Glutathione S-methyl transferase, mu 3
0.00073	0.6	7	130.086 - 130.378	26	*Ctsd*	Cathepsin D
0.00099	0.65	8	123.353 - 123.677	19	*Abcb10*	ATP-binding cassette, sub-family B, member 10
0.0011	0.64	9	96.184 - 96.187	10	*Atp1b3*	ATPase, Na+/K+ transporting, beta 3
0.0013	0.48	9	96.179 - 96.184	9	*Atp1b3*	ATPase, Na+/K+ transporting, beta 3
0.0027	0.52	9	96.1760 - 96.1766	4	*Atp1b3*	ATPase, Na+/K+ transporting, beta 3
0.0029	0.58	17	42.388514-42.388517	4	*Clic5*	Riken cDNA clone
0.0038	0.5	9	98.260 - 98.261	12	*Crbp*	RNA-binding protein 1

Table 10. Chromosome 10 genes identified by microarray as differentially expressed

Unigene	Cytoband	Gene	A Control	A Tx	B6 Control	B6 Tx	Strain *p*	Tx *p*	Interaction *p*	Max fold
Genes with strong interaction effect (Regulation depends on both strain and treatment)										
Mm.200373	32.0 cM	**Sgpl1**	442	519	461	296	0.088	0.283	0.045	0.64
Mm.45124	57.0 cM	**Kitl**	302	341	296	174	0.015	0.073	0.021	0.77
Mm.278577	C1	**A230046K03Rik**	1029	683	597	735	0.051	0.337	0.012	0.59
Mm.268389	C1	**MGC69704**	351	222	240	255	0.211	0.069	0.029	0.66
Genes with strong one-way treatment effect (Regulation depends primarily on treatment)										
none on Chr. 10										
Genes with strong one-way strain effect (Regulation depends primarily on strain)										**Fold B6/A**
Mm.9213	12.0 cM	**Esr1**	301	322	443	579	0.020	0.319	0.515	0.72
Mm.6458	18.0 cM	**Timeless**	2347	2057	1383	1417	0.003	0.687	0.467	0.65
Mm.22264	26.0 cM	**Apg5l**	275	340	153	193	0.033	0.348	0.836	0.83
Mm.4504	29.0 cM	**Gja1**	3036	3395	2241	1845	0.009	0.680	0.282	0.65
Mm.4504	29.0 cM	**Gja1**	4936	5550	3681	3042	0.023	0.744	0.340	0.64
Mm.240150	30.0 cM	**D10Ucla1**	850	818	532	444	<0.001	0.207	0.467	0.77
Mm.277498	35.0 cM	**Psap**	900	1253	732	657	0.018	0.599	0.159	0.63
Mm.235960	38.0 cM	**Ank3**	1706	1148	2129	2238	0.011	0.211	0.124	0.61
Mm.2400	43.0 cM	**Gpx4**	7592	9161	4552	4590	0.001	0.512	0.427	0.87
Mm.317188	43.0 cM	**Tdg**	877	943	640	553	0.001	0.652	0.235	0.61
Mm.9257	46.0 cM	**D10Wsu52e**	2432	2836	1830	1513	0.022	0.742	0.273	0.66
Mm.132958	47.0 cM	**Timp3**	6603	6919	2503	2571	<0.001	0.737	0.939	1.41
Mm.132958	47.0 cM	**Timp3**	3887	4467	2173	2412	<0.001	0.085	0.789	0.87
Mm.132958	47.0 cM	**Timp3**	1061	1301	608	594	<0.001	0.432	0.379	0.97
Mm.268521	48.0 cM	**Igf1**	609	780	438	371	0.003	0.777	0.134	0.78
Mm.159684	49.0 cM	**Tmpo**	252	401	193	182	0.021	0.523	0.163	0.80
Mm.22670	66.0 cM	**Mdm2**	357	367	256	224	0.023	0.720	0.518	0.59
Mm.31379	67.5 cM	**Hmga2**	622	643	308	275	<0.001	0.629	0.427	1.12
Mm.289371	72.0 cM	**Rdh5**	523	462	358	231	0.002	0.052	0.289	0.74
Mm.248648	A1	**Stx11**	258	257	344	433	0.002	0.281	0.290	0.59

Unigene	Cytoband	Gene	A Control	A Tx	B6 Control	B6 Tx	Strain *p*	Tx *p*	Interaction *p*	
Genes with strong one-way strain effect (Regulation depends primarily on strain)										**Fold B6/A**
Mm.227794	A1	**Shprh**	725	839	488	501	0.003	0.436	0.592	0.66
Mm.193041	A1	**Map3k7ip2**	603	643	338	464	0.006	0.138	0.347	0.64
Mm.101115	A1	**E130306M17Rik**	367	304	129	95	0.012	0.739	0.753	1.58
Mm.27154	A1-B2	**Vnn1**	382	399	210	152	<0.001	0.317	0.191	1.11
Mm.86670	A3	**Tbpl1**	982	1193	701	731	0.001	0.179	0.339	0.60
Mm.294783	A3	**2610102K23Rik**	844	849	1354	1318	0.003	0.885	0.879	0.66
Mm.35251	B1	**Tube1**	191	279	426	359	0.004	0.425	0.073	0.74
Mm.36664	B1	**LOC270711**	336	307	662	559	0.005	0.507	0.718	0.93
Mm.64104	B1	**2410016F19Rik**	347	358	236	231	0.006	0.909	0.731	0.59
Mm.243941	B3	**Man1a**	319	389	256	190	0.003	0.632	0.065	0.67
Mm.234437	B4	**1700056O17Rik**	1024	1194	786	686	<0.001	0.935	0.058	0.59
Mm.29344	B4	**Tde2**	4916	6086	3617	3383	0.003	0.583	0.204	0.65
Mm.19325	B5.3	**1200003C15Rik**	415	680	336	322	0.007	0.097	0.076	0.73
Mm.27104	C1	**2700078H01Rik**	209	240	458	576	<0.001	0.128	0.754	1.20
Mm.256981	C1	**1700129L13Rik**	466	543	129	185	<0.001	0.292	0.784	1.68
Mm.278577	C1	**A230046K03Rik**	1060	1199	682	797	0.006	0.222	0.898	0.61
Mm.236214	C1	**Grin3b**	1584	1684	957	1074	0.029	0.658	0.871	0.69
Mm.289431	C1	**Eef2**	6894	6039	2896	3871	0.047	0.978	0.495	0.93
Mm.27651	C2	**BC030932**	500	557	212	198	<0.001	0.767	0.234	1.37
Mm.34980	C2	**(hypothetical)mRNA**	428	519	121	112	<0.001	0.676	0.376	2.02
Mm.252843	C2	**1700023M03Rik**	419	352	897	902	<0.001	0.388	0.431	1.22
Mm.27886	C2	**2410011G03Rik**	3890	3198	7648	6801	<0.001	0.123	0.659	1.03
Mm.11982	C2	**(hypothetical)mRNA**	4110	4058	2068	2168	<0.001	0.898	0.818	0.95
Mm.11982	C2	**(hypothetical)mRNA**	4508	3705	2689	2630	<0.001	0.197	0.260	0.63
Mm.252843	C2	**1700023M03Rik**	344	241	145	140	0.001	0.167	0.256	1.03
Mm.256845	C2	**AI854408**	566	649	395	392	0.005	0.619	0.577	0.63
Mm.268400	C3	**2810442I22Rik**	1997	2226	1463	1337	0.017	0.890	0.408	0.59
Mm.2020	D1	**Csrp2**	625	588	1051	1011	<0.001	0.636	0.959	0.77
Mm.37266	D1	**8430438D04Rik**	1526	1416	898	948	0.005	0.841	0.725	0.67
Mm.268025	D1	**Lin7a**	1608	1544	1078	1016	0.022	0.891	0.979	0.59
Mm.22270	D2	**Tm4sf3**	4558	4763	7877	7821	<0.001	0.868	0.813	0.75
Mm.294120	D3	**Rnf41**	153	130	1090	1069	<0.001	0.575	0.723	2.93
Mm.252213	D3	**Baz2a**	1062	998	638	732	0.003	0.649	0.320	0.59
Mm.296915	D3	**5730551F12Rik**	457	468	317	297	0.011	0.780	0.608	0.59

Table 11: Known genes in the *Nociq2* QTL region

104 genes between 67.5 and 70.0 cM

cM	Genome Coordinates	Symbol, Name
67.5	119939359-120054668(-)	**Hmga2**, high mobility group AT-hook 2
	120365529-120482386(-)	**Msrb3**, methionine sulfoxide reductase B3
	120506867-120563151(-)	**Lemd3**, LEM domain containing 3
	120617453-120684092(+)	**Wif1**, Wnt inhibitory factor 1
	121021345-121053500(+)	**Gns**, glucosamine (N-acetyl)-6-sulfatase
	121066610-121132513(-)	**Rassf3**, Ras association (RalGDS/AF-6) domain family 3
	121202715-121243002(-)	**Tbk1**, TANK-binding kinase 1
	121243640-121282408(-)	**Xpot**, exportin, tRNA (nuclear export receptor for tRNAs)
	121441553-121611197(-)	**Srgap1**, SLIT-ROBO Rho GTPase activating protein 1
	121736973-121755708(-)	**Tmem5**, transmembrane protein 5
	122099735-122104689(+)	**Avpr1a**, arginine vasopressin receptor 1A
	122369396-122633107(+)	**Ppm1h**, protein phosphatase 1H (PP2C domain containing)
	122685727-122767072(-)	**Mon2**, MON2 homolog (yeast)
	122802307-122887864(-)	**Usp15**, ubiquitin specific peptidase 15
	124920049-125022548(-)	**Slc16a7**, solute carrier family 16 (monocarboxylic acid transporters), member 7
	125665573-125714974(+)	**Lrig3**, leucine-rich repeat and immunoglobulin-like domains 3
	126601327-126634252(-)	**Xrcc6bp1**, XRCC6 binding protein 1
70	126728332-126732689(+)	**Ctdsp2**, CTD (carboxy-terminal domain, RNA polymerase II, polypeptide A) small phosphatase 2
	126733459-126753708(+)	**Avil**, advillin
	126755052-126763534(-)	**Tsfm**, Ts translation elongation factor, mitochondrial
	126774652-126778181(+)	**Mettl1**, methyltransferase-like 1
	126780970-126785726(+)	**Cyp27b1**, cytochrome P450, family 27, subfamily b, polypeptide 1
	126789291-126795433(-)	**March9**, membrane-associated ring finger (C3HC4) 9
	126796335-126800115(+)	**Cdk4**, cyclin-dependent kinase 4
	126800000-126802984(-)	**Tspan31**, tetraspanin 31
	126808152-126825249(+)	**Centg1**, centaurin, gamma 1
69.25	126897961-126905118(+)	**B4galnt1**, beta-1,4-N-acetyl-galactosaminyl transferase 1
	126923438-126929486(-)	**Dtx3**, deltex 3 homolog (Drosophila)
	126932897-126947385(-)	**Pip5k2c**, phosphatidylinositol-4-phosphate 5-kinase, type II, gamma
70	126965002-126999708(-)	**Kif5a**, kinesin family member 5A
69.5	127003037-127018445(+)	**Dctn2**, dynactin 2
69.5		**Evi5-rs1**, ecotropic viral integration site 5 related sequence 1
70	127018594-127025409(-)	**Mbd6**, methyl-CpG binding domain protein 6
	127027446-127032926(+)	**Ddit3**, DNA-damage inducible transcript 3
	127032866-127048316(-)	**Mars**, methionine-tRNA synthetase
	127059481-127066603(+)	**Arhgap9**, Rho GTPase activating protein 9
69	127066527-127078227(-)	**Gli1**, GLI-Kruppel family member GLI1
69	127086040-127088410(-)	**Inhbe**, inhibin beta E
69	127092958-127107069(-)	**Inhbc**, inhibin beta-C
	127136789-127236021(+)	**R3hdm2**, R3H domain containing 2
	127238355-127245453(+)	**Stac3**, SH3 and cysteine rich domain 3
	127253777-127259073(-)	**Shmt2**, serine hydroxymethyl transferase 2 (mitochondrial)
	127262111-127271196(-)	**Nxph4**, neurexophilin 4
	127274818-127357765(-)	**Lrp1**, low density lipoprotein receptor-related protein 1
70	127343745-127397114(+)	**Stat6**, signal transducer and activator of transcription 6
70	127397630-127403389(-)	**Nab2**, Ngfi-A binding protein 2
70	127441967-127457649(+)	**Myo1a**, myosin IA

	127461189-127468478(+)	**Tac2**, tachykinin 2
	127476249-127484066(+)	**Zbtb39,** zinc finger and BTB domain containing 39
72	127486333-127488404(-)	**Admr**, adrenomedullin receptor
70	127496521-127505007(+)	**Rdh1,** retinol dehydrogenase 1 (all trans)
	127513116-127614028(+)	**Rdh16,** retinol dehydrogenase 16
	127513116-127529408(+)	**Rdh9**, retinol dehydrogenase 9
70	127586639-127597887(+)	**Rdhs,** retinol dehydrogenase similar
	127620739-127682049(-)	**Rdh7,** retinol dehydrogenase 7
	127635246-127648472(+)	**Sdro,** orphan short chain dehydrogenase/reductase
	127727647-127744219(-)	**Hsd17b9,** hydroxysteroid (17-beta) dehydrogenase 9
77	127751903-127766741(+)	**Prim1,** DNA primase, p49 subunit
	127772284-127785348(+)	**Naca,** nascent polypeptide-associated complex alpha polypeptide
	127795693-127866122(+)	**Baz2a,** bromodomain adjacent to zinc finger domain, 2A
	127795693-127813965(+)	**Ptges3,** prostaglandin E synthase 3 (cytosolic)
	127820018-127827099(+)	**Atp5b,** ATP synthase, H+ transporting mitochondrial F1 complex, beta subunit
	127869927-127913299(-)	**Rbms2,** RNA binding motif, single stranded interacting protein 2
	127930839-127946754(+)	**Gls2**, glutaminase 2 (liver, mitochondrial)
	127946726-127948614(-)	**Spryd4,** SPRY domain containing 4
74	127962658-127968631(+)	**Mip**, major intrinsic protein of eye lens fiber
18	127968912-127989763(+)	**Timeless,** timeless homolog (Drosophila)
76	127990951-127992721(+)	**Apon,** apolipoprotein N
73	128004817-128006971(+)	**Apof,** apolipoprotein F
70	128007396-128029669(+)	**Stat2,** signal transducer and activator of transcription 2
	128032960-128034904(-)	**Il23a,** interleukin 23, alpha subunit p19
	128040155-128058167(+)	**Usp52,** ubiquitin specific peptidase 52
72	128059409-128064373(+)	**Tmem4,** transmembrane protein 4
	128074652-128099299(+)	**Cs**, citrate synthase
	128099917-128105817(-)	**Coq10a,**coenzyme Q10 homolog A (yeast)
	128113944-128130826(+)	**Ankrd52,** ankyrin repeat domain 52
	128132754-128138005(-)	**Slc39a5**, solute carrier family 39 (metal ion transporter), member 5
	128138215-128146616(-)	**Obfc2b**, oligonucleotide/oligosaccharide-binding fold containing 2B
72	128148477-128178261(+)	**Rnf41,** ring finger protein 41
	128198102-128227202(+)	**Smarcc2,** SWI/SNF related, matrix associated, actin dependent regulator of chromatin, subfamily c, member 2
	128227889-128230853(-)	**Myl6,** myosin, light polypeptide 6, alkali, smooth muscle and non-muscle
	128231185-128235715(-)	**Myl6b,** myosin, light polypeptide 6B
	128247347-128262961(-)	**Mbc2**, membrane bound C2 domain containing protein
	128279054-128284865(-)	**Zc3h10,** zinc finger CCCH type containing 10
	128285208-128286207(-)	**Rpl41,** ribosomal protein L41
	128294857-128303029(-)	**Pa2g4,** proliferation-associated 2G4
70	128304622-128327612(-)	**Erbb3,** v-erb-b2 erythroblastic leukemia viral oncogene homolog 3 (avian)
	128361627-128363574(-)	**Rps26,** ribosomal protein S26
	128369506-128382917(-)	**Zfpn1a4,** zinc finger protein, subfamily 1A, 4 (Eos)
	128406985-128410952(-)	**Suox,** sulfite oxidase
	128414968-128433355(-)	**Rab5b,** RAB5B, member RAS oncogene family
	128435036-128442103(-)	**Cdk2**, cyclin-dependent kinase 2
70	128443349-128457215(+)	**Si**, silver
71	128457225-128481147(-)	**Dgka,** diacylglycerol kinase, alpha

	128484980-128503654(+)	**Wibg,** within bgcn homolog (Drosophila)
70	128528146-128536967(+)	**Mmp19,** matrix metallopeptidase 19
	128542767-128556537(+)	**Dnajc14**, DnaJ (Hsp40) homolog, subfamily C, member 14
	128554993-128558685(-)	**Ormdl2,** ORM1-like 2 (S. cerevisiae)
	128621636-128628776(-)	**Gdf11**, growth differentiation factor 11
72	128647020-128649913(+)	**Cd63**, Cd63 antigen
72	128650679-128656364(-)	**Rdh5,** retinol dehydrogenase 5
72	128657005-128660615(-)	**Bloc1s1,** biogenesis of lysosome-related organelles complex-1, subunit 1
72	128670909-128695373(+)	**Itga7**, integrin alpha 7
	128695368-128698079(-)	**Mettl7b,** methyltransferase like 7B

MGI queried August 16, 2006.

Appendix B: Figure Captions

Fig 1. Genetic map of the mouse genome showing marker distribution.

Fig 2. Frequency histograms of B6129PF2 for multiple phenotypes. (a) Baseline tail-withdrawal latency. Analgesia produced by (b) clonidine (3 mg/kg), (c) morphine (15 mg/kg), and (d) WIN55,212-2 (10 mg/kg) is quantified as percentage of the maximum possible effect (checkered) and as percent analgesia (diagonal lines).

Fig 3. LOD score plots of thermal sensitivity. The Y-axis is the LOD score. Horizontal lines indicate level of significance: dashed line is significant ($\alpha = 0.05$), dashed-and-dotted line is highly significant ($\alpha = 0.001$), and dotted line is suggestive ($\alpha = 0.63$). (a) Full genome scan of baseline tail-withdrawal latency. Chromosome number is given on the X-axis, with ticks above the axis representing microsatellite markers. The X-axis of interval mapping plots for individual chromosomes (b) 7, (c) 11, and (d) 4 gives the distance from the centromere in centiMorgans. The black horizontal bars represent 1-LOD drop-off confidence intervals for each peak. The chromosome 4 graph shows interval mapping results in the presence (solid line) and absence (dashed line) of the covariate "sex."

Fig 4. Full genome QTL scan of composite analgesia score. The Y-axis is the LOD score. Horizontal lines indicate level of significance: dashed line is significant ($\alpha = 0.05$), dashed-and-dotted line is highly significant ($\alpha = 0.001$), and dotted line is suggestive ($\alpha =$

0.63). Chromosome number is given on the X-axis, with ticks above the axis representing microsatellite markers.

Fig 5. Full genome QTL scans of analgesia phenotypes: (a) clonidine, (b) morphine, and (c) WIN55,212-2. The Y-axis is the LOD score. Horizontal lines indicate level of significance: dashed line is significant ($\alpha = 0.05$), and dotted line is suggestive ($\alpha = 0.63$). Chromosome number is given on the X-axis, with ticks above the axis representing microsatellite markers.

Fig 6. Linkage to distal chromosome 1 for multiple analgesia phenotypes. The phenotypes plotted are 3 mg/kg clonidine (dashed line), 10 mg/kg morphine (dotted line), 10 mg/kg WIN55,212-2 (dashed-and-dotted line), and baseline tail-withdrawal latency (solid line). The Y-axis is the LOD score. The X-axis gives the distance from the centromere in centiMorgans. The black horizontal bar represents the 1-LOD drop-off confidence interval for all analgesia peaks. Significance thresholds are not indicated, as they were determined by permutation analysis and are different for each phenotype.

Fig 7. Full genome Digital Disease mapping output for composite analgesia Z-scores. Bars represent the 19 autosomes broken into 10 Mb haplotype segments (see text); the height of each bar indicates the strength of correlation between genotype and phenotype, in terms of the number of standard deviations away from the mean standard deviation for all correlations. The dashed line represents the top 10% of correlated haplotype segments.

Fig 8. Full genome Digital Disease mapping output for single-drug analgesia Z-scores: a) clonidine, b) epibatidine, c) morphine, d) U50,488, and e) WIN55,212-2. Bars represent the 19 autosomes broken into 10 Mb haplotype segments (see text); the height of each bar indicates the strength of correlation between genotype and phenotype, in terms of the number of standard deviations away from the mean standard deviation for all correlations. The dashed line represents the top 10% highest-correlated haplotype segments.

Fig 9. *Fcgr3* Knockout/congenic interval of Chromosome 1. Introgressed 129 DNA is shown in gray on a white C57BL/6 background. Microsatellite markers are labeled above the figure; other markers are shown below.

Fig 10. *Fcgr3* KO vs. C57BL/6 wild-type: three analgesic drugs. Percent analgesia scores for wild-type C57BL/6 (solid line) and Fcgr3 KO (dashed line) mice at multiple doses are shown for a) clonidine, b) morphine, and c) WIN55,212-2.

Fig 11a. Comparison of wild-type C57BL/6, knockout/congenic Fcgr3, and heterozygotic mice for analgesia produced by 20 mg/kg clonidine. Significance levels: ** $p < 0.01$, *** $p < 0.001$.

Fig 11b. Comparison of subcongenic strains derived from Fcgr3KO, and wild-type C57BL/6 and Fcgr3KO strains, on analgesia produced by 20 mg/kg clonidine. Significance levels: *** $p < 0.001$.

Fig 12. Expression of *Kcnj9* in three central nervous system sites: periaqueductal gray (PAG), rostroventral medulla (RVM), and spinal cord (SC).

Fig 13. GIRK3 KO vs. C57BL/6 wild-type: three analgesic drugs. Percent analgesia scores for wild-type C57BL/6 (solid line) and GIRK3 KO (dashed line) mice at multiple doses are shown for a) clonidine, b) morphine, and c) WIN55,212-2.

Fig 14. Effect of oabain treatment on formalin response. In a) and b), the Y-axis indicates the number of five second samples in which a nocifensive behavior towards the injured paw was observed in the early or late phase, respectively. Fig. c) shows the percent difference in paw weight between treated and untreated paws is shown. Significance levels: * $p < 0.05$.

Fig 15. PCR of ATPase channel subunits. a) Basal expression of *Atp1b3* relative to GAPDH in the dorsal root ganglia (DRG) of A/J and C57BL/6. b) Relative basal expression of three ATPase subunit genes in the DRG, as expressed as a ratio of A/J to C57BL/6 transcript levels. Ratios near 1.0 indicate no difference between the two strains. c) Expression of *Atp1b3*, relative to GAPDH, in the DRG 45 minutes post-formalin injection among five inbred strains.

Fig 16. Recombinant inbred phenotype correlations—formalin. The top figure indicates the Mb position of microsatellite markers on Chr. 10. The long bars in the lower figure represent the parental derivation for the queried section of Chr. 10 for each inbred and RI strain. White bars indicate A/J-derived genome; black bars indicate B6-derived genome.

The phenotypic response is indicated by the mean number of positive samples (standard error in parentheses), and the phenotype is characterized as either A-like or B6-like (white or black squares) for purposes of correlation. The correlations shown below the long bars indicate the Pearson *r* between the given marker and the formalin strain means.

Fig 17. Recombinant congenic phenotype correlations—formalin. The top figure indicates the Mb position of microsatellite markers on Chr. 10. The long bars in the lower figure represent the parental derivation for the queried section of Chr. 10 for each inbred and RC strain. White bars indicate A/J-derived genome; black bars indicate B6-derived genome. The phenotypic response is indicated by the mean number of positive samples (standard error in parentheses).

Fig 18. Congenic strain comparison—formalin. a) AcB64-derived congenic strains in which wild-type or congenic alleles have been maintained at the QTL locus. b) BcA72-derived congenic strains in which wild-type or congenic alleles have been maintained at the QTL locus. The Y-axis expresses the formalin response of each strain as the percentage of five second samples in which nocifensive behavior toward the injured paw was observed. The strain means of each type were averaged for comparison; significance levels: * $p < 0.05$.

Appendix C: Figures

Fig. 1. Genetic map of the mouse genome showing marker distribution

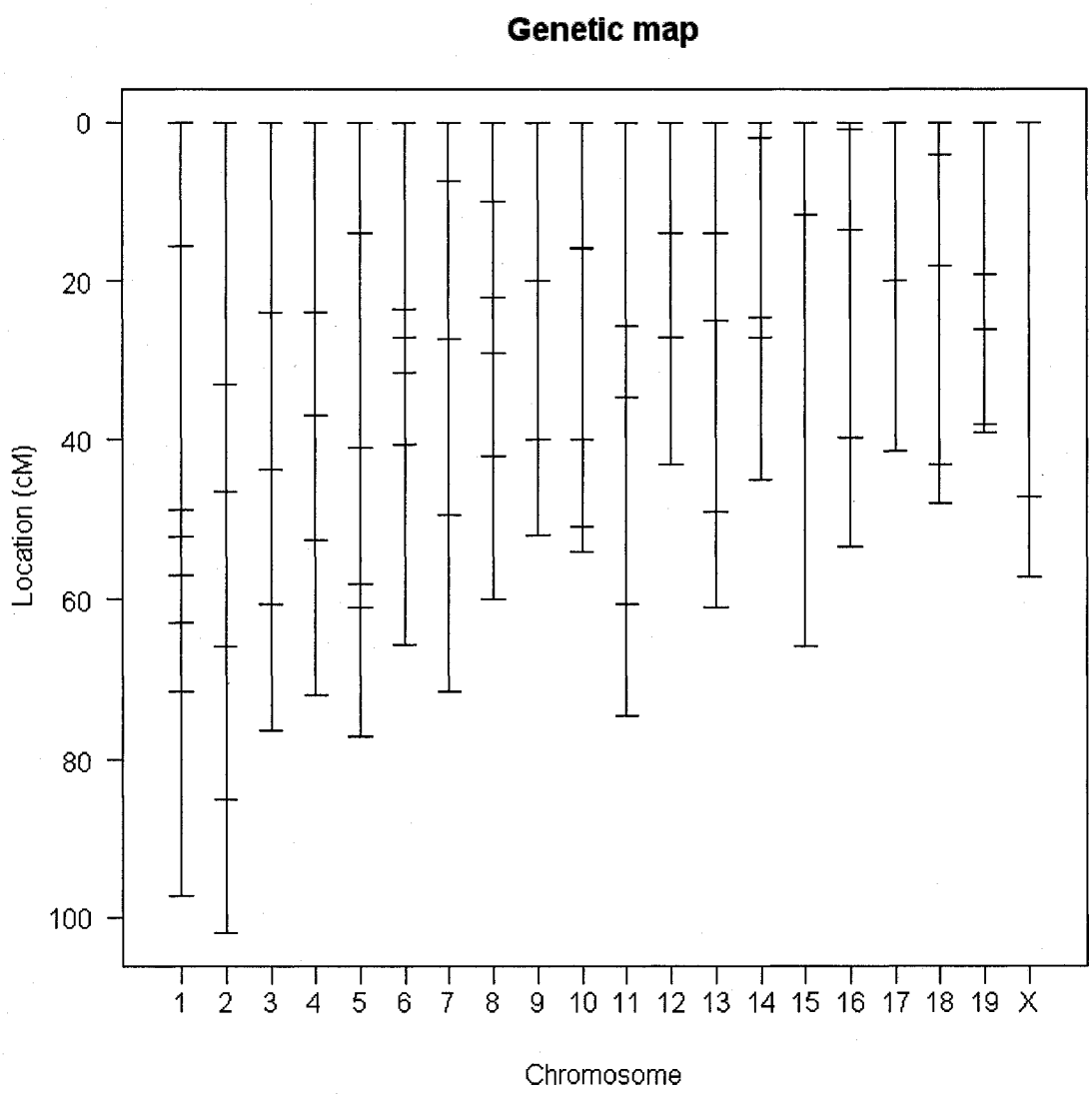

Fig. 2a-2d. Frequency histograms of B6129PF2 on multiple phenotypes

a. Baseline latencies

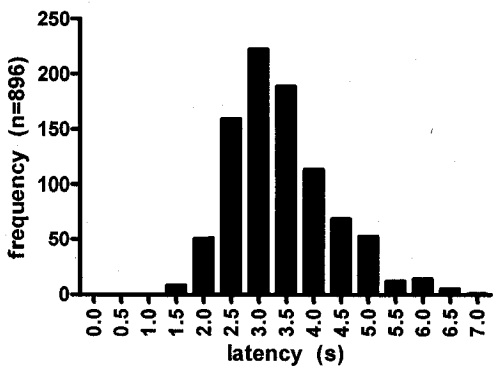

b. Clonidine analgesia

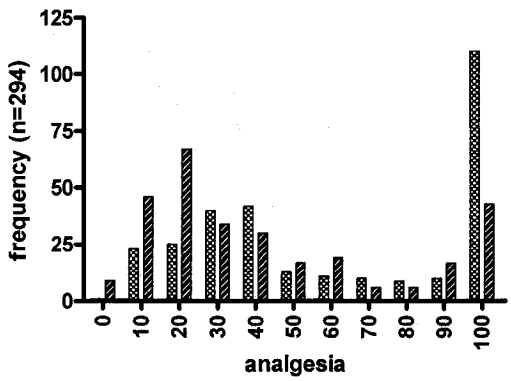

c. Morphine analgesia

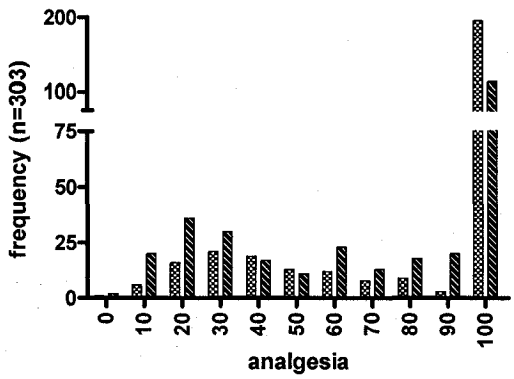

d. WIN55,212-2 analgesia

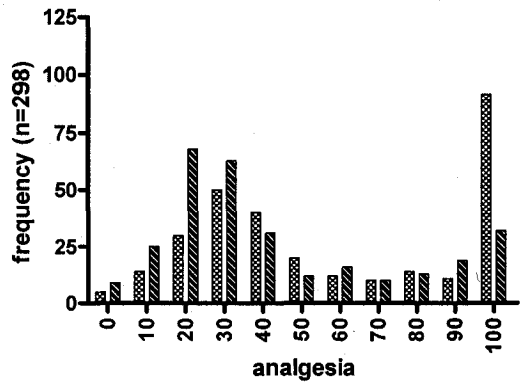

Fig. 3a-3d. LOD score plots of thermal sensitivity

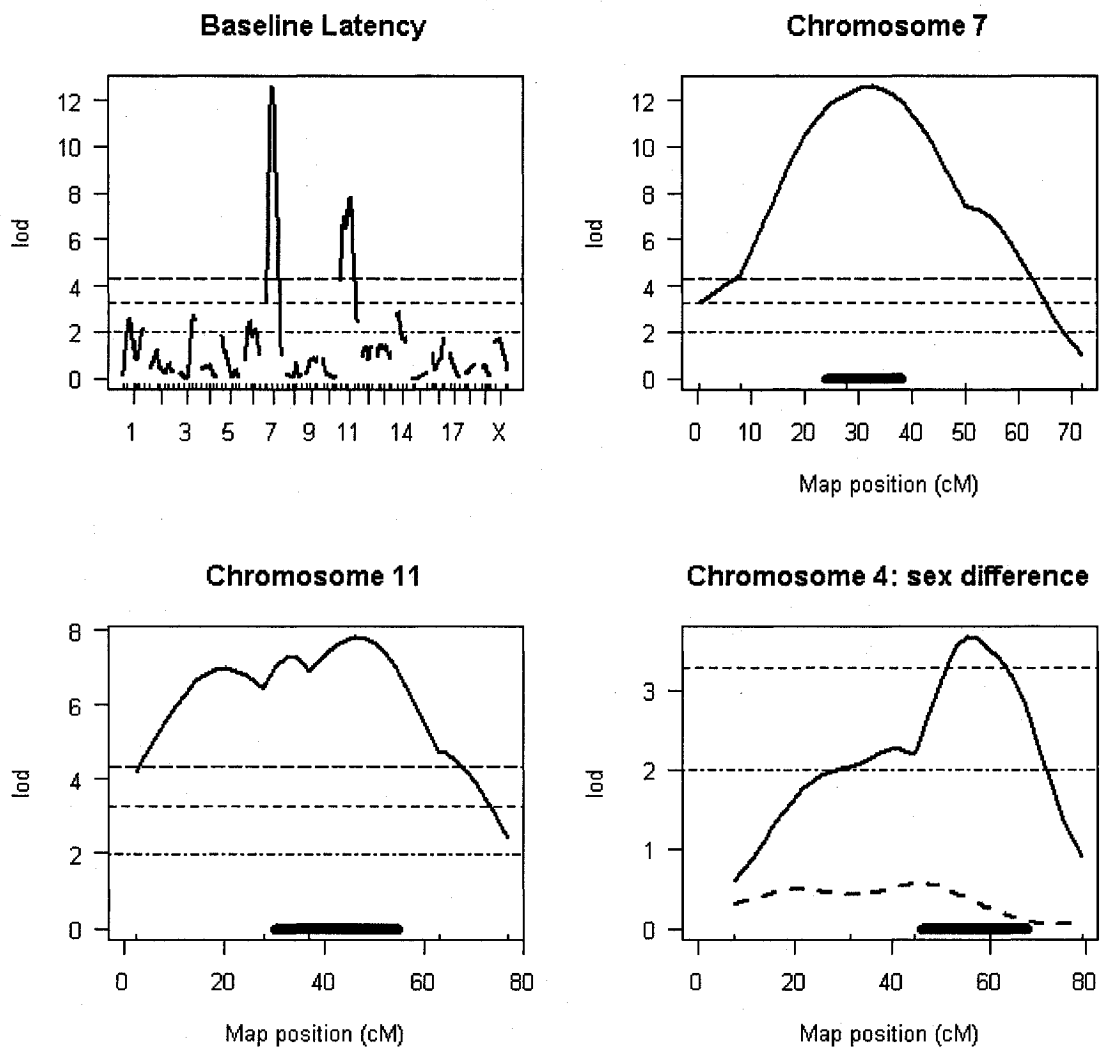

Fig. 4. Full genome QTL scan of composite analgesia score

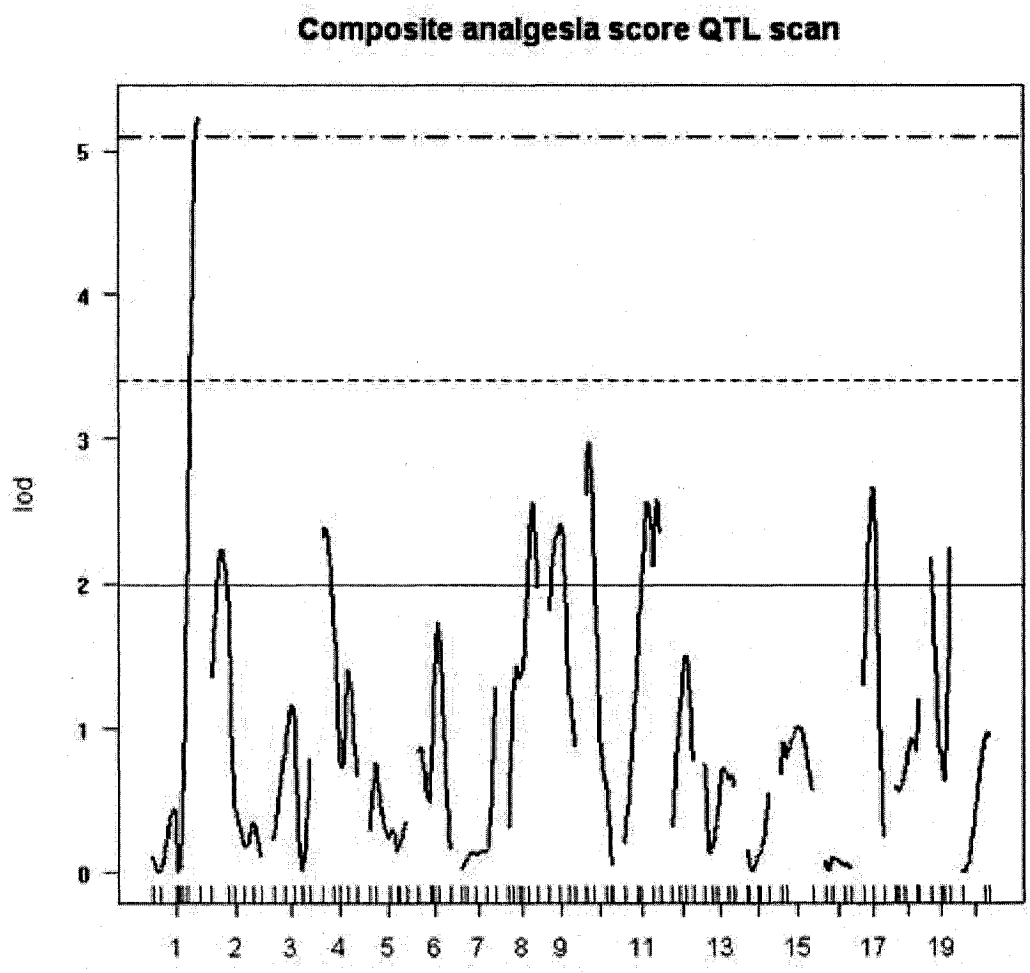

Fig. 5. Full genome QTL scans of analgesia phenotypes

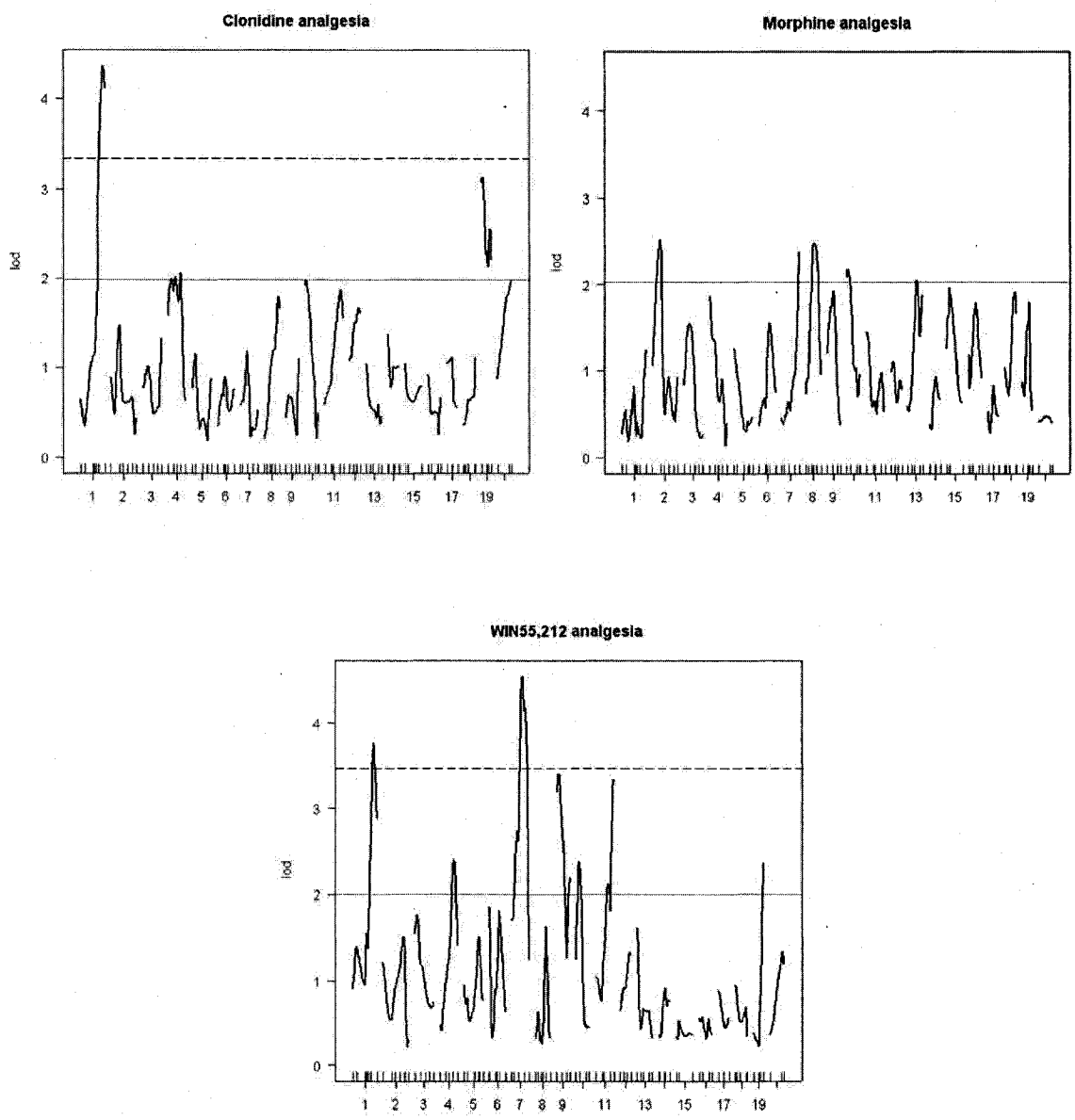

Fig. 6. Linkage to distal chromosome 1 in multiple analgesia phenotypes

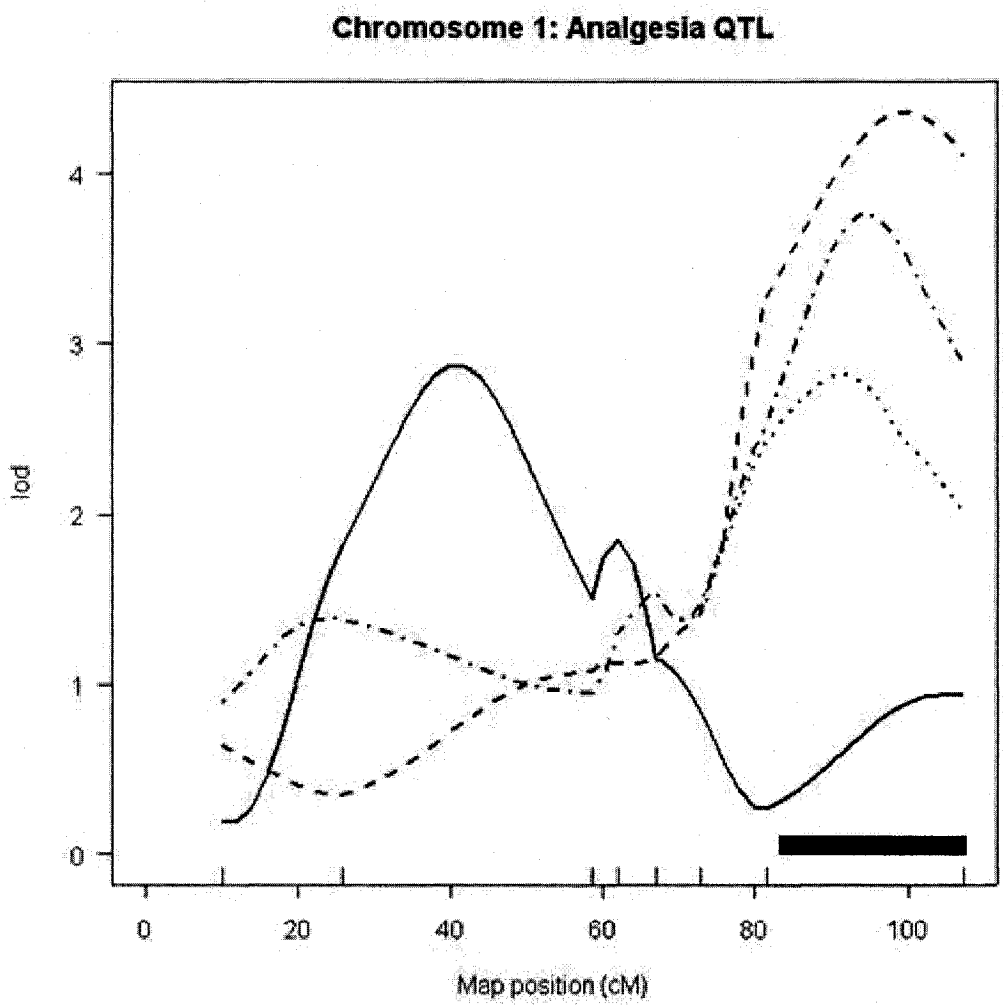

Fig. 7. Full genome Digital Disease mapping output for composite analgesia Z-scores

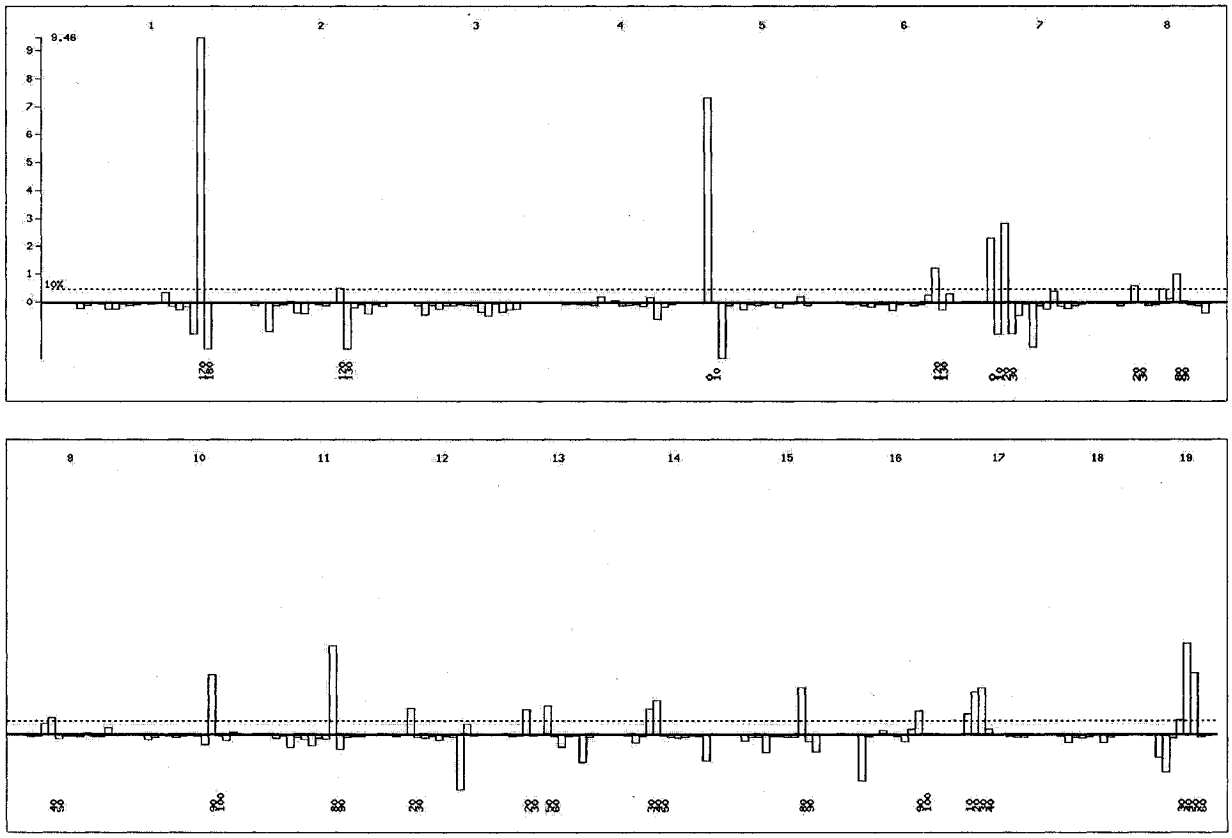

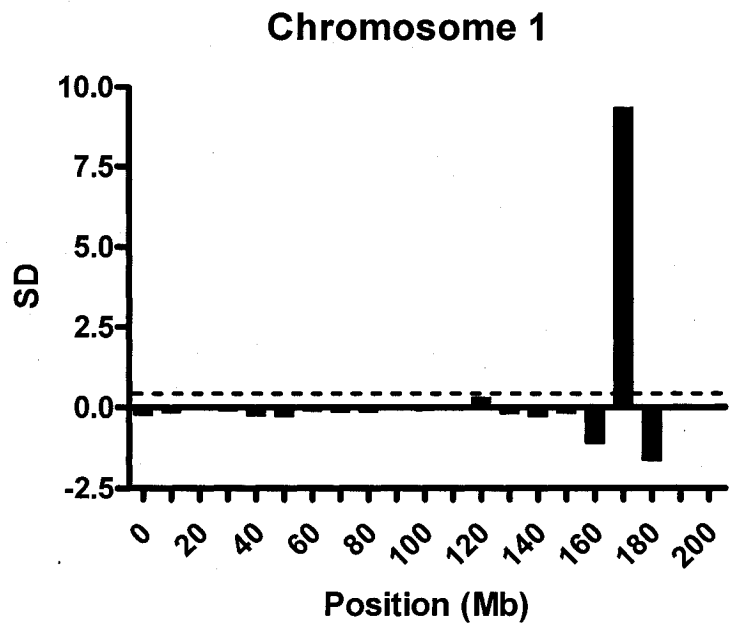

Fig. 8a. Full genome Digital Disease mapping output for clonidine analgesia Z-scores

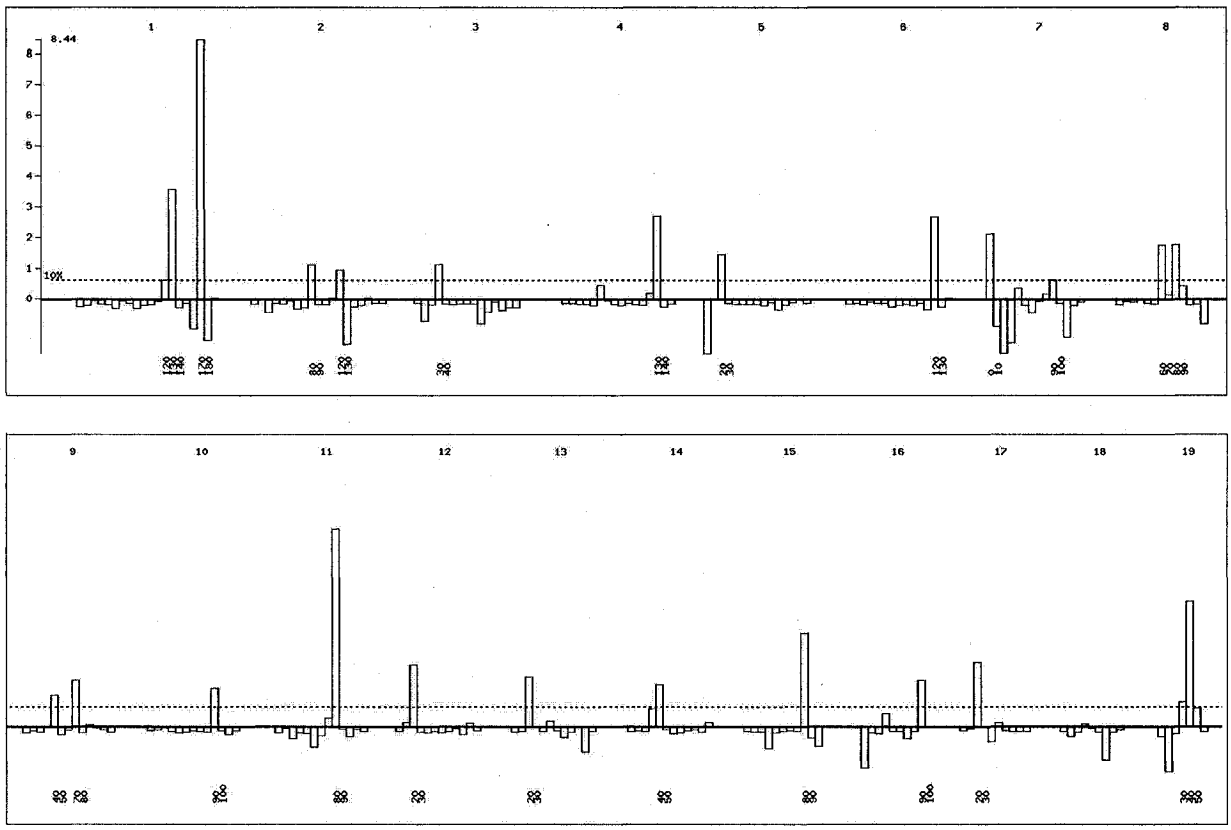

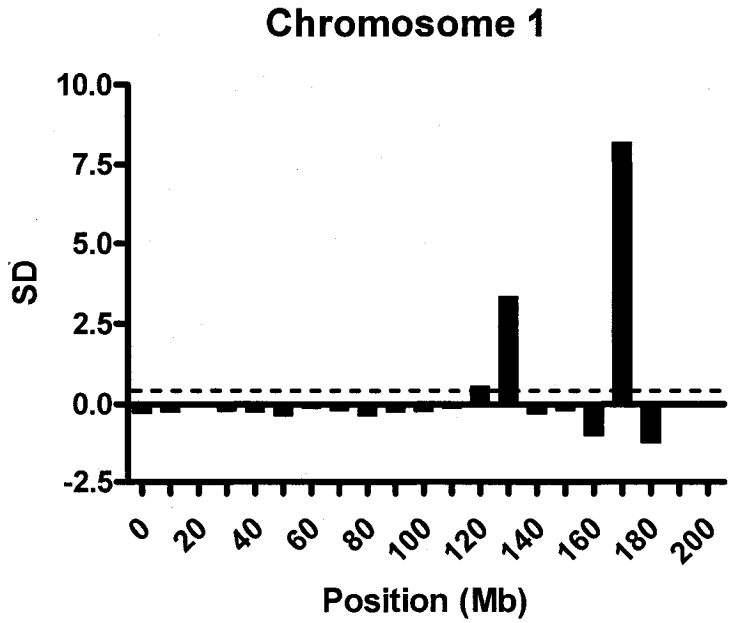

Fig. 8b. Full genome Digital Disease mapping output for epibatidine analgesia Z-scores

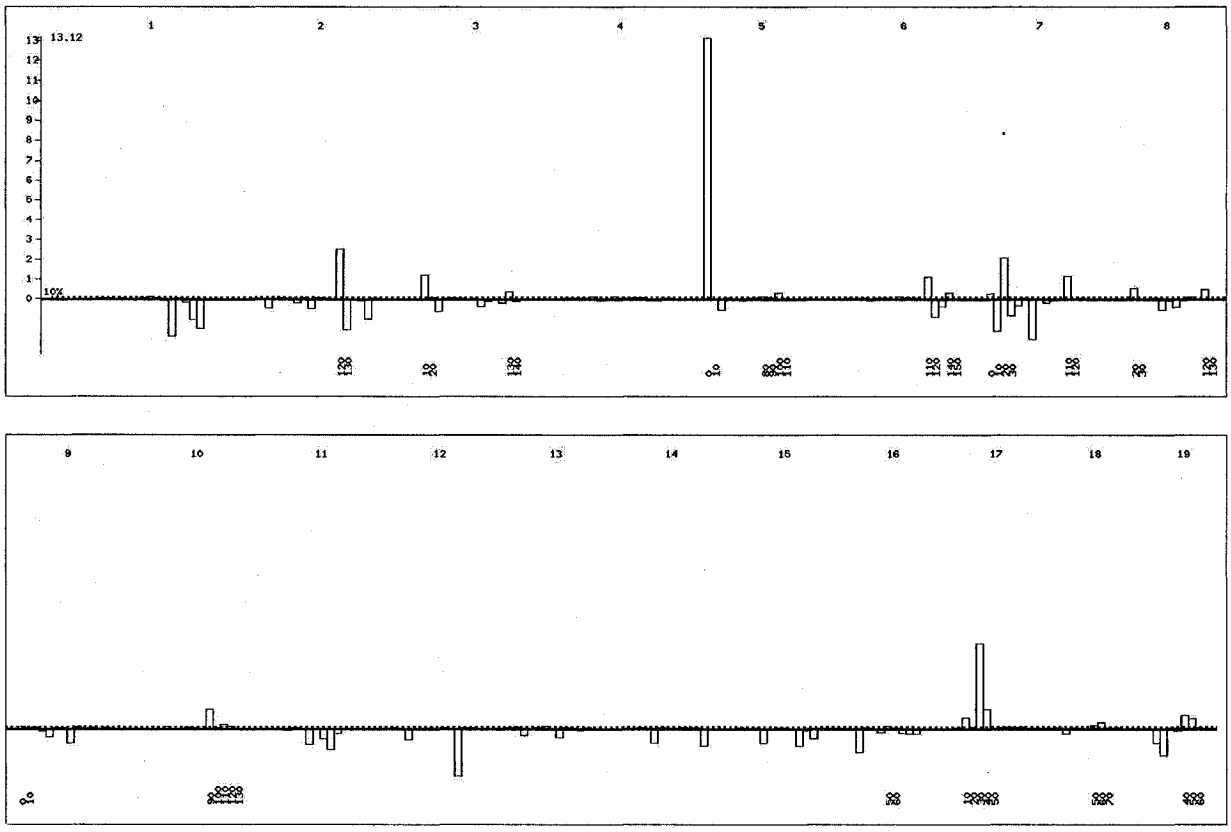

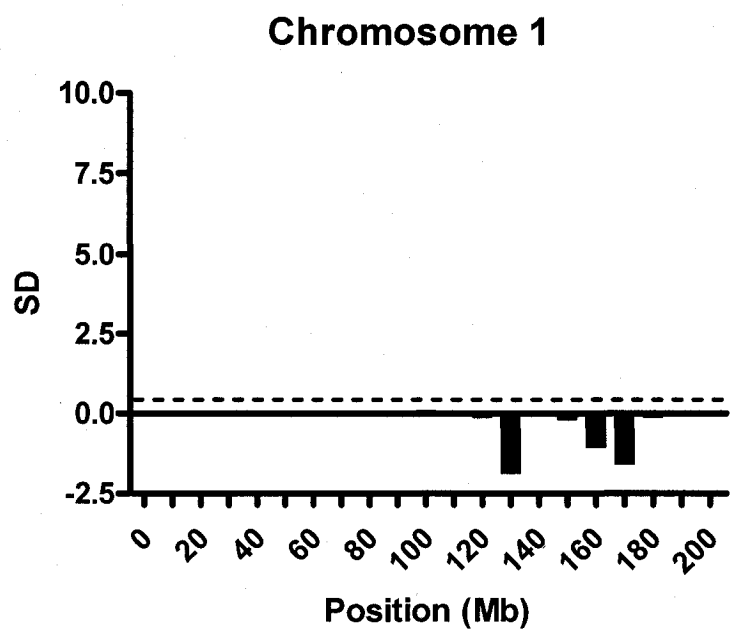

Fig. 8c. Full genome Digital Disease mapping output for morphine analgesia Z-scores

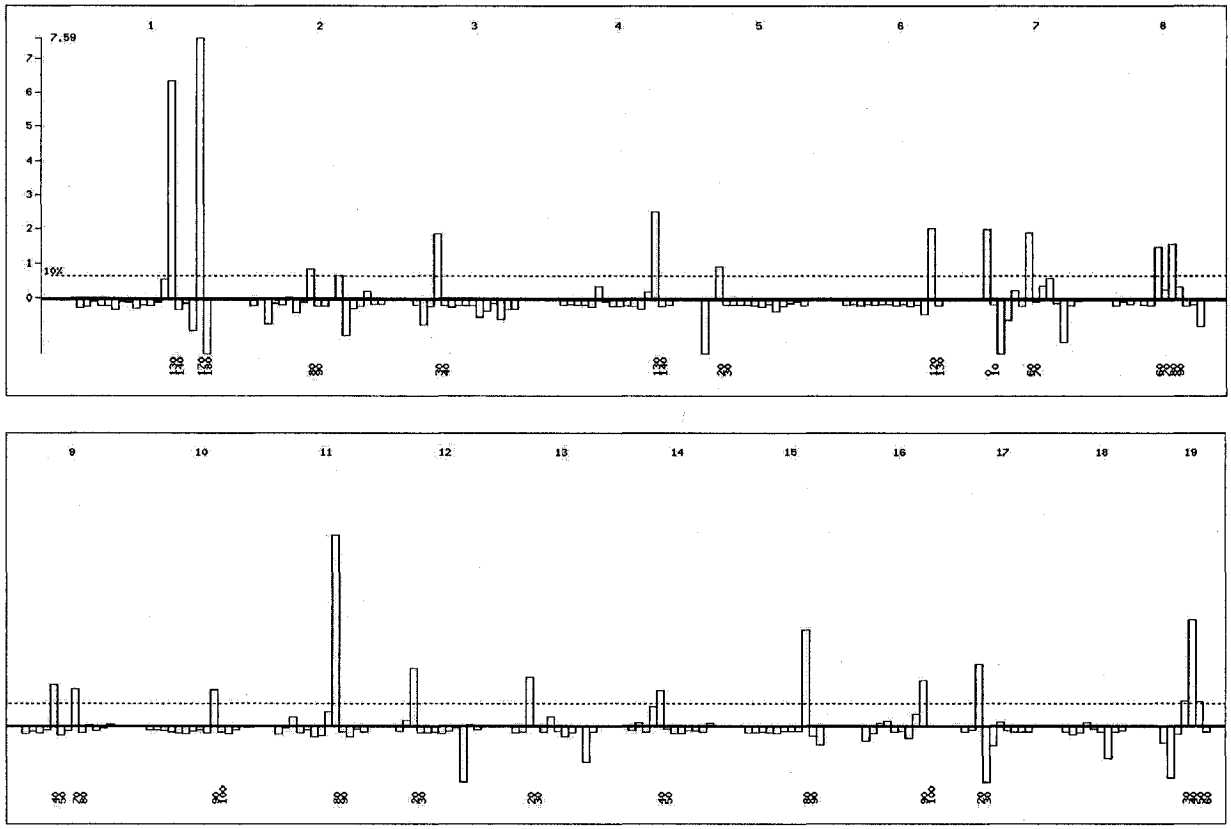

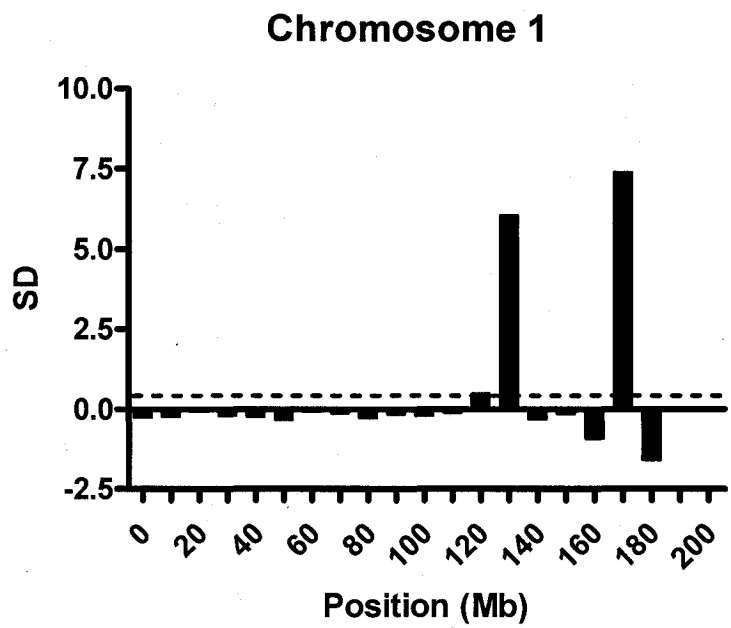

Fig. 8d. Full genome Digital Disease mapping output for U50,488 analgesia Z-scores

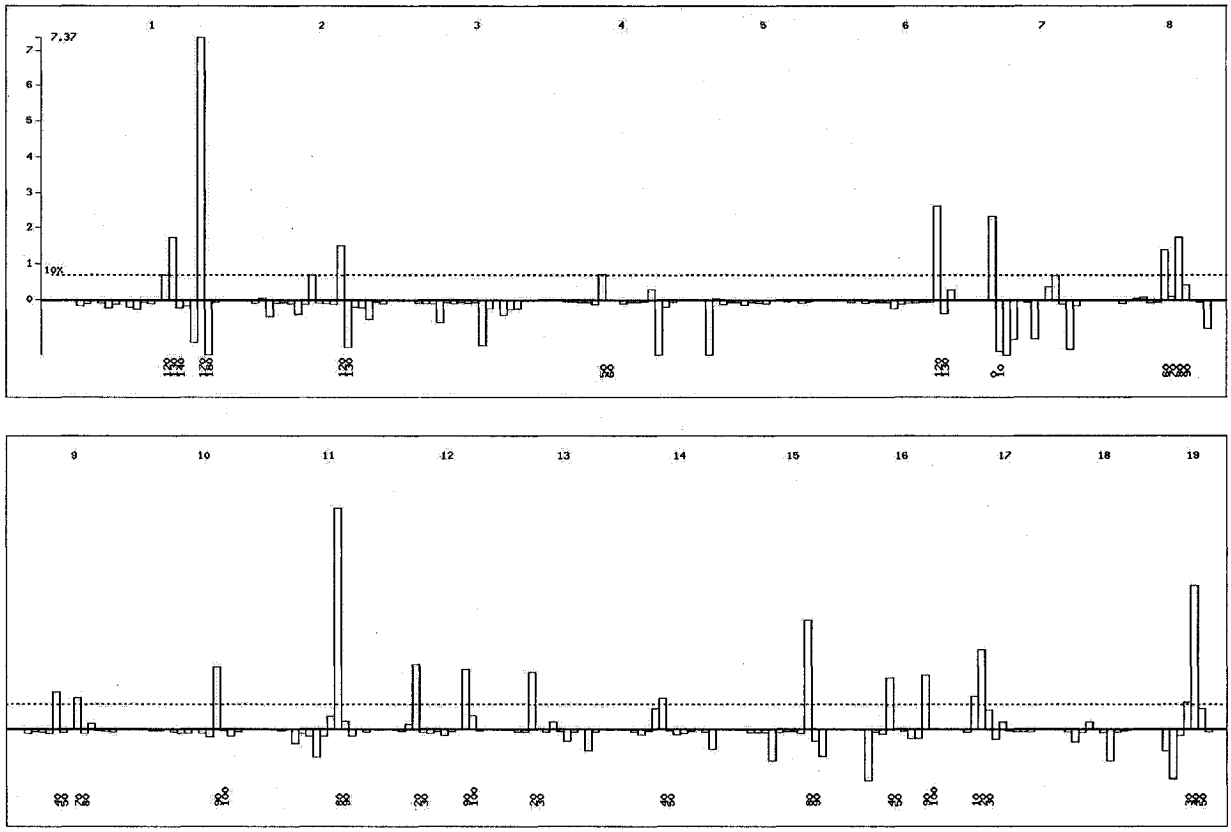

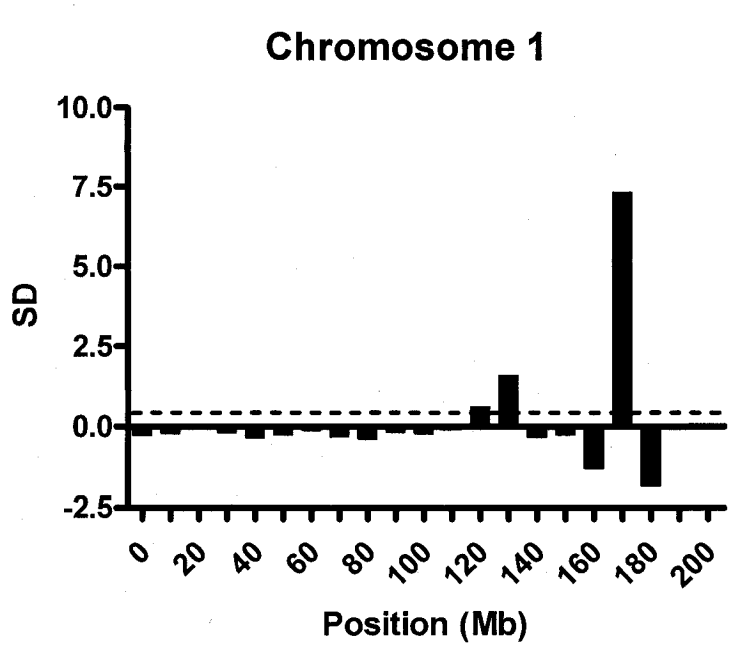

Fig. 8e. Full genome Digital Disease mapping output for WIN55,212-2 analgesia Z-scores

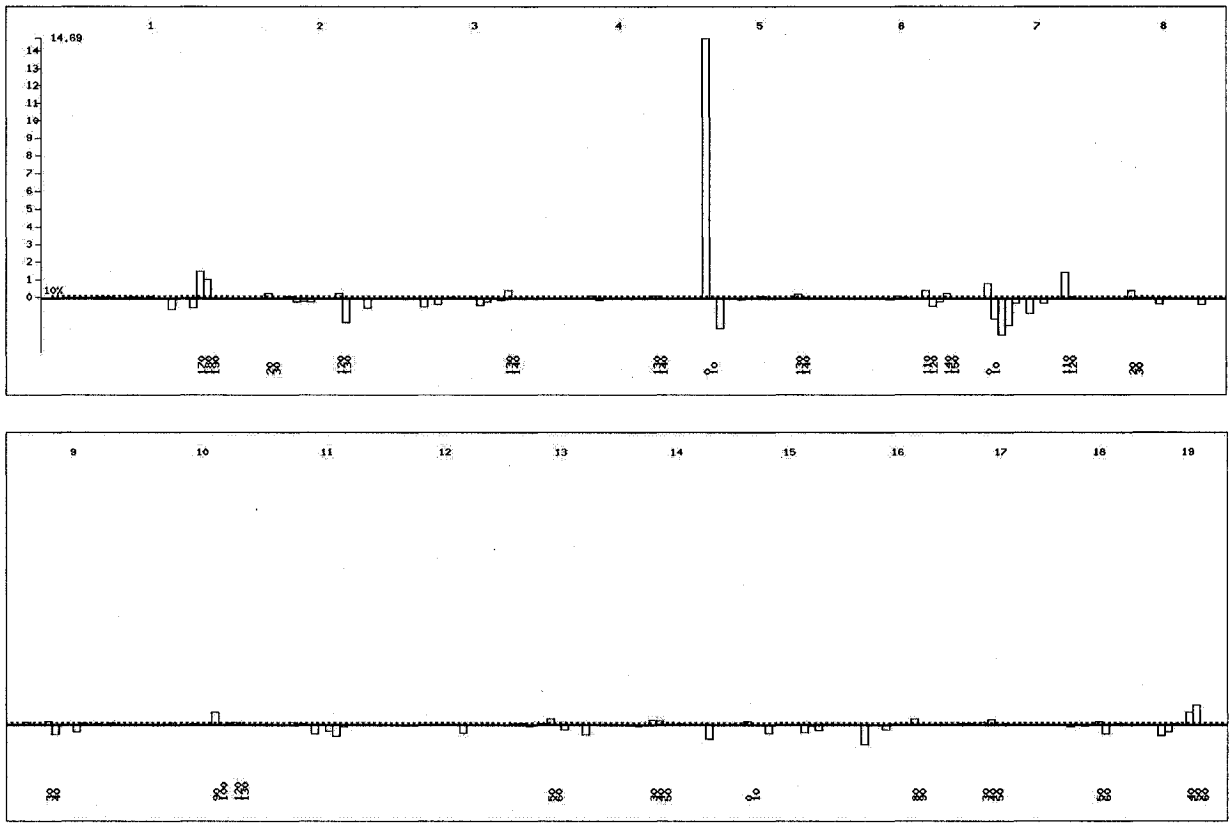

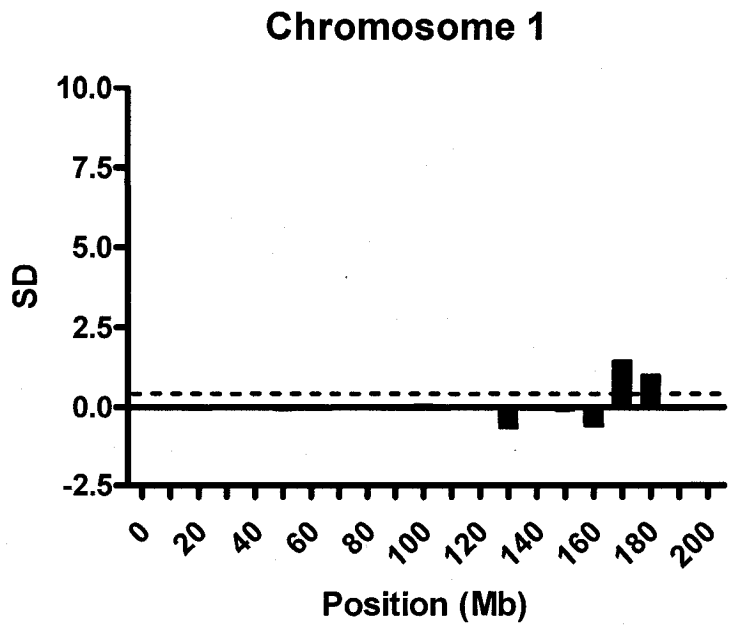

Fig. 9. Fcgr3 Knockout/congenic interval

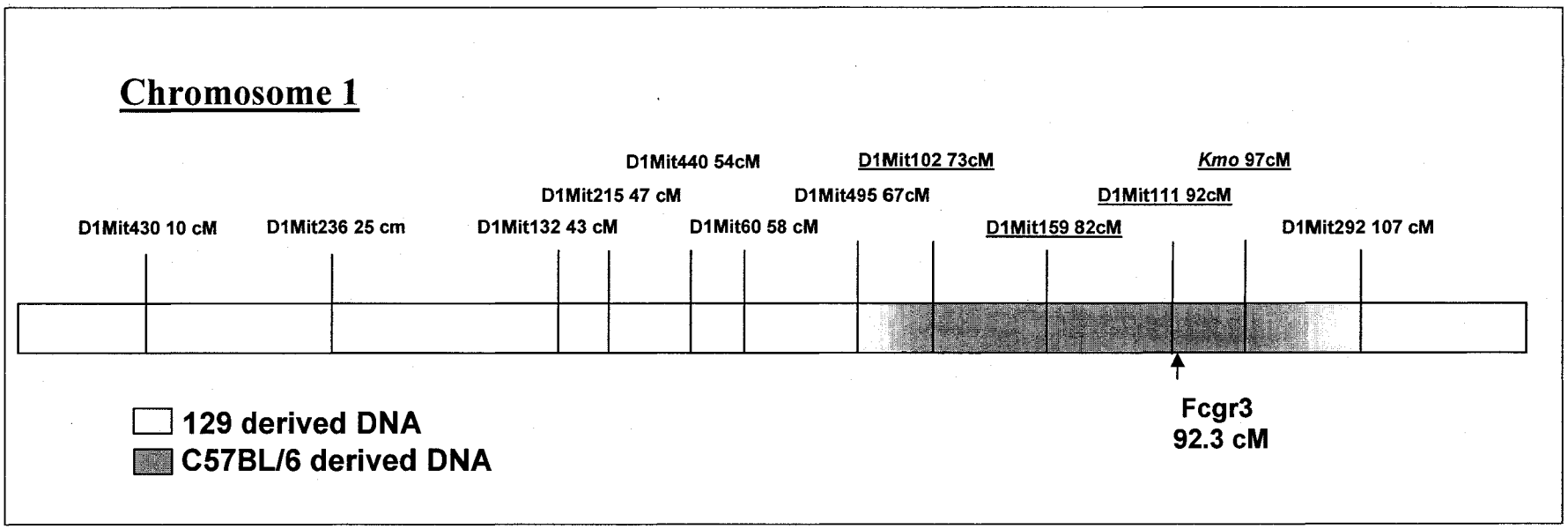

Fig. 10. Fcgr3 KO vs. C57BL/6 wild-type: three analgesic drugs

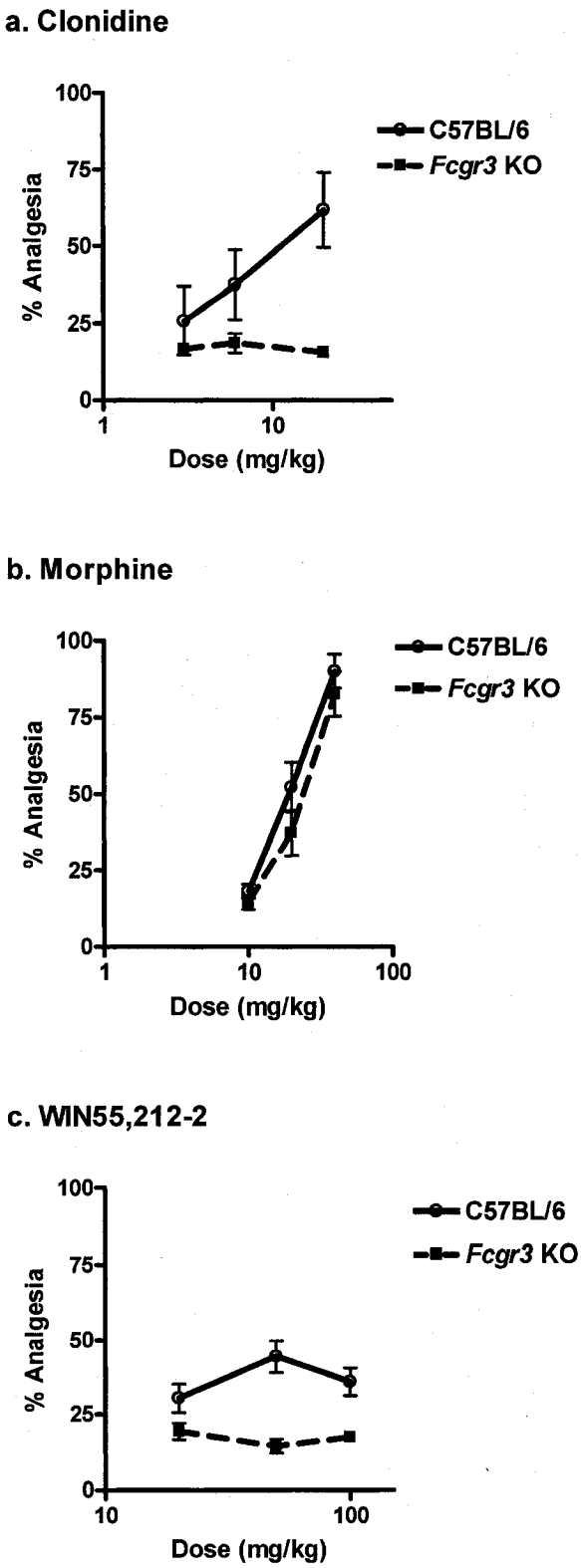

Fig. 11a. Dominance effects of the 129 vs. B6 allele in clonidine analgesic magnitude.

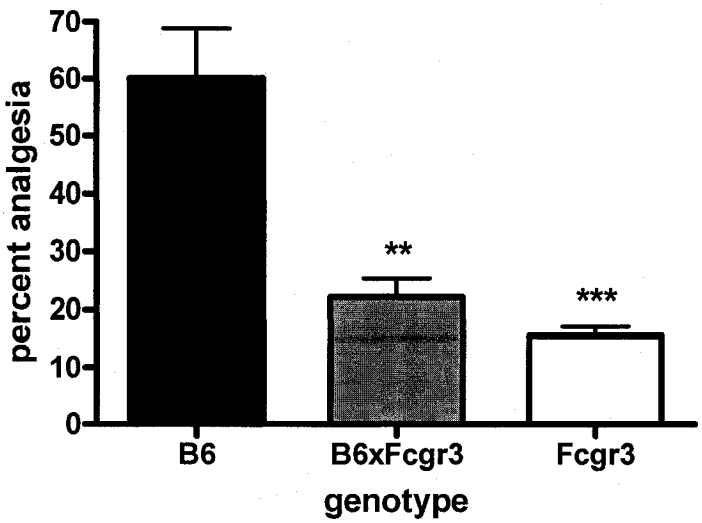

b. Subcongenic strains

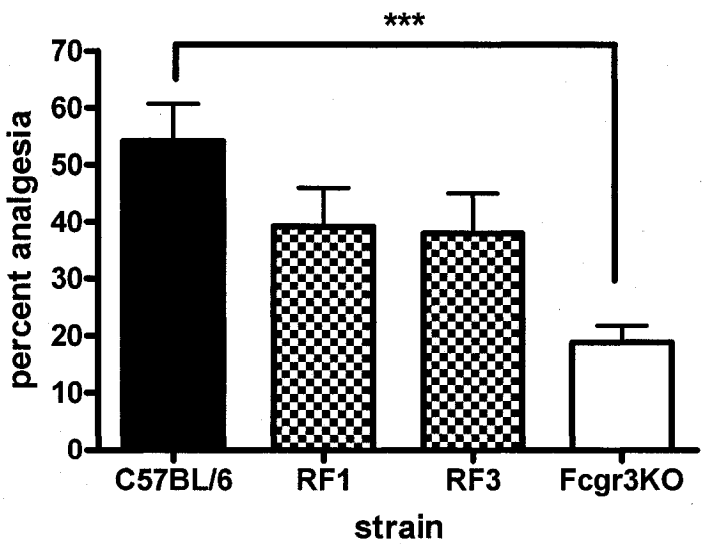

Fig. 12. Expression of *Kcnj9* in three central nervous system sites

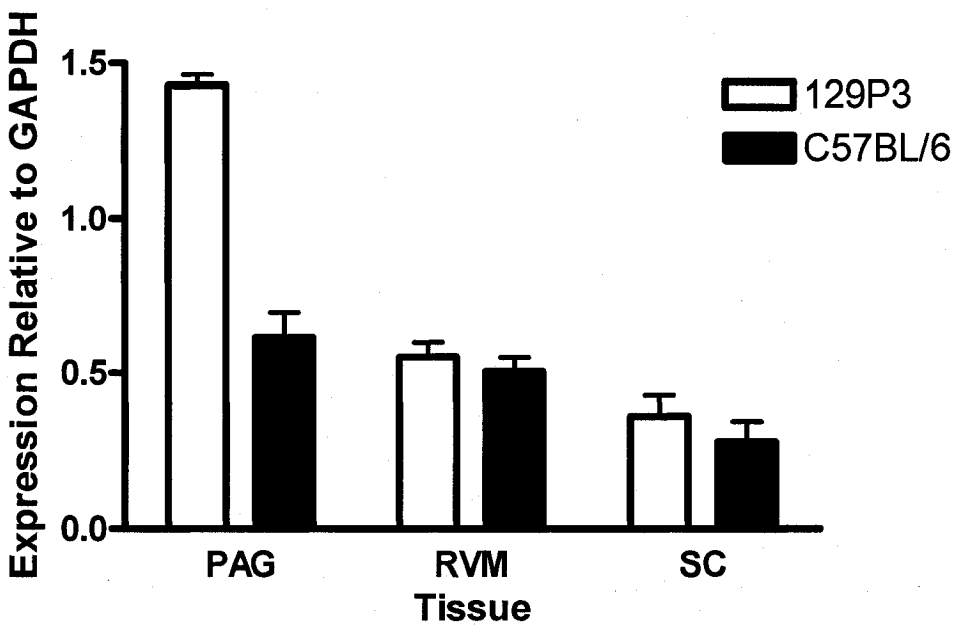

Fig. 13. GIRK3 KO vs. C57BL/6 wild-type: three analgesic drugs

a. Clonidine

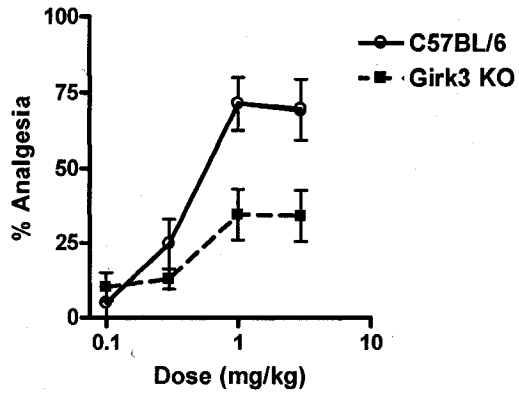

b. Morphine

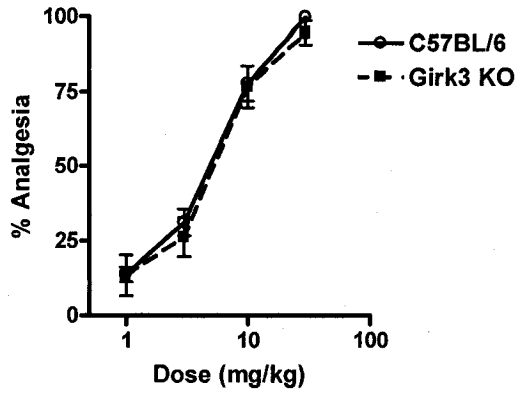

c. WIN55,212-2

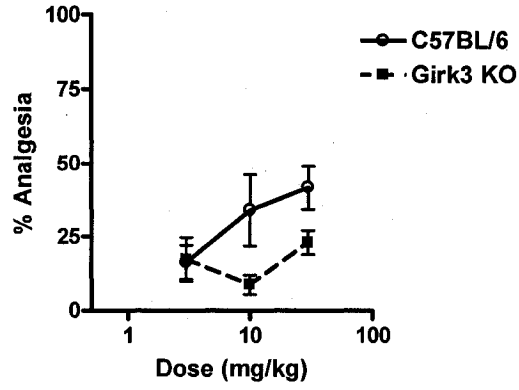

Fig. 14. Effects of 1 mg/kg systemic ouabain on A vs. B6 strain differences

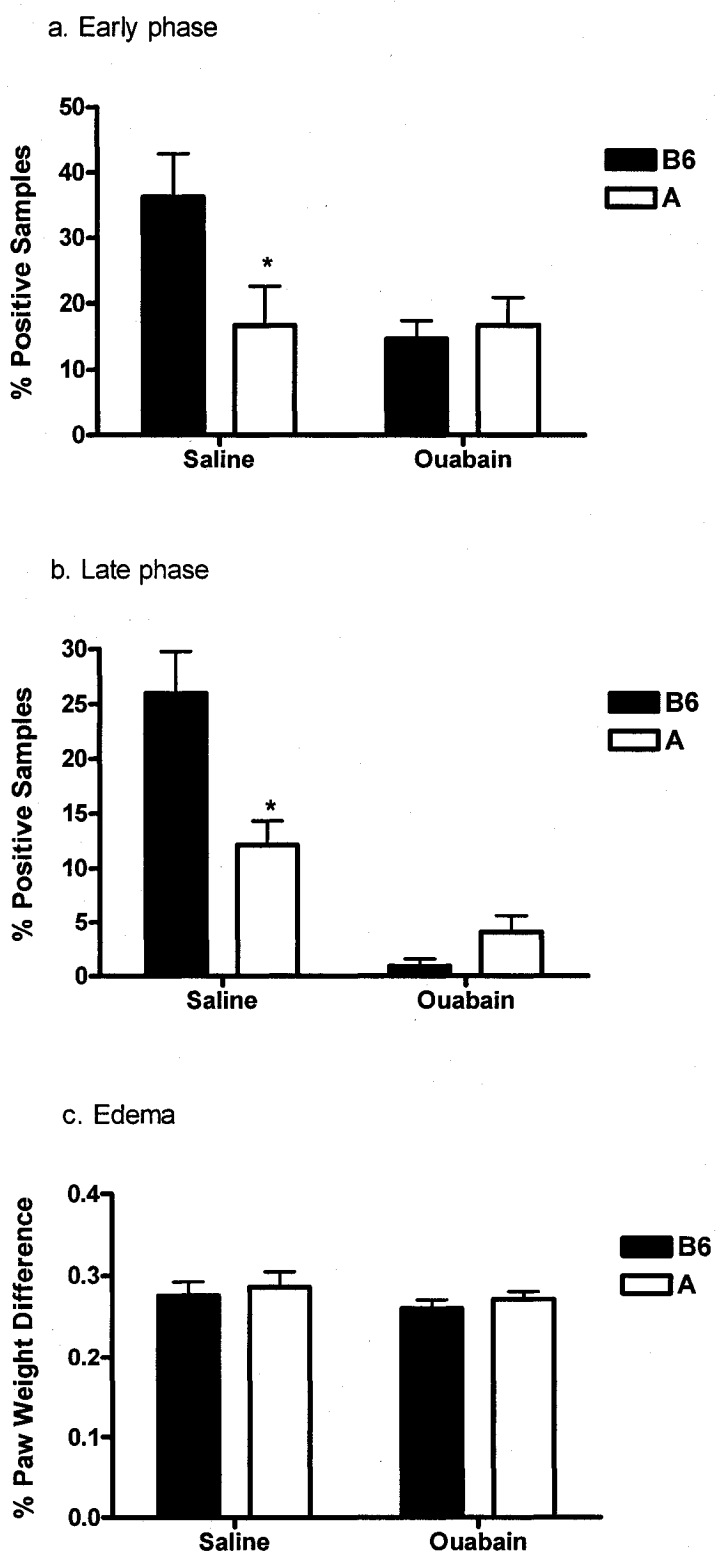

Fig. 15. qPCR of Na,K ATPase channel subunits

a. Basal expression of *Atp1b3* in the DRG of two mouse strains

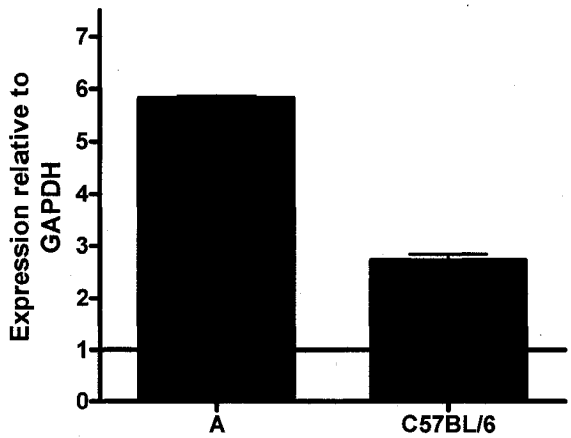

b. Relative basal expression of ATPase subunit genes in the DRG of two mouse strains

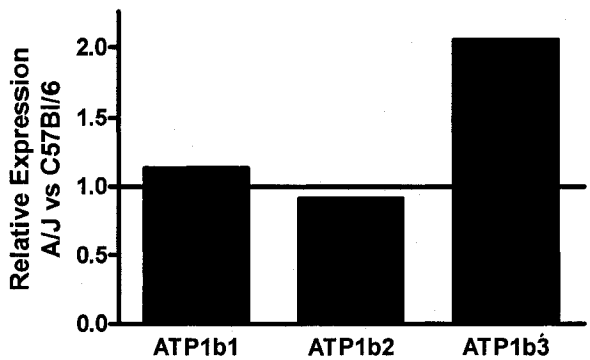

c. Expression of *Atp1b3* in the DRG following formalin injection

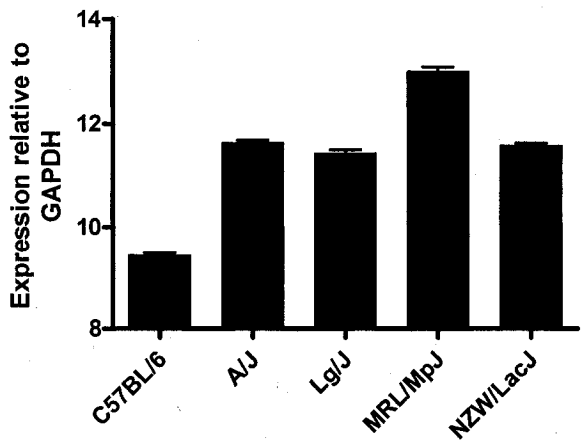

Fig. 16. Recombinant inbred phenotype correlations

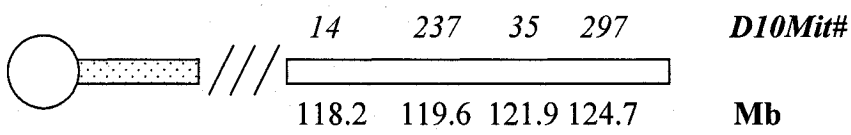

		F_{late}	Phenotype
A/J:		9.7 (1.5)	(0)
B6:		31.8 (3.9)	(1)
BXA-4:		13.6 (3.0)	
AXB-4:		13.9 (2.5)	
AXB-19:		22.6 (1.4)	
BXA-17:		23.3 (1.7)	
AXB-8:		25.2 (1.8)	
AXB-18:		26.9 (1.6)	
BXA-8:		32.7 (2.5)	
BXA-26:		40.6 (4.5)	

Correlation: -0.25 -0.02 0.52 0.61

Fig. 17. Recombinant congenic strain phenotypes

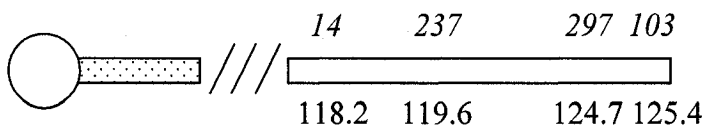

		F_{late}	Phenotype
A/J:		19.9 (1.8)	
AcB63:		17.1 (1.8)	
AcB64:		25.0 (1.3)	
B6:		28.0 (2.3)	
BcA70:		23.2 (2.6)	
BcA72:		19.7 (1.3)	
BcA79:		31.5 (2.6)	
BcA81:		31.1 (1.9)	

Fig. 18. Congenic strain comparisons.

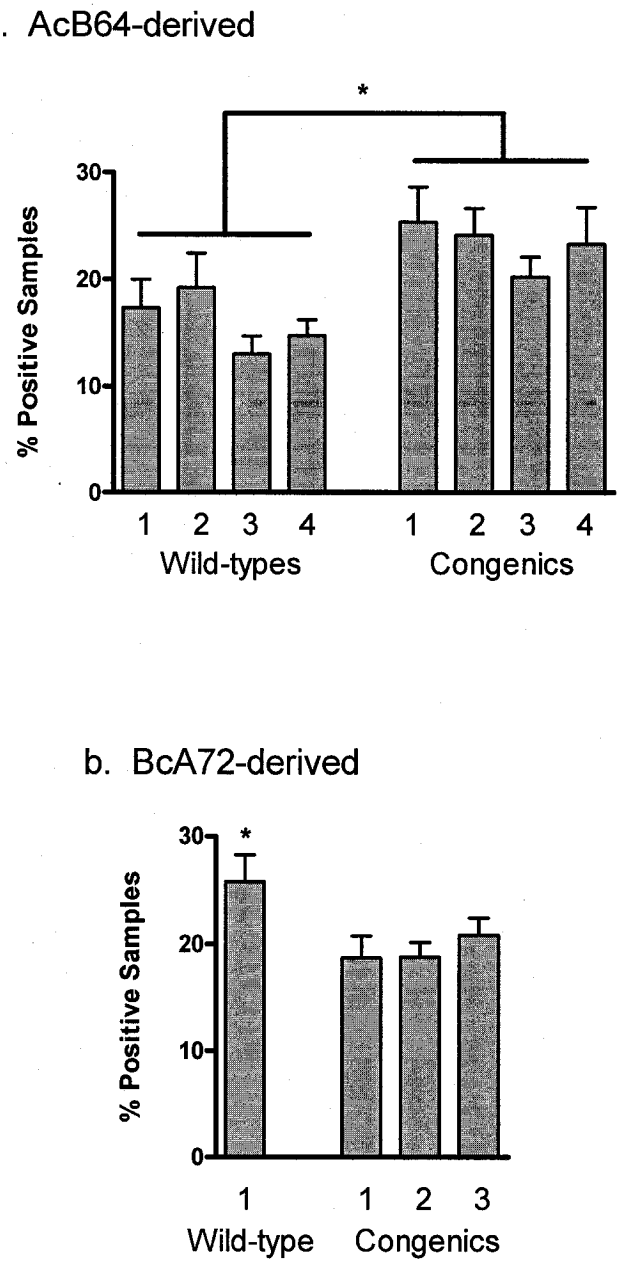

VITA

Shad Benjamin Smith was born in Provo, Utah on October 5, 1975. He graduated in the top ten of his class from Hoggard High School in Wilmington, North Carolina, in 1993. He obtained a B.S. degree in Psychology from Brigham Young University in 2000, with minors in Zoology and Chemistry. Following graduation Shad Benjamin Smith worked for over a year as a substance abuse counselor at New Hanover Metro Treatment Center in Wilmington, North Carolina. He then began graduate studies in Psychology and Behavioural Neuroscience in the laboratory of Dr. Jeffrey S. Mogil at McGill University. Following completion of his Ph.D., Shad will begin post-doctoral research with Dr. William Maixner and Dr. Luda Diatchenko in the Dental Research Department of the University of North Carolina at Chapel Hill.